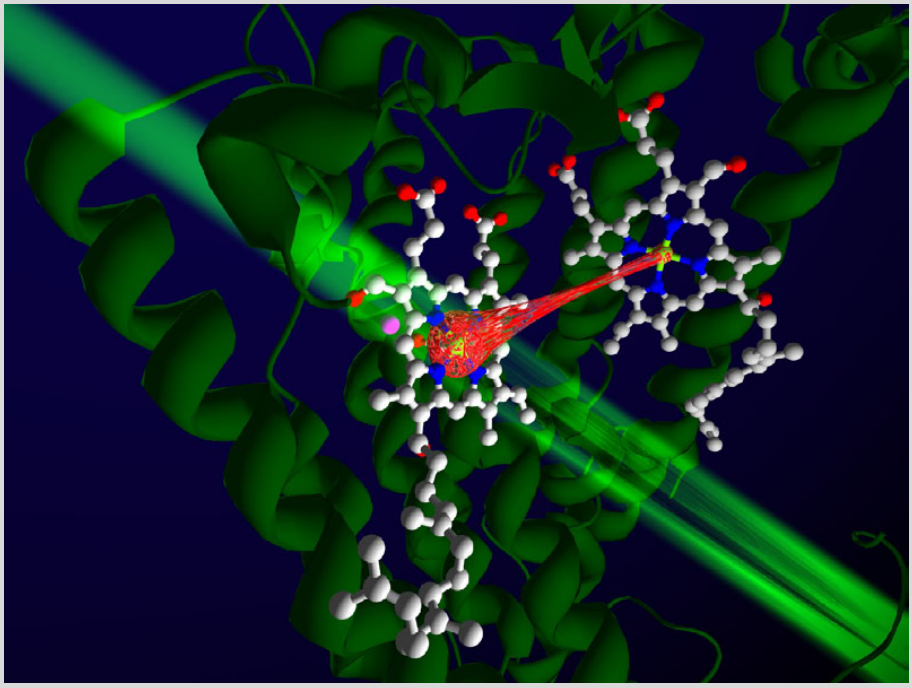

Proton Translocation Coupled to Electron Transfer Reactions in Terminal Oxidases

ILYA BELEVICH

Institute of Biotechnology
Division of Biochemistry
Department of Biological and Environmental Sciences
Faculty of Biosciences
University of Helsinki

Dissertationes bioscientiarum molecularium Universitatis Helsingiensis in Viikki

22/2007

PROTON TRANSLOCATION COUPLED TO ELECTRON TRANSFER REACTIONS IN TERMINAL OXIDASES

Ilya Belevich

Institute of Biotechnology
Division of Biochemistry
Department of Biological and Environmental Sciences
Faculty of Biosciences
University of Helsinki

ACADEMIC DISSERTATION

To be presented for public criticism, with permission of the Faculty of Biosciences, University of Helsinki in the auditorium 1041 of Biocenter 2 (Viikinkaari 5) on November 8th, 2007 at 12 noon

HELSINKI 2007

Supervisors:

Dr. **Michael I. Verkhovsky**
Institute of Biotechnology
University of Helsinki
Finland

Prof. **Mårten Wikström**
Institute of Biotechnology
University of Helsinki
Finland

Reviewers:

Prof. **Ilmo Hassinen**
Department of Medical Biochemistry and Molecular Biology
Faculty of Medicine, University of Oulu
Finland

Research Assistant Prof. **Joel Morgan**
Department of Biology
Rensselaer Polytechnic Institute, Troy, NY
USA

Opponent:

Prof. **Peter R. Rich**
Glynn Laboratory of Bioenergetics
Department of Biology
University College London, London, UK

Kustos:

Prof. **Carl G. Gahmberg**
Division of Biochemistry
Department of Biological and Environmental Sciences
University of Helsinki, Finland

Cover art - artistic representation of electron backflow reaction in cytochrome *c* oxidase. Two hemes (heme a_3, left and heme *a*, right) and Cu_B centers among α-helices are shown. A laser flash induces CO dissociation from the two-electron reduced state, which is followed by electron redistribution between the hemes as shown on the picture.

ISBN 978-952-10-4176-1 (paperback)
ISBN 978-952-10-4177-8 (PDF, http://ethesis.helsinki.fi)

ISSN 1795-7079

Yliopistopaino, Helsinki University Printing House
Helsinki, 2007

To my family

For every complex problem, there is a solution

that is simple, neat, and wrong.

paraphrase of H. L. Mencken

CONTENTS

ABBREVIATIONS AND NOMENCLATURE

Chemical compounds:

ADP - adenosine 5'-diphosphate
ATP - adenosine 5'-triphosphate
DM - *n*-dodecyl-β-D-maltoside
$FADH_2$ - flavin adenine dinucleotide (reduced)
Fe-S - iron-sulfur cluster
FMN - flavin mononucleotide
NAD^+/ NADH - nicotinamide adenine dinucleotide (oxidized/reduced form)
Q/QH_2 - ubiquinone/ubiquinol
RubiPy - tris (2,2'-bipyridyl) ruthenium (II)

Intermediates of the catalytic cycle

O - fully-oxidized, ground state
E or **E_H** - one-electron reduced state
R - fully-reduced state
A - ferrous-oxy intermediate
P - peroxy intermediate
F - ferryl-oxo intermediate
O_H (H or O~) - fully-oxidized, high-energy state

Other abbreviations:

CcO - cytochrome *c* oxidase
COFR - fully-reduced oxidase ligated by carbon monoxide
COMV - "mixed-valence" (two-electron reduced) oxidase ligated by carbon monoxide
d - relative dielectric depth of the binuclear center within the membrane
E_m - midpoint redox potential relative to the Standard Hydrogen Electrode
EPR - electron paramagnetic resonance
Ferryl form - state of heme-iron with +4 charge (extra oxidized)
Ferric form - state of heme-iron with +3 charge (oxidized)
Ferrous form - state of heme-iron with +2 charge (reduced)
N-side - electrically negative side of the membrane (matrix in mitochondria or cytoplasm in bacteria)
P-side - electrically positive side of the membrane (intermembrane space in mitochondria or periplasmic space in bacteria)
K_d - dissociation constant
K_m - Michaelis-Menten constant
ROS - reactive oxygen species
$\Delta\mu_H^+$ - electrochemical proton gradient
$\Delta\Psi$ - electric membrane potential
τ - time constant, $^1/_k$

Amino acids:

A	Ala	Alanine	**I**	Ile	Isoleucine	**R**	Arg	Arginine
C	Cys	Cysteine	**K**	Lys	Lysine	**S**	Ser	Serine
D	Asp	Aspartic acid	**L**	Leu	Leucine	**T**	Thr	Threonine
E	Glu	Glutamic acid	**M**	Met	Methionine	**V**	Val	Valine
F	Phe	Phenylalanine	**N**	Asn	Asparagine	**W**	Trp	Tryptophan
G	Gly	Glycine	**P**	Pro	Proline	**Y**	Tyr	Tyrosine
H	His	Histidine	**Q**	Gln	Glutamine			

The numbering of amino acid residues mainly refers to the *Paracoccus denitrificans* enzyme; at the same time the corresponding residue numbers for the bovine (*Bos taurus*) cytochrome *c* oxidase are given in parentheses.

LIST OF ORIGINAL PUBLICATIONS

I. **Ilya Belevich**, Vitaliy B. Borisov, Alexander A. Konstantinov, and Michael I. Verkhovsky
Oxygenated complex of cytochrome *bd* from *Escherichia coli*: Stability and photolability.
(2005) *FEBS Letters*, Vol. 579, p. 4567-4570
http://linkinghub.elsevier.com/retrieve/pii/S0014-5793(05)00854-9

II. **Ilya Belevich**, Anne Tuukkanen, Mårten Wikström, and Michael I. Verkhovsky
Proton coupled electron equilibrium in soluble and membrane bound cytochrome *c* oxidase from *Paracoccus denitrificans*
(2006) *Biochemistry*, Vol. 45, p. 4000-4006
http://dx.doi.org/10.1021/bi052458p

III. Dmitry Bloch, **Ilya Belevich**, Audrius Jasaitis, Camilla Ribacka, Anne Puustinen, Michael I. Verkhovsky, and Mårten Wikström
The catalytic cycle of cytochrome c oxidase is not the sum of its two halves
(2004) *Proc. Nat. Acad. Sci. USA*, Vol.101, p. 529-533
http://www.pnas.org/cgi/content/full/101/2/529

IV. **Ilya Belevich**, Michael I. Verkhovsky, and Mårten Wikström
Proton-coupled electron transfer drives the proton pump of cytochrome *c* oxidase
(2006) *Nature*, Vol. 440, p. 829-832
http://www.nature.com/nature/journal/v440/n7085/abs/nature04619.html

V. **Ilya Belevich**, Dmitry A. Bloch, Nikolai Belevich, Mårten Wikström, and Michael I.Verkhovsky
Exploring the proton pump mechanism of cytochrome *c* oxidase in real time
(2007) *Proc. Nat. Acad. Sci. USA*, Vol. 104, p. 2685-2690
http://www.pnas.org/cgi/content/full/104/8/2685

1. INTRODUCTION

1.1 Energy Cycle in Living Organisms

All living organisms require energy for growth and reproduction, and the most important task of all organisms is to find a way to absorb the energy in an available form and then transform it into a usable form. The major source of energy in the biosphere is sunlight. About three billion years ago some bacteria learned to utilize the energy of photons from the Sun and convert it into the energy of chemical bonds in a process called photosynthesis. In this complex process the energy of a light quantum drives the electron flux from water to carbon dioxide forming carbohydrates – mainly glucose (Equation 1), sucrose, and starch – which eventually form the basis for the building of biomass and growth. As a side product of the photosynthetic reaction, molecular oxygen is released into the atmosphere.

$$6\,CO_2 + 6\,H_2O \xrightarrow[\text{photosynthesis}]{h\nu} C_6H_{12}O_6 + 6\,O_2 \qquad (1)$$

After some time in the past, the amount of dioxygen in the atmosphere was greatly increased and about 2-2.5 billion years ago a new line of organisms appeared. This new form of life was able to obtain the energy it needed by transferring electrons from foodstuffs, created in photosynthesis, to oxygen thereby releasing a great deal of energy (Equation 2). This latter process is called respiration.

$$C_6H_{12}O_6 + 6\,O_2 \xrightarrow{\text{respiration}} 6\,CO_2 + 6\,H_2O + \text{energy (ATP)} \qquad (2)$$

Taken together these two processes form a closed carbon cycle, responsible for the circulation and transformation of energy among living organisms on Earth.

1.2 Cellular Respiration

The main foodstuffs used by cells in the cellular respiration are carbohydrates, fatty acids, and proteins. As an example, the catabolic reaction of carbohydrates in higher organisms consists of three main stages. The first stage is glycolysis and it takes place in the cytoplasm of the cell. In this process glucose and other sugars are transformed into three-carbon molecules of pyruvate with the generation of ATP and NADH. However, the amount of ATP and NADH formed at this stage is rather small, especially when compared to subsequent steps of pyruvate disintegration.

The next two steps of energy transformation occur in mitochondria. The mitochondrion consists of two closed membrane layers, identified as the outer and inner membranes, which divide the

mitochondrion into two isolated compartments: the internal matrix and intermembrane space. The outer membrane, which encloses the entire organelle, has a large number of pores formed by the protein *porin*. Porin contains a relatively large internal channel that makes the outer membrane permeable to all kinds of molecules up to 1 500 Daltons. In contrast, the inner membrane is impermeable to any water-soluble molecules and ions, and transport of molecules through this membrane is carried out selectively through specific transporters. The physiological functions of the inner membrane are to house the enzymatic complexes of the respiratory chain (also known as the electron transport chain) and to maintain an electrochemical transmembrane proton gradient, which is subsequently used for ATP synthesis (Mitchell, 1961). Depending on environmental conditions the inner mitochondrial membrane can be extremely enlarged into the matrix space, increasing its capacity to contain the proteins of the respiratory chain. Unlike eukaryotes, prokaryotes lack mitochondria and in these organisms the enzymes of the respiratory chain are situated in the cytoplasmic membrane.

At the second stage of the catabolic reaction the molecules of pyruvate are transferred into the matrix compartment of the mitochondria. In the matrix space pyruvate is converted to acetyl-CoA - the substrate for the citric acid cycle (*Krebs cycle*), where it is finally oxidized to carbon dioxide. In this sequential process the oxidation of one molecule of acetyl-CoA produces one molecule of ATP, one molecule of QH_2 and three molecules of NADH. The latter two substances are used as electron donors in the last stage of cellular respiration by the enzymes of the respiratory chain.

The respiratory chain (Fig. 1) consists of four membrane-bound protein complexes containing redox-active cofactors (see review by Saraste, 1999). The first enzyme in this chain is complex I (NADH:ubiquinone oxidoreductase or NADH dehydrogenase). Complex I is the largest enzyme of the respiratory chain composed of up to 45 different subunits (Carroll *et al.*, 2002) with noncovalently bound flavin mononucleotide (FMN) and at least eight iron-sulfur clusters (Fe-S) as prosthetic groups (Hinchliffe and Sazanov, 2005). Complex I receives electrons from NADH and use them to reduce the quinone pool in the membrane. This reaction is coupled to proton translocation across the membrane in the stoichiometry of two protons per electron (Wikström, 1984; Bogachev *et al.*, 1996; reviews by Yano, 2002; Hirst, 2005). It should be noted however that in some organisms e.g. the yeast *Saccharomyces cerevisiae* (baker's yeast), the mitochondrial respiratory chain does not contain complex I as such, but several alternative

NADH dehydrogenases. These alternative dehydrogenases can oxidize matrix and cytoplasmic NADH but do not contribute to production of a membrane potential (Joseph-Horne *et al.*, 2001).

The reduced quinone pool is also maintained by complex II (succinate:ubiquinone oxidoreductase or succinate dehydrogenase), which is a component of the citric acid cycle. Complex II contains a covalently bound FAD (flavin-adenine dinucleotide) and several Fe-S clusters as redox cofactors and couples the oxidation of succinate to the reduction of ubiquinone (review by Horsefield *et al.*, 2004). In addition, the membrane domain of complex II contains heme *b*, which does not participate in electron transfer itself, but most likely serves as a regulator of the redox potentials of the cofactors and facilitates electron transfer to ubiquinone. Complex II is not involved in proton translocation across the membrane and serves only as an electron entry point to the energy transducing part of the respiratory chain.

Complex III (ubiquinol:cytochrome *c* oxidoreductase or bc_1 complex) has 11 subunits with several redox centers: two protohemes (cytochromes *b*), a membrane-anchored cytochrome c_1 and a Rieske-type center (Fe_2S_2). Complex III transfers electrons from ubiquinol to cytochrome *c* and translocates one charge across the membrane dielectric for each electron delivered to cytochrome *c*, by a mechanism known as the protonmotive Q-cycle (Mitchell, 1976; Crofts, 2004 for reviews).

Finally, the terminal oxidase - complex IV (cytochrome *c* oxidase, CcO) - uses the electrons from cytochrome *c* to reduce dioxygen to water, and links this process to proton pumping across the membrane. Mammalian CcO consists of 13 subunits and has 4 redox-active centers: a bimetallic copper site (Cu_A), two hemes (*a* and a_3[1]), and another copper ion (Cu_B). Heme a_3 and Cu_B together form a catalytic site where all the chemistry of oxygen reduction to water occurs.

In the respiration process electrons from NADH are sequentially transferred through the enzymes of the respiratory chain to the terminal electron acceptor – dioxygen. The energy released in this reaction drives proton translocation across the membrane and creates an electrochemical transmembrane proton gradient ($\Delta\mu_H^+$).The full drop of redox potential from NADH to dioxygen is about 1.15 V; however since the inner membrane cannot sustain over ~200 mV, the release of energy in a single step would be extremely inefficient. Thus, the

[1] Because oxygen-binding heme has specific chemical and spectroscopic properties subscript '3' after the heme letter is used to distinguish it.

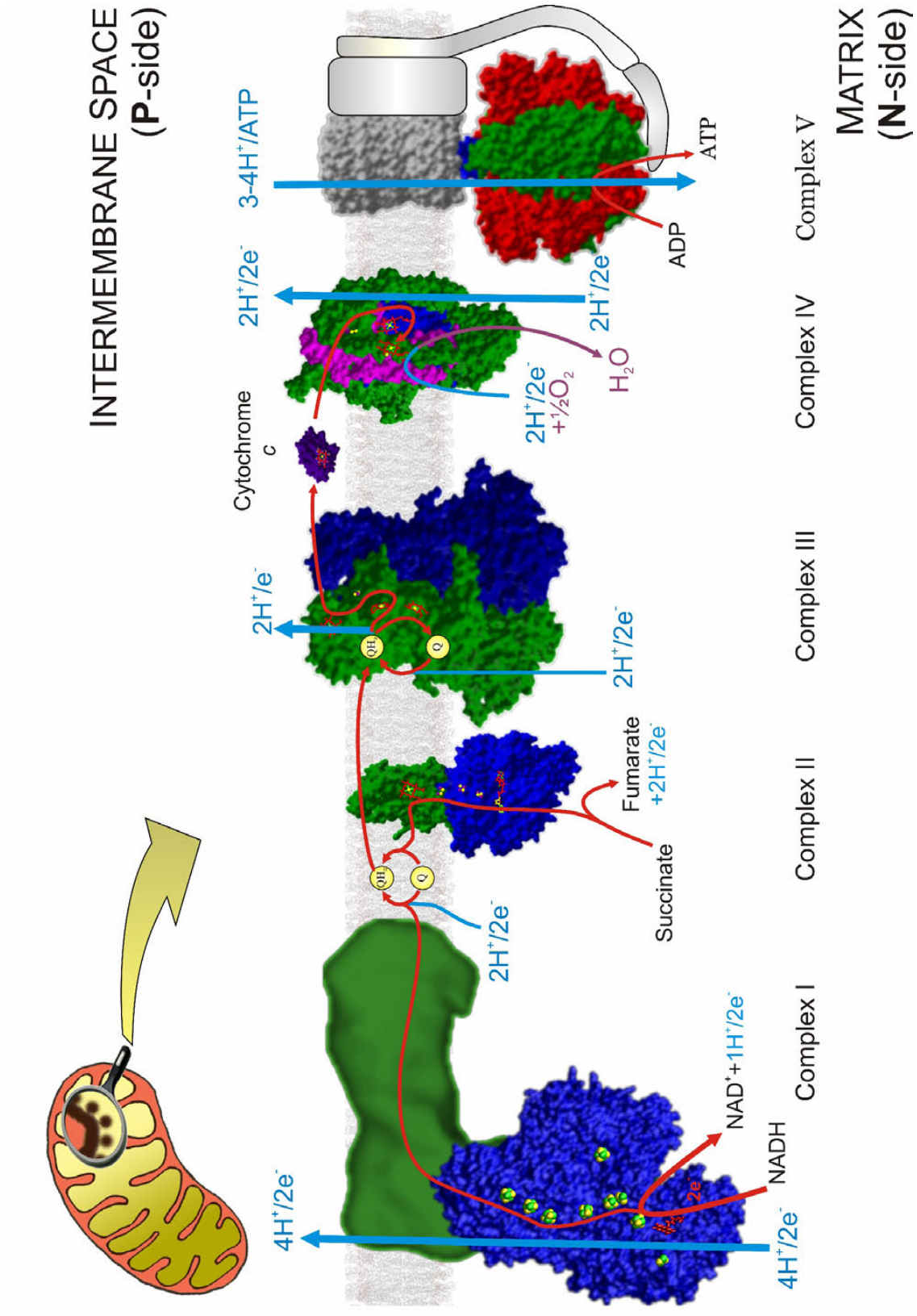

Figure 1. Schematic representation of the mitochondrial inner membrane, including the enzymes of the respiratory chain and ATP synthase. Based on the crystallographic structures 2FUG, 1YQ3, 1BGY, 2B4Z, 1QLE, 1BMF, 1YCE)

respiratory chain releases the energy sequentially, step by step and can be described as a molecular transformer that accepts the voltage provided by the redox reaction (1.15 V) and lower it to a voltage that the membrane can sustain (~200 mV), while conserving energy by making a corresponding increase in the current. Since the overall drop of energy from NADH to dioxygen is in about 5 times higher than the potential on the membrane, the sequential organization of the respiratory chain allows the utilization of the energy into the translocation of 5 charges (protons) across the membrane. The $\Delta\mu_H^+$ created in this way is mostly used by the ATP synthase (complex V) for formation of ATP (Mitchell, 1961; Stock *et al.*, 2000).

The sequential oxidation of glucose to carbon dioxide is extremely efficient and provides sufficient energy for formation of up to 31 molecules of cytoplasmic ATP per molecule of glucose (Fig. 2). One of the main tasks in cellular bioenergetics is to understand individual functional mechanisms of the enzymes in the respiratory chain. The present study is focused on the terminal oxidases of the respiratory chain, which are responsible for final utilization of electrons supplied from NADH.

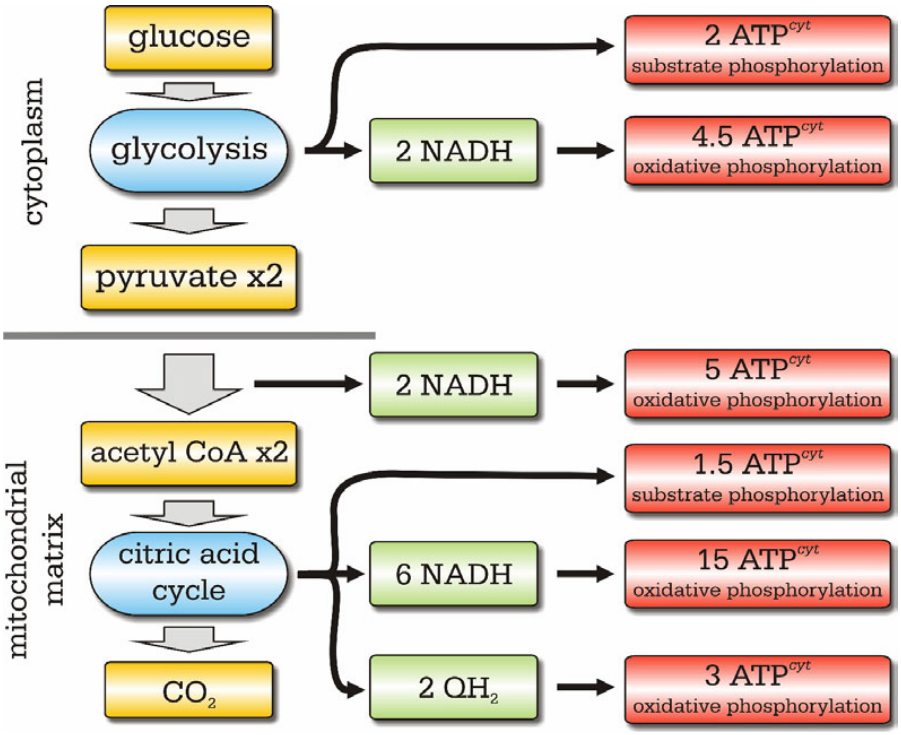

Figure 2. The approximate overall efficiency of oxidation of one molecule of glucose to carbon dioxide in the eukaryotic cell (assuming that: oxidation of 1 $NADH_{matrix}$ is coupled to transfer of 10 H^+ across the membrane; $H^+/ATP_{cytoplasm}$ ratio at the ATP synthase is 3 (ATP synthase efficiency) + 1 (ATP/ADP exchanger); and delivery of $NADH_{cytoplasm}$ into the matrix space occurs via glutamate-aspartate shuttle and consumes 1 H^+).

2. STRUCTURE AND FUNCTION OF TERMINAL OXIDASES

2.1 Function

Cytochrome *c* oxidase (CcO) catalyzes the final step of respiration - reduction of molecular oxygen. Reduction of one dioxygen to water requires four electrons that are supplied one-by-one from the water-soluble cytochrome *c* on the P-side, and four protons, taken up from the N-side of the membrane:

$$4\ \text{cyt}\ c_P^{2+} + 4\ H_N^+ + O_2 \longrightarrow 4\ \text{cyt}\ c_P^{3+} + 2\ H_2O + \text{energy}$$

There are several main aspects in the functioning of CcO. First, even though the reduction of oxygen to water is an exergonic process, coupled to release of large amounts of energy, this reaction does not proceed spontaneously under normal conditions. The reason is the high activation barrier. Hence, the first main role of CcO is to form favorable conditions for catalysis and to facilitate the process of oxygen reduction to water.

Secondly, the energy released in the reaction of oxygen reduction is conserved in the form of a transmembrane electrochemical gradient of protons across the membrane ($\Delta\mu_H^+$). Formation of $\Delta\mu_H^+$ by CcO is based on two principles: vectorial chemistry and proton pumping. Since the protons and electrons for oxygen reduction to water are taken from the different sides of the membrane, the reaction results in net transfer of four charges across the membrane. At the same time, the enzyme is able not only to catalyze the oxygen reduction but also to utilize the released energy for proton pumping. In 1977 Wikström showed that reduction of molecular oxygen to water by CcO is linked to pumping of four protons across the membrane dielectric (Wikström, 1977). Hence, the overall reaction carried out by cytochrome *c* oxidase can be described by the following equation:

$$4\ \text{cyt}\ c_P^{2+} + 8\ H_N^+ + O_2 \longrightarrow 4\ \text{cyt}\ c_P^{3+} + 2\ H_2O + 4\ H_P^+$$

Thirdly, all processes involving oxygen redox chemistry are potentially extremely dangerous for a cell due to possible formation of highly toxic reactive oxygen species (hydroxyl radical, hydrogen peroxide, and superoxide - *ROS*). These oxygen compounds can induce chain reactions of oxidative damage to fatty acids and other lipids, DNA molecules, proteins, *etc*. Therefore, the mechanism of oxygen catalysis in CcO organized such that it excludes the formation of ROS and assures complete reduction of oxygen to water (Babcock and Wikström, 1992).

2.2 Terminal Oxidases

In contrast to eukaryotes, where only one type of terminal oxidases (aa_3-type cytochrome *c* oxidase) is present, the respiratory chains in bacteria can vary extensively (Anraku and Gennis, 1987; Garcia-Horsman *et al.*, 1994) and have multiple types of terminal oxidases (Fig. 3). The main function of such branching is to provide bacteria with better elasticity in a variety of environmental growth conditions. In brief, in bacteria the composition of the respiratory pathways has been evolved for optimal growth based on the following factors:

- *Maintaining the highest possible coupling efficiency* (H^+/e^- ratio) under many different environmental conditions for maximal yield of ATP. For example, if the oxygen tension in the growth medium is high, then the terminal oxidases in *Escherichia coli* will be mostly represented by the highly efficient cytochrome bo_3, which uses the energy of oxygen reduction to water to pump protons. In contrast, under low-oxygen conditions, the most pronounced will be the expression of cytochrome *bd* (Rice and Hempfling, 1978; Poole, 1983). This oxidase has higher affinity to oxygen (Paper I) but does not pump protons (Miller and Gennis, 1985; Puustinen *et al.*, 1991). Hence, the overall amount of energy formed in low-oxygen conditions will be decreased, but the respiratory chain will still be able to work, providing the bacteria with energy.
- *Rapid removal of excess reducing equivalents* such as NADH/NADPH. Even though the main function of the respiratory chain is to generate $\Delta\mu_{H^+}$, it also regulates the NAD^+/NADH ratio by eliminating excess reducing equivalents. This function is very important for organisms that have access to some alternative sources of energy such as photosynthesis. For instance, under high-light conditions in cyanobacteria reducing equivalents are formed extremely rapidly, and even CcO and the b_6f complex working together can not prevent over-reduction of the quinone pool in the membrane. In such a situation cytochrome *bd* starts to play an important role due to its lower coupling efficiency (Berry *et al.*, 2002).
- *Regulation of intracellular oxygen concentration.* Under some specific conditions it may be very important for bacteria to decrease the intracellular amounts of oxygen to protect oxygen-sensitive enzymes from inhibition. For example, nitrogenases from the strict aerobe *Azotobacter vinelandii* (Kelly *et al.*, 1990) or from some enteric bacteria (Hill *et al.*, 1990) can be easily inhibited by high concentrations of dioxygen. Thus, on one hand the oxygen concentration in these organisms must be kept low enough to allow nitrogen fixation and on the other hand it must be high enough for adequate synthesis of ATP. It

has been shown that in these bacteria cytochrome *bd* is a key element in the respiratory chain, involved in the oxygen regulating process (Hill *et al.*, 1990; Kelly *et al.*, 1990).

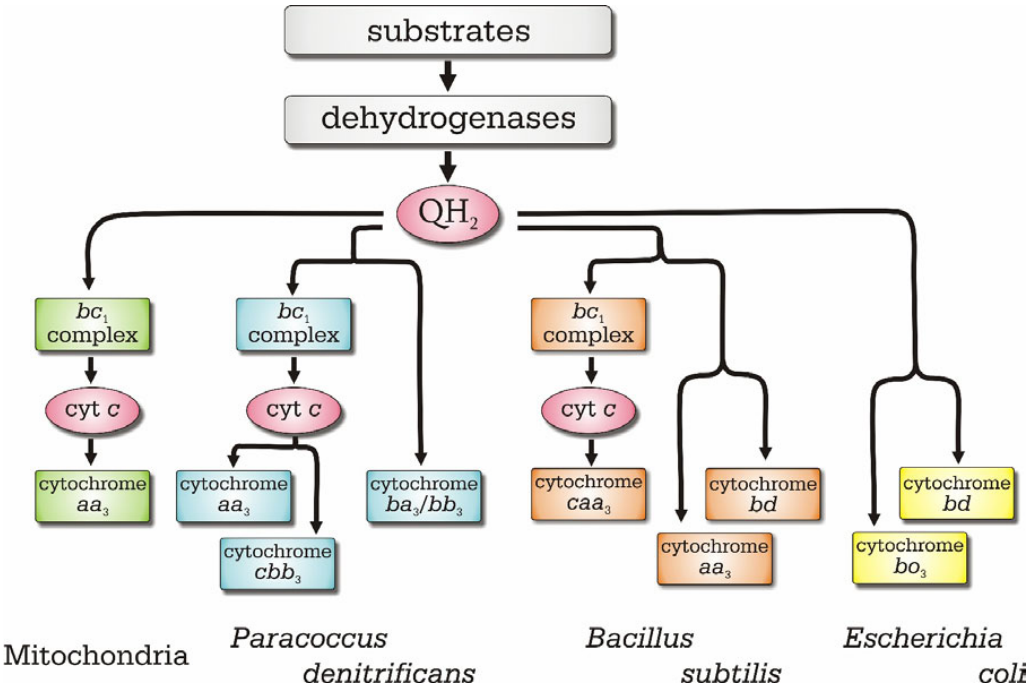

Figure 3. Schematic drawing of respiratory chain branching in several aerobic organisms.

Depending on the construction of the catalytic site, terminal oxidases can be divided into two families: the heme-copper superfamily and the cytochrome *bd*-type family. Most terminal oxidases belong to the heme-copper superfamily (Garcia-Horsman *et al.*, 1994); they are characterized by a unique binuclear catalytic site, where all the chemistry of oxygen reduction to water occurs. The binuclear site is located in subunit I and consists of a high-spin heme and a copper atom, called Cu_B. Both high-spin heme and Cu_B are retained in the protein by ligation to one and three histidine residues, respectively. In addition to the binuclear site, subunit I also harbors a low-spin heme, which is ligated by two histidine residues, and serves as a donor of electrons to the binuclear center. Together, the binuclear center and the electron-donating heme form the core of the protein, which is common to all members of the heme-copper oxidase superfamily. In bacteria, several different types of hemes (B, O or A) can be found as redox cofactors (Calhoun *et al.*, 1994) (Fig. 4). In addition to the core functional group, some oxidases of this class have extra prosthetic groups: for example, a bimetallic copper site Cu_A (in cytochrome aa_3[2]), a single *c*-type heme (in caa_3), or even several *c*-type hemes (cbb_3).

[2] The designation cytochrome $aa_3/bo_3/caa_3/cbb_3$ refers to the entire protein complex. The letter with subscript 3 defines the oxygen-binding heme; the letter next to it defines the type of the electron-donating low-spin heme. When additional heme(s) is present in the oxidase its type is designated by the first italic letter.

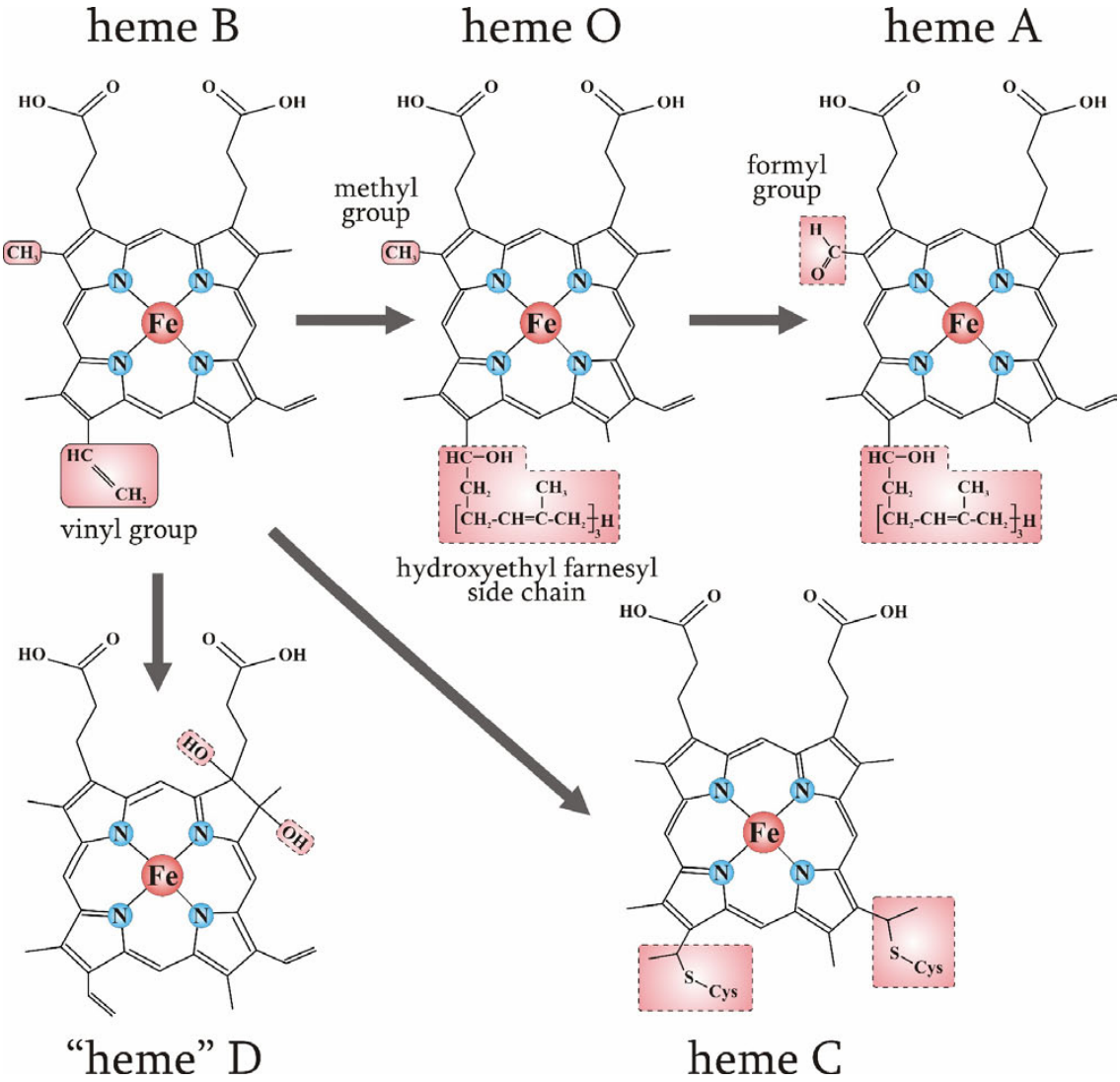

Figure 4. Structures of heme B, heme O, heme A, heme D (in this heme one double bond in a pyrrole ring has been reduced, so it is actually a chlorin, rather than a real heme), and heme C (structure of heme C is similar to heme B except that heme C is covalently bound to polypeptide via thioether bridges).

Heme-copper oxidases can be divided into two main subgroups based on the source of electrons, which they are able to utilize. The members of this first subgroup - cytochrome *c* oxidases - receive electrons from the water-soluble cytochrome *c* and are found in both eukaryotic and bacterial organisms. The most extensively studied examples of these oxidases are mitochondrial CcO from bovine heart; bacterial aa_3-type oxidases from *Paracoccus denitrificans* and *Rhodobacter sphaeroides*; cytochromes ba_3 and caa_3 from *Thermus thermophilus*; and cytochrome cbb_3 from various species. The second subgroup is represented by quinol-oxidases, which are found only in bacteria. Quinol oxidases accept electrons directly from quinols in the

cytoplasmic membrane. The best known member of this class is cytochrome bo_3 from *Escherichia coli*.

The second family of terminal respiratory oxidases is *bd*-type quinol oxidases. Compared to heme-copper oxidases, cytochrome *bd* has a completely different structure at the catalytic site. It lacks a copper atom and is most likely formed by two high-spin hemes: heme *d* (Fig, 4) and heme b_{595}. In addition to these hemes, cytochrome *bd* contains a low-spin heme b_{558}, which is directly involved in accepting electrons from quinols (Green *et al.,* 1986). Although this oxidase does not pump protons across the membrane (Miller and Gennis, 1985; Puustinen *et al.,* 1991), it can still create $\Delta\mu_H^+$ by virtue of vectorial chemistry. This results in reduced coupling efficiency which in fact turns out to have an adaptive importance for bacteria.

2.3 Structure of Cytochrome c Oxidase

A clear understanding of the mechanism of protein function is almost impossible without a knowledge of its 3D structure. The last decade was extremely successful in resolving the structures of membrane bound proteins by X-ray crystallography. Even though the information about basic composition and functioning of terminal oxidases was already known before the crystal structures were established, the great advantage was obtained when the first crystallographic structures of CcO were resolved (Iwata *et al.* 1995; Tsukihara *et al.,* 1995).

At present, mitochondrial and bacterial, reduced and oxidized, ligand-bound and unliganded, wild-type and mutant, cytochrome *c* and quinol terminal oxidases' structures from five organisms have been resolved with resolution up to 1.8 Å (Table 1). However, these structures have not, by themselves, provided an explanation of the catalytic mechanism of the enzyme. For example, the structures of the oxidized and reduced states of CcO reveal no large differences in the spatial organization of the protein, and the molecular mechanism of CcO is still enigmatic. Solving the structures of all intermediates in the catalytic cycle of CcO could help to answer this question. In some cases such approach has provided invaluable information about the mechanism of protein functioning. For instance, the structure of the light-driven proton pump bacteriorhodopsin was solved in all main states of the photocycle, which made it possible to create a picture of the function of this protein (Lanyi, 2004). Unfortunately, the intermediates of the catalytic cycle of CcO are quite unstable, which makes this approach extremely difficult.

Table 1. The list of resolved crystallographic structures of terminal oxidases.

Type	Source	Resolution	PDB number[3]	Reference
aa_3	bovine	2.80 Å	-	Tsukihara *et al.*, 1995
aa_3	bovine	2.80 Å	1OCC	Tsukihara *et al.*, 1996
aa_3	bovine	2.30 Å	2OCC	Yoshikawa *et al.*, 1998
aa_3-reduced	bovine	2.35 Å	1OCR	Yoshikawa *et al.*, 1998
aa_3-CO bound	bovine	2.80 Å	1OCO	Yoshikawa *et al.*, 1998
aa_3-N_3 bound	bovine	2.90 Å	1OCZ	Yoshikawa *et al.*, 1998
aa_3	bovine	1.80 Å	1V54	Tsukihara *et al.*, 2003
		1.80 Å	2DYR	Muramoto *et al.*, 2007
aa_3-reduced	bovine	1.90 Å	1V55	Tsukihara *et al.*, 2003
		1.90 Å	2EIJ	Muramoto *et al.*, 2007
aa_3-Cd^{2+} bound	bovine	2.10 Å	2EIK, 2EIL	Muramoto *et al.*, 2007
aa_3-Zn^{2+} bound	bovine	2.70 Å	2EIM, 2EIN	Muramoto *et al.*, 2007
aa_3	*P. denitrificans*	2.80 Å	-	Iwata *et al.*, 1995
aa_3	*P. denitrificans*	2.70 Å	1AR1	Ostermeier *et al.*, 1997
aa_3	*P. denitrificans*	3.00 Å	1QLE	Harrenga and Michel, 1999
aa_3	*Rh. sphaeroides*	2.30 Å	1M56	Svensson-Ek *et al.*, 2002
aa_3-E286Q	*Rh. sphaeroides*	3.00 Å	1M57	Svensson-Ek *et al.*, 2002
aa_3	*Rh. sphaeroides*	2.00 Å	2GSM	Qin *et al.*, 2006
ba_3	*Th. thermophilus*	2.40 Å	1EHK	Soulimane *et al.*, 2000
ba_3	*Th. thermophilus*	2.30 Å	1XME	Hunsicker-Wang *et al.*, 2005
bo_3, quinol oxidase	*E. coli*	3.50 Å	1FFT	Abramson *et al.*, 2000

Mammalian CcO has a molecular weight of about 200 kDa and contains 13 different polypeptide subunits (Table 2). The three largest form the core of the enzyme and are encoded by the mitochondrial genome, whereas the remaining 10 subunits originate from nuclear DNA (Capaldi, 1990). Bacterial CcO (Table 2) are simpler in structure and have only from three to four subunits (Fig. 5A), but the sequence homology of subunits I, II, and III to the corresponding ones of mitochondrial CcO is extremely high (Raitio et al., 1987; Steinrucke *et al.*, 1987). The sequence identity between CcO from *R. sphaeroides* and from bovine heart is 52% for subunit I (Shapleigh and Gennis, 1992), 39% for subunit II (Cao *et al.*, 1991), and 50% for subunit III (Cao *et al.*, 1992). Thus, the bacterial terminal oxidases can be excellent models of more complex eukaryotic oxidases for functional studies, mainly because there are easier and faster ways to manipulate them using molecular genetic methods (Hosler *et al.*, 1993).

[3] Three-dimensional structures of terminal oxidases and other biological macromolecules can be downloaded from RCSB Protein Data Bank (*http://www.rcsb.org/pdb*).

2.3.1 Subunit I

Subunit I is the largest and the most conserved (Saraste, 1990) subunit of CcO with a molecular weight of about 60 kDa (Table 2). It consists of 12 transmembrane helices without any large extramembrane domain (Fig. 5A, shown in yellow). The helices are not perpendicular to the membrane plane but tilted about 20-35^{o} with respect to the membrane normal. When viewed from the top (P-side), the 12 segments of subunit I form three semicircular arcs twisted anticlockwise, and arranged around a quasi-threefold axis of symmetry (Fig. 5B). Three pores (pores *A*, *B*, and *C*) are formed in the center of the arcs. Pore *B* houses the binuclear center (heme a_3 and Cu_B) of the oxidase and includes the proton conductive K-channel that connects the binuclear center with the N-side of the membrane (see below). Pore *C* retains heme *a*; the remaining pore, *A* contains no cofactors but is the location of the proton conductive D-channel as well as a plausible pathway for oxygen delivery to the binuclear site (Riistama *et al.*, 1996).

Heme *a* is located in pore *C* at a depth of about $^{1}/_{3}$ of the membrane thickness from the P-side and is oriented perpendicular to the membrane plane such that its propionates are pointing towards the P-side of the membrane. In both reduced (S=0) and oxidized (S=$^{1}/_{2}$) states (Tweedle *et al.*, 1978; Babcock *et al.*, 1981) the heme iron is bound to four nitrogens of the porphyrin ring and to two conserved histidines of subunit I. The latter two histidine axial ligands of heme *a*: His_I 94(61) and His_I413(378) are located in helices II and X respectively (Shapleigh *et al.*, 1992; Iwata *et al.*, 1995; Tsukihara *et al.*, 1995); the bonds between the histidines and the heme iron hold the heme in the protein.

Biosynthesis of heme A is a sequential process (Fig. 4) that involves initial farnesylation of protoheme (heme B) at the 2-position (Saiki *et al.*, 1993) to form heme O. In the next step, the heme O product is modified by hydroxylation of the methyl group at 8-position of the porphyrin ring to formyl (Caughey *et al.*, 1975).

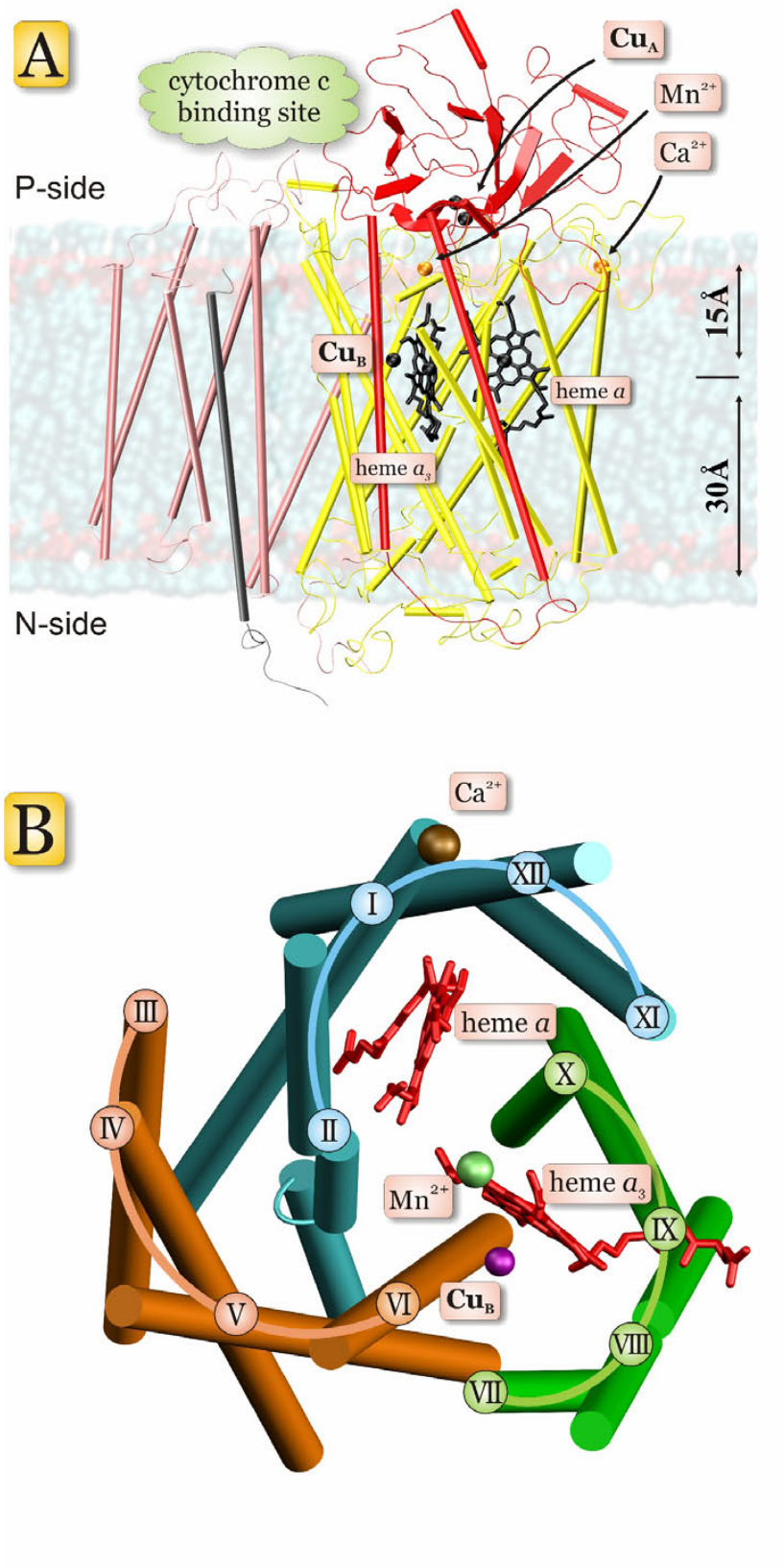

Figure 5. The structure of cytochrome *c* oxidase from *P. denitrificans* (PDB entry 1AR1). **A.** Organization of subunits and redox-active centers: subunit I is shown in yellow, subunit II in red, subunit III in pink, subunit IV in ice blue; hemes and coppers are shown in black (heme a_3 on the left and heme *a* on the right side). **B.** Top view of subunit I; only metal centers and transmembrane helices are shown. Helices form three semicircular arcs denoted A (orange), B (green), and C (blue).

The low-spin hemes in terminal oxidases are responsible for most absorption in the visible part of the spectrum. The decomposed oxidized spectrum of heme *a* has peaks at 426 nm (ε ~ 120 $mM^{-1}cm^{-1}$, Soret band) and 595 nm (ε ~ 19.5 $mM^{-1}cm^{-1}$, alpha band) (Vanneste, 1966). Absorption properties of heme *a* depend on the reduction state of the heme, making this center an easy target for optical spectroscopy. The reduced -*minus*- oxidized difference spectrum of heme *a*, produced by the ligand-binding method introduced by Horie and Morrison (1963), has a peak at 445 nm (ε ~ 57 $mM^{-1}cm^{-1}$), and a trough at 425 nm (ε ~ –41$mM^{-1}cm^{-1}$) in the Soret region as well as another peak at 605 nm (ε ~ 20.5 $mM^{-1}cm^{-1}$) in the alpha region (Vanneste, 1966). The absorption maximum at 605 nm in the reduced -*minus*- oxidized spectrum of heme *a* in CcO is quite unusual for low-spin A-type heme (Lemberg, 1962). This maximum is red shifted by about 15 nm compared to an isolated bis-imidazole heme A model compound (Callahan and Babcock, 1983) due to formation of a strong hydrogen bond between the formyl group of heme *a* and the neighboring $Arg_I54(38)$ (Kannt *et al.*, 1999; Riistama *et al.*, 2000b).

The second A-type heme is situated at about 13 Å (center-to-center distance) from heme *a* and is denoted as a_3. The plane of heme a_3 is also perpendicular to the membrane and its propionates point towards the P-side in a manner similar to heme *a*. The two hemes face each other at an angle of 104-108° (Iwata *et al*, 1995; Tsukihara *et al.*, 1995). Heme a_3 is a high-spin heme in both the fully-reduced *ferrous* state (S=2) (Babcock *et al.*, 1976) and the resting *ferric* state ($S=^5/_2$) (Babcock *et al.*, 1981). Depending on conditions, heme a_3 can be five- or six- coordinated (Babcock *et al.*, 1981): the permanent bonds of the heme iron include four bonds with nitrogens of the porphyrin ring and one extra bond with the conserved $His_I411(376)$ (Stevens and Chan, 1981; Shapleigh *et al.*, 1992; Iwata *et al.*, 1995; Tsukihara *et al.*, 1995) that fixes the heme in the protein. This five-fold coordination of the heme iron leaves one side of the heme empty and available for binding of ligands such as dioxygen, carbon monoxide, azide, hydroxide ions, water molecules *etc.* The binding of ligands can modulate the spin state of this heme: for example, binding of cyanide to the ferric form changes the spin-state of heme a_3 from high to low ($S=^1/_2$) (Babcock *et al.*, 1981).

The absolute absorption spectrum of oxidized heme a_3 has a highly pronounced maximum in the Soret region at 414 nm (ε ~ 81 $mM^{-1}cm^{-1}$) and low intensity bands in the alpha region including a maximum at around 600 nm and a beta-band at around 560 nm (Vanneste, 1966). The main absorption changes in the reduced -*minus*- oxidized spectrum of heme a_3 also correspond to the

Soret region – peak at 444 nm (ε ~112 $mM^{-1}cm^{-1}$) and trough at 411 nm (ε ~ -50 $mM^{-1}cm^{-1}$), whereas the absorbance in the alpha region is much less pronounced with a single peak at around 601 nm (ε ~ 4.9 $mM^{-1}cm^{-1}$) and a shoulder at around 579 nm (ε ~ 3.9 $mM^{-1}cm^{-1}$) (Vanneste, 1966; Liao and Palmer, 1996). In addition, oxidized heme a_3 has one extra band, detected at around 655 nm (*charge-transfer* band) attributed to charge-transfer to a ligand of heme a_3 (Beinert *et al.*, 1976; Shaw *et al.*, 1978; Mitchell *et al.*, 1991).

The last redox metal center of subunit I is ~5 Å away from heme a_3 iron and is formed by a copper atom denoted as Cu_B. Together, heme a_3 and Cu_B form the binuclear catalytic center of the oxidase (Fig. 6), where all the chemistry of dioxygen splitting and reduction to water takes place. The distance between the heme a_3 iron and Cu_B seems to be the same in both reduced and oxidized states of the enzyme (Harrenga and Michel, 1999) or fluctuates slightly in a range of about 0.1-0.3 Å (Yoshikawa *et al.*, 1998; Tsukihara *et al.*, 2003). The oxidized Cu_B is a tetragonal center (Fann *et al.*, 1995); it has three permanent histidine imidazole ligands, identified by both genetic (Hosler *et al.*, 1993) and X-ray spectroscopic approaches (Iwata *et al.*, 1995; Tsukihara *et al.*, 1995; Ostermeier *et al.*, 1997), as well as one mobile oxygen ligand with exchangeable proton/protons (Fann *et al.*, 1995). The imidazole ligands originate from $His_I276(240)$ in helix VI, and from $His_I325(290)$ and $His_I326(291)$ both located in the loop between helices VII and VIII.

Due to an extremely low extinction coefficient, the absorbance spectrum of Cu_B is still unknown, though it is possible to obtain information about the redox state of this center by optical spectroscopy. Existing data indicate that the appearance of the *charge-transfer* band (655 nm) requires both components of the binuclear center to be in the oxidized state; so reduction of Cu_B, when heme a_3 is oxidized, will induce decay in the intensity of the *charge-transfer* band (Beinert *et al.*, 1976; Mitchell *et al.*, 1991). The other technique that can be used to observe the Cu_B center is electron paramagnetic resonance (EPR) which spectroscopy is sensitive to molecules and ions with unpaired electron spins. Since in the oxidized (cupric) state the copper atom contains one unpaired electron in the highest orbital, in theory the redox state of Cu_B can be followed by EPR. Unfortunately, the presence of the heme a_3 iron in proximity to the copper atom results in a strong antiferromagnetic interaction between these two centers making them both EPR silent (van Gelder and Beinert, 1969) in most situations. Only when one or the other of them is reduced, or the magnetic coupling has been broken by other means, does the EPR signal from the oxidized center appear. For example, in a reaction of the fully-reduced CcO with

dioxygen done at low-temperature (Reinhammar et al., 1980; Karlsson and Andreasson, 1981; Karlsson *et al.*, 1981; Blair *et al.*, 1985; Morgan *et al.*, 2001), or by decoupling of the heme a_3-Cu_B pair using techniques including: ligand binding, gamma radiation, saturated ammonium sulfate treatment, incubation in some detergents, *etc.* (Pezeshk *et al.*, 2001). The EPR signal of Cu_B exhibits the four characteristic hyperfine peaks of a type 2 cupric center and is centered near g = 2.25.

Another important structure identified in CcO consists in the covalent bond between $His_I276(240)$ and $Tyr_I280(244)$ (Fig. 6). Because of this connection the 3 histidines and the tyrosine form a conjugated π-electron system around the Cu_B center. In addition to crystallographic studies, the existence of the histidine-tyrosine cross-link was also confirmed by protein sequencing and mass-spectroscopic analysis of CcO from several species (Buse *et al.*, 1999; Rauhamäki *et al.*, 2006). Formation of this bond could considerably reduce the pK_a of the tyrosine (Yoshikawa *et at.*, 1998; McCauley *et al.*, 2000), allowing it to participate in the oxygen reduction process by donating both the proton and the fourth electron required for the reaction, and forming a tyrosine radical (Proshlyakov et al., 1998; Proshlyakov et al, 2000).

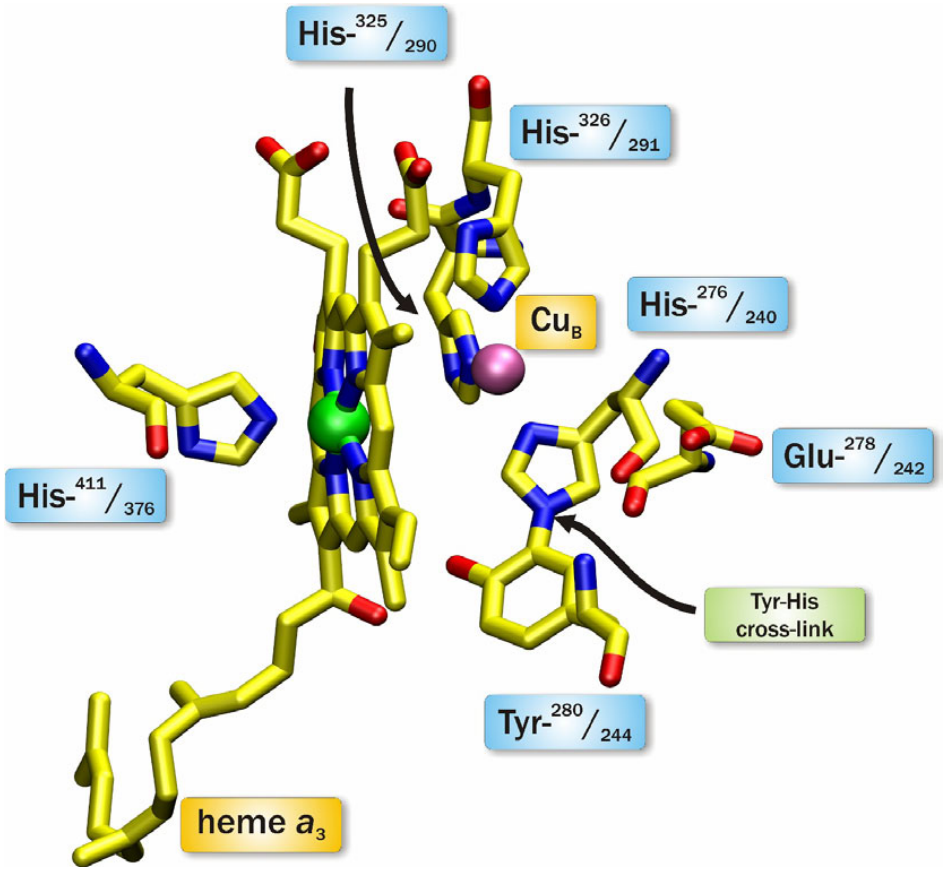

Figure 6. Catalytic center of cytochrome *c* oxidase (PDB entry 1V54): high-spin heme a_3, Cu_B, histidine-tyrosine cross-linked structure, and their ligands. Amino-acid numbering from *P. denitrificans* / bovine enzymes.

In addition to the redox-active centers, subunit I also contains tightly bound non-redox active metal centers. A Mg^{2+}/Mn^{2+} binding site is located at the interface between subunits I and II, approximately half way between the heme a_3 and Cu_A centers. The metal atom is ligated to $His_I403(368)$, $Asp_I404(369)$, $Glu_{II}198(218)$, and to three water molecules (Hosler *et al.*, 1995; Ostermeier *et al.*, 1997; Tsukihara *et al.*, 1995; Yoshikawa *et al.*, 1998; Svensson-Ek *et al.*, 2002). In mitochondrial CcO this site is occupied by magnesium (Einarsdóttir and Caughey, 1985; Tsukihara *et al.*, 1995), whereas in bacterial oxidases it can be partially substituted by a manganese atom (Seelig *et al.*, 1981). The function of this metal site is unknown, but it was shown that Mn^{2+} is located in the expulsion pathway for the waters that are produced in the binuclear center of the oxidase (Schmidt *et al.*, 2003). Site-specific mutagenesis of the metal-ligating residues did not cause either a change in pumping efficiency or a significant decrease in the enzymatic activity (Hosler *et al.*, 1995; Fetter *et al.*, 1995). In addition, proton-translocating quinol oxidases lack this center (Abramson *et al.*, 2000) without any effect on the proton translocation ratio (Puustinen *et al.*, 1989; Verkhovskaya *et al.*, 1992). However, since both subunits I and II have a number of negatively charged residues at their common interface, the Mg^{2+}/Mn^{2+} site may be important for their stabilization.

Another non-redox active metal site has been found in a loop between helices I and II close to the P-side of the membrane. The identity of the metal ion in this center is not completely clear: based on ligand coordination pattern it has been predicted to be occupied by sodium in mitochondrial oxidases (Yoshikawa *et al.*, 1998) and by calcium in bacterial ones (Ostermeier *et al.*, 1997; Svensson-Ek *et al.*, 2002). At the same time, cation-binding experiments suggest that in the mitochondrial CcO this site can reversibly bind either calcium or sodium (Kirichenko *et al.*, 1998), whereas in bacterial oxidases this site contains only a tightly bound calcium that cannot be removed even by an excess of chelating agents such as EGTA (ethyleneglycol-bis-(β-aminoethyl either)*N,N'*-tetra-acetic acid) (Riistama *et al.*, 1999; Pfitzner *et al.*, 1999; Lee *et al.*, 2002). The role of the tightly bound Ca^{2+} may be in structural stabilization of the bacterial oxidases (Lee *et al.*, 2002).

2.3.2 Subunit II

Subunit II is another CcO subunit, which contains redox active cofactors. It has a molecular weight of about 27 kDa (Table 2), and forms two transmembrane helices interacting with subunit

Table 2. Subunit composition of terminal oxidases in mitochondria and bacteria.

Subunit[1]	bovine (heart) aa_3			*P. denitrificans* aa_3	
	M_r[2]	composition	encoded by	M_r[3]	composition
I	56993	12 α-helices	mitochondria	62500	12 α-helices
II	26049	2 α-helices	mitochondria	27999	2 α-helices
III	29918	7 α-helices	mitochondria	30671	7 α-helices
IV	17153	1 α-helix	nucleus	5364	1 α-helix
Va	12434	at the N-side	nucleus		
Vb	10670	at the N-side	nucleus		
VIa	9418	1 α-helix	nucleus		
VIb	10068	at the P-side	nucleus		
VIc	8480	1 α-helix	nucleus		
VIIa	6234	1 α-helix	nucleus		
VIIb	6350	1 α-helix	nucleus		
VIIc	5541	1 α-helix	nucleus		
VIII	4962	1 α-helix	nucleus		

[1] Mitochondrial subunit nomenclature from Kadenbach and Merle, 1981;

[2] Molecular masses for bovine aa_3 from Capaldi, 1990;

[3] Haltia *et al.*, 1994; Witt and Ludwig, 1997.

I (Figure 5A) and a large C-terminal hydrophilic globular domain at the P-side of the membrane (Iwata *et al.*, 1995; Tsukihara *et al.*, 1996). The redox active copper center, conventionally referred to as Cu_A, is formed by two copper atoms. There has been a long discussion in the oxidase field concerning the type and number of copper atoms in the Cu_A center and only at the beginning of the 1990s this issue was finally resolved (Kroneck *et al.*, 1990; van der Oost *et al.*, 1992; Antholine *et al.*, 1992; Malmström and Aasa, 1993; Kelly *et al.*, 1993; Lappalainen *et al.*, 1993). The Cu_A center in the oxidized state of the enzyme was found to be in mixed-valence configuration that can be formally represented as $[Cu^{1.5+}\text{-}Cu^{1.5+}]$. Upon reduction Cu_A holds an electron by sharing it between both copper atoms. This redox center is situated in the globular domain almost on the border with subunit I. As was shown by site-directed mutagenesis (Kelly *et al.*, 1993) and confirmed later by X-ray crystallography (Iwata *et al.*, 1995; Tsukihara *et al.*, 1995), Cu_A is ligated to two cysteines ($Cys_{II}216(196)$ and $Cys_{II}220(200)$), two histidines

($His_{II}181(161)$ and $His_{II}224(204)$), one methionine ($Met_{II}227(207)$) and one carbonyl oxygen of $Glu_{II}218(198)$.

The redox state of Cu_A can be followed by optical absorbance spectroscopy. The spectrum of oxidized Cu_A has two clear maxima: a broad peak at around 820 nm ($\varepsilon \sim 1.6$ $mM^{-1}cm^{-1}$) and a rather sharp peak at 480 nm ($\varepsilon \sim 3.0$ $mM^{-1}cm^{-1}$) with a shoulder at about 530 nm (Lappalainen *et al.*, 1993; Jasaitis *et al.*, 2001). Even though the extinction coefficient of the latter peak is higher, the practical characteristic wavelength of Cu_A in the intact CcO is in the region of around 820 nm, where hemes do not absorb, thus making it possible to follow redox changes of Cu_A only. In addition to optical absorbance spectroscopy, the EPR technique has proved to be a valuable tool for studies of Cu_A. Oxidized Cu_A possesses a strong and characteristic EPR signal in the $g \sim 2$ region (Beinert *et al.*, 1962; Aasa *et al.*, 1976) measured at the temperature of liquid nitrogen and lower.

2.3.3 Subunit III

Subunit III is the biggest subunit of CcO (Fig. 5A) that has no redox cofactors. It has a molecular weight of about 30 kDa (Table 2), and consists of seven transmembrane helices without any extensive extramembrane domain. The helices of subunit III are arranged into two bundles: the first one is formed by helices I and II, and the other by helices from III to VII (Iwata *et al.*, 1995; Tsukihara *et al.*, 1996). The bundles of helices are tilted with respect to each other forming a large V-shaped cleft joined at the N-side of the membrane. Subunit III is in side-to-side contact with the helices of pore A of subunit I.

The function of this subunit is unknown: it contains no prosthetic groups, and, it is not involved in proton pumping as shown using a two-subunit enzyme preparation from *P. denitrificans* reconstituted into liposomes (Solioz *et al.*, 1982; Hendler *et al.*, 1991) and by a mutagenesis study (Haltia *et al.*, 1991). However, it might be involved in the stabilization of the mature oxidase and in ensuring correct assembly of the enzyme (especially at the final folding step of subunit I), including structural adjustment of the heme centers (Haltia *et al.*, 1989). At the same time, the V-shaped cleft is located at the mouth of the oxygen conducting channel and may secure a constant flux of oxygen into the catalytic center (Riistama *et al.*, 1996, see below). It is also possible that the membrane-anchored cytochrome c_{552}, which is a physiological electron donor for CcO from *P. denitrificans* (Berry and Trumpower, 1985), might use this cleft for

binding and placing itself in an appropriate position for electron transfer to Cu_A (Iwata *et al.*, 1995).

2.3.4 Other Subunits

In addition to the three core subunits, heme-copper terminal oxidases can have extra subunits. CcO from *P. denitrificans* has one additional subunit (Haltia *et al.*, 1994; Iwata *et al.*, 1995) with a molecular weight of about 5 kDa (Witt and Ludwig, 1997). It has one transmembrane helix, which is in contact with all other subunits. The function of this subunit is unknown: deletion of its gene has no effect on either protein integrity or enzymatic and spectral properties of the oxidase (Witt and Ludwig, 1997).

In mammalian CcO the three mitochondrially-encoded core subunits (homologous to the three main subunits of the bacterial enzyme) are supplemented by ten additional subunits, which are encoded by nuclear DNA (Table 2). Seven out of ten nuclear encoded subunits consist of one transmembrane helix each, whereas subunits Va, Vb and VIb are small globular proteins. Subunits Va and Vb are bound to the oxidase on the matrix side of the protein, while subunit VIb is bound on the intermembrane side. Because none of the nuclear encoded subunits are associated with the active site, it is quite unlikely that they are important in the functional mechanism of CcO. However based on the fact that binding sites for ATP/ADP (Tsukihara *et al.*, 1996; Kadenbach *et al.*, 2000), protein kinase A (Yang *et al.*, 1998), and 3,5-diiodothyronine (Arnold *et al.*, 1998) have been found within some of them, it has been assumed that the nuclear encoded subunits have a regulatory function. The role of these subunits in the regulation of the enzymatic activity is also supported by the presence of tissue-specific isoforms in mammals (Kadenbach *et al.*, 2000). Studies on yeast subunit VIb, which exhibits high amino acid sequence identity to bovine CcO, show that this subunit can be important during assembly of the oxidase, though it can be removed from the mature enzyme without any effect on activity (LaMarche *et al.*, 1992). The crystal structure of bovine CcO indicates that subunits VIa and VIb might be involved in stabilization of a dimer state of the protein (Tsukihara *et al.*, 1996). In addition, mitochondrial oxidase contains Zn^{2+}, which is tightly bound to subunit Vb (Tsukihara *et al.*, 1995&1996).

2.4 Pathways

The chemical reaction of oxygen reduction to water, which triggers proton translocation across the membrane, occurs at the binuclear center in the middle of the protein and requires both delivery of substrates (*i.e.* electrons, protons, and oxygen) and release of products (water). All these aforementioned reactants, which are necessary for the functioning of the oxidase, are transported to the catalytic site through specialized pathways. These pathways have been identified and they can be divided into electron-, proton- and oxygen- transfer structures.

2.4.1 Electron-transfer Pathways

The transfer of electrons within proteins is a quite complicated process defined by a number of factors. According to electron-transfer theory (Marcus and Sutin, 1985) the rate of electron transfer depends on the distance between donor and acceptor, the difference in their redox potentials, and the reorganization energy (*i.e.* the energy required to alter the equilibrium geometry of the initial state into the equilibrium geometry of the product). There are two main theories to describe the mechanism how the electron is transferred within a protein. In the first conceptualization (Gray and Winkler, 1996), electron tunneling is considered to occur specifically through bonds and can be modulated by conformational changes of the secondary structure of the protein. In contrast, the other theory (Moser *et al.*, 1992; Page *et al.*, 1999) postulates that efficient tunneling of electrons is not limited to any specially designed pathway within the protein, but rather occurs via multiple pathways through the protein medium; and in the simplest view it can be defined by edge-to-edge distance between donor and acceptor, modified by atomic density of the intervening medium.

The reduction of dioxygen to water requires four electrons. These electrons are donated one by one from water-soluble cytochrome *c*, which serves as one-electron mediator between the cytochrome bc_1-complex and CcO. Cytochrome *c* binds in a cleft between subunits II and III on the P-side of the membrane (Fuller *et al.*, 1981; Iwata *et al.*, 1995). This area is enriched in acidic residues (Iwata *et al.*, 1995; Tsukihara *et al.*, 1996) that could interact with positively charged lysines and arginines on the surface of cytochrome *c* (Ferguson-Miller *et al.*, 1978; Rieder and Bosshard, 1980; Bushnell *et al.*, 1990). Thus, it is likely that the formation of cytochrome *c* – CcO complex is defined mostly by electrostatic interactions between the proteins; this is also supported by the fact that there is a strong dependence of the reaction of

reduced cytochrome *c* with the oxidase on the ionic strength of the medium (Antalis and Palmer, 1982; Hazzard *et al.*, 1991; Witt *et al.*, 1998; Zhen *et al.*, 1999). However, it cannot be excluded that complex formation is additionally modulated by hydrophobic forces (Pelletier and Kraut, 1992). As soon as cytochrome *c* binds to the oxidase, the electron is rapidly transferred via the highly conserved $Trp_{II}121(104)$ (Witt *et al.*, 1998; Zhen *et al.*, 1999) to the primary electron acceptor – the bimetallic copper center, Cu_A (Kobayashi *et al.*, 1989; Hill, 1991). The rate of electron transfer in this process has been found to be of the order of $0.6 - 1 \times 10^5$ s^{-1} (Hill, 1991; Hill, 1994; Geren *et al.*, 1995).

The Cu_A center is situated near the membrane surface on the P-side of the membrane, while all other redox centers are buried at an equal depth, approximately $^1/_3$ (13 Å) of the membrane thickness below the membrane surface from the P-side (Iwata *et al.*, 1995; Tsukihara *et al.*, 1995). The centre-to-centre distance between Cu_A and the iron atom of heme *a* is 19.5 Å and this is only 2.6 Å closer than the distance between Cu_A and the iron atom of heme a_3 (22.1 Å). However despite such similarity in distances, the preference in electron transfer from Cu_A is completely biased towards heme *a*. The reason for this effect may be purely thermodynamic. The electron transfer from Cu_A to heme *a* is not coupled to proton uptake to compensate the negative charge at the heme *a*; at the same time, the midpoint redox potential of heme a_3 without protonation is far too low to permit electron transfer (Mitchell and Rich, 1994; Verkhovsky *et al.*, 2006); thus the rate of heme a_3 reduction may be limited by slow proton uptake for charge compensation (Verkhovsky *et al.*, 1995; Brzezinski, 1996), thereby leading to the observed results.

From electron injection experiments, the rate of electron equilibration between Cu_A and heme *a* is estimated to be about 1.8×10^4 s^{-1} in mitochondrial (Kobayashi *et al.*, 1989; Nilsson, 1992; Zaslavsky *et al*, 1993; Winkler *et al.*, 1995) and about 1.1×10^5 s^{-1} in bacterial oxidases (Konstantinov *et al.*, 1997; Zaslavsky *et al.*, 1998; Verkhovsky *et al.*, 2001b; Papers III&V). The same equilibration, measured by perturbed equilibrium methods (see sections 4.1&5.2), has similar rates for the mitochondrial enzyme (Morgan *et al.*, 1989; Oliveberg and Malmström, 1991; Verkhovsky *et al.*, 1992; Jasaitis *et al.*, 1999), while in bacteria it seems to be three-four fold slower ~ 2.8×10^4 s^{-1} (Ädelroth *et al*, 1995; Paper II).

Heme *a* serves as a donor of electrons to the heme a_3-Cu_B center. The planes of the two hemes are perpendicular to the membrane, forming an interplanar angle of 104-108°, with a minimal

edge-to-edge distance between the hemes of about 4.7 Å (Iwata *et al.*, 1995; Tsukihara *et al.*, 1995). The measured rate of electron equilibration between heme *a* and heme a_3 varies significantly, depending on the particular circumstances under which the measurements are made. When the electron is delivered into the oxidized enzyme from reduced cytochrome *c*, the equilibrium is reached with a time constant of the order 0.3 - 1.0 s (Antalis and Palmer, 1982); alternatively, when fully-reduced oxidase reacts with dioxygen, electron equilibration is much faster and has a time constant of about 30 μs (Hill, 1991; Verkhovsky *et al.*, 1994). But the fastest rate of electron equilibration between the hemes can be measured after CO photodissociation from the mixed-valence (two-electron reduced) enzyme. In this case, a phase with a time constant of 3-5 μs was identified and assigned to electron transfer from heme a_3 to heme *a* (Oliveberg and Malmström, 1991; Verkhovsky *et al.*, 1992; Einarsdóttir *et al.*, 1995; Ädelroth *et al*, 1995). However the rate of this process is still at least three orders of magnitude slower than predicted by electron transfer theory (Moser *et al.*, 1992; Page *et al.*, 1999), where the expected time constant of electron tunneling between these two heme centers is estimated to be in the nanosecond time domain. Recently, based on detailed analysis of the "photolysis" spectra of the CO-bound fully-reduced and mixed-valence states, measured with submicrosecond time resolution, it was proposed that in mixed-valence state about 20% of heme a_3 oxidation occurs faster than 3 μs, and presumably faster than 40 ns (Verkhovsky *et al.*, 2001a). Later this proposal was confirmed by sensitive pump-probe transient absorbance spectroscopy with femtosecond time resolution (Pilet *et al.*, 2004). Thus, dissociation of CO from the binuclear center induces an initial phase of ultra-fast electron equilibration between the hemes with a time constant of about 1.2 ns, followed by a slower equilibration phase with a time constant of 3 μs, which is possibly determined by the kinetics of CO dissociation from the Cu_B center (Verkhovsky *et al.*, 2001a; Pilet *et al.*, 2004). Such a large magnitude of difference in the observed rates of electron equilibration between the hemes is attributed to possible structural rearrangement of the protein, or to coupling of electron transfer to protonation or ligand state changes of neighboring groups (Verkhovsky *et al.*, 1995; Brzezinski, 1996; Verkhovsky *et al.*, 2001a; Pilet *et al.*, 2004).

2.4.2 Proton-transfer Pathways

Since the redox centers of the oxidase are buried within the protein they have no direct contact with the aqueous phase. However, maintenance of high rates of respiration requires both fast proton delivery to the catalytic center and corresponding fast proton translocation across the membrane. It should be noted that the proton transfer pathways in CcO have been much less investigated than the electron transfer pathways. The unstructured protein medium itself cannot facilitate efficient proton delivery towards the binuclear center, or across the membrane, and in order to overcome this limitation the oxidase has specialized proton-conductive structures. It is proposed that these structures are based on chains of hydrogen bonds between hydrogen-bonding protein side groups (polar and/or protonatable) and water molecules, where the proton is transferred by a Grotthuss type mechanism (de Grotthuss, 1806&2006; Nagle and Morowitz, 1978; Agmon, 1995). In this mechanism the excess proton on a hydronium ion is transferred to an acceptor water molecule by means of O-H covalent bond breakage in the donor molecule, and its reforming in the acceptor as a result of proton exchange between these two molecules (Fig. 7). After such proton hopping from donor to acceptor, the whole hydrogen-bonded chain is aligned in the wrong direction for further transfers and has to be reoriented. Only after reorientation the next proton can be transferred in the same direction as the previous one.

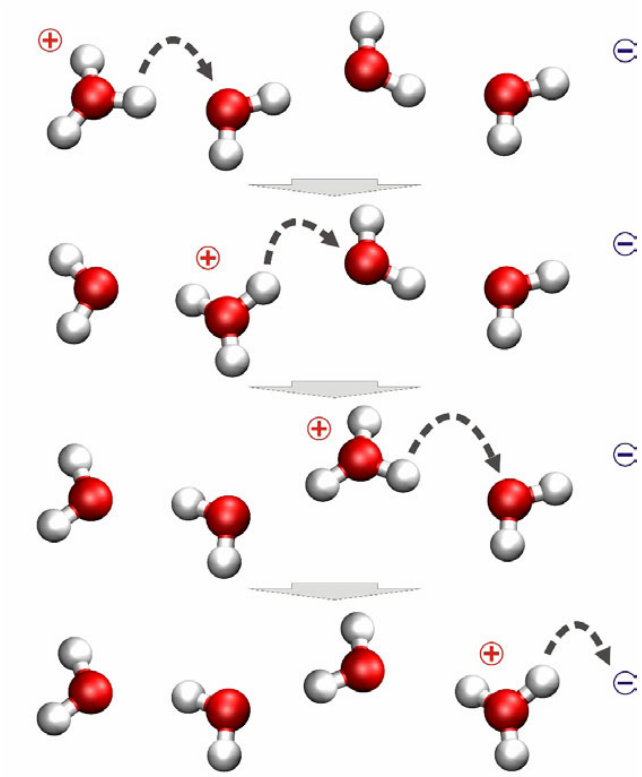

Figure 7. Schematics of the Grotthuss mechanism.

At least two proton-conductive channels have been identified by site-directed mutagenesis (Hosler *et al.*, 1993; Thomas *et al.*, 1993ab; Fetter *et al.*, 1995) and later confirmed by X-ray spectroscopy (Iwata *et al.*, 1995; Tsukihara *et al.*, 1996; Abramson *et al.*, 2001; Svensson-Ek *et al.*, 2002). Both channels are situated in subunit I and lead from the N-side of the membrane towards the catalytic center of the oxidase (Fig. 8).

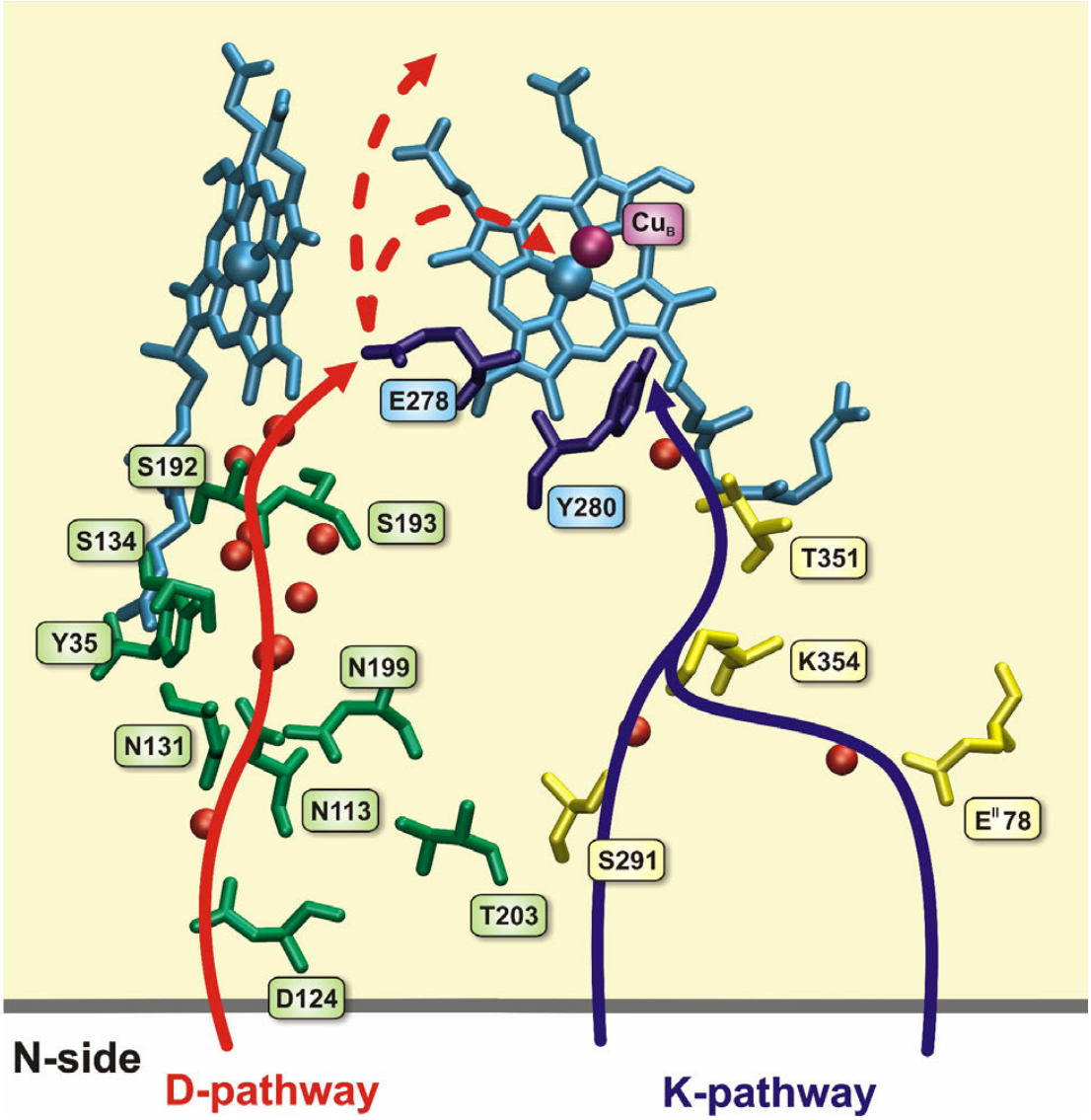

Figure 8. Proton conducting pathways together with the redox centers heme *a*, heme a_3, and Cu_B in cytochrome *c* oxidase (PDB entry 1AR1). The red spheres are structurally identified water molecules (based on the bovine 1V54 x-ray structure). *P. denitrificans* amino-acid numbering.

One of these is the K-pathway, named after the highly conserved lysine 354_I(319) (Hosler *et al.*, 1993; Thomas *et al.*, 1993b), which is situated approximately halfway through the channel. This pathway starts with either Ser_I291(255) (Iwata *et al.*, 1995; Tsukihara *et al.*, 1996) or $Glu_{II}78$(62) (Kannt *et al.*, 1998; Ma *et al.*, 1999; Brändén *et al.*, 2002) and continues through conserved residues Lys_I354(319), Thr_I351(316), towards the hydroxyethyl farnesyl side chain of heme a_3 and Tyr_I280(244), in the proximity to the binuclear center. Tyr_I280 at the end of the K-pathway is covalently linked to His_I276(240) by post-translational modification, and is assumed to be involved in oxygen reduction catalysis. The importance of Tyr_I280 is supported by site-directed mutagenesis studies, in which all mutational substitutions for this tyrosine result in complete elimination of oxidase activity (Hosler *et al.*, 1993; Thomas *et al.*, 1994; Pfitzner *et al.*, 1998). Two or three tightly bound water molecules can be found in this pathway in the X-ray structures.

One water molecule is situated between Thr_I351 and the hydroxyl group of the hydroxyethyl farnesyl side chain of heme a_3, another between Ser_I291 and Lys_I354, and finally a possible third between $Glu_{II}78$ and Lys_I354 (in 1V54, 1V55, Table 1). The amino acid residues of the K-pathway are connected by hydrogen bonds; however this connection seems to be interrupted by a large hydrophobic gap between Lys_I354 and Thr_I351, where no water molecules have been found so far. It is proposed that this gap might be bridged by a movement of lysine residue (Hofacker and Schulten, 1998).

The other channel, named D after the highly conserved $Asp_I124(91)$ (Thomas *et al.*, 1993a; Fetter *et al.*, 1995; Pfitzner *et al.*, 1998), that is situated near the surface of the enzyme on the N-side. Asp_I124 together with $Thr_I203(167)$ and $Asn_I199(163)$ form a mouth that leads via polar residues $Asn_I113(80)$, $Asn_I131(98)$, $Tyr_I35(19)$, $Ser_I134(101)$, $Ser_I192(156)$, $Ser_I193(157)$ and crystallographically identified bound water molecules to $Glu_I278(242)$, which is an important residue for proton pumping (Svensson-Ek *et al.*, 1996; Ädelroth *et al.*, 1997; Verkhovskaya *et al.*, 1997; Konstantinov *et al.*, 1997). The mode of proton translocation after Glu_I278 is not clear because no proton connectivity beyond this residue has been detected in the crystallographic structures. However, it is proposed that this space is occupied by three to four mobile water molecules (Riistama *et al.*, 1997; Zheng *et al.*, 2003) that form a proton conductive pathway directing protons either to the Δ-propionate of heme a_3 for pumping or to the binuclear center for water formation (Hofacker and Schulten, 1998; Wikström *et al.*, 2003). Release of the pumped proton takes place through the highly hydrophilic domain above the heme groups. This area contains an extended hydrogen-bonded network of charged and polar amino acid residues, the propionates of the hemes, bound metal centers and water molecules, and presumably is involved in the transfer of pumped protons towards the P-side of the membrane (Iwata *et al.*, 1995; Tsukihara *et al.*, 1996; Ostermeier *et al.*, 1997). Based on results of site-directed mutagenesis studies it is believed that the exit channel for pumped protons may start at the conserved residues $Arg_I473(438)$ and $Arg_I474(439)$ (Puustinen and Wikström, 1999; Brändén *et al.*, 2005), which are hydrogen-bonded to the Δ-propionates of the hemes, and then continue through the chains of mobile water molecules.

The presence of two independent proton conducting pathways in the oxidase was suggested immediately after the discovery of proton pumping (Wikström *et al.*, 1977; Artzatbanov *et al.*, 1978). The initial hypothesis was appealingly simple: the presence of two channels in the oxidase was explained in terms of a different role for each channel in the proton transfer

mechanism. It was proposed that the D-channel is responsible for translocation of "pumped" protons, while the K-channel is used for uptake of "chemical" protons for water formation. However, this idea turned out to be incorrect, and more recent results have indicated more complicated mechanism. The D-channel is involved in the transfer of all four "pumped" protons and two "chemical" protons used in the oxidative part of the catalytic cycle (Konstantinov *et al.*, 1997; Ädelroth *et al.*, 1997), while the K-channel is responsible for the uptake of another two "chemical" protons during the reductive part of the cycle (Hosler *et al.*, 1996; Konstantinov *et al.*, 1997; Ädelroth *et al.*, 1998a; Wikström *et al.*, 2000; Paper III). In addition, Lys_I354 may also be involved in the oxidative part of the cycle (Brändén *et al.* 2001) providing charge compensation upon electron transfer from heme *a* to the binuclear site and formation of the **P** intermediate.

Interestingly, based on structural analysis of bovine heart CcO in the reduced and oxidized states, one additional proton-conductive pathway has been proposed (Tsukihara *et al.*, 1996; Yoshikawa *et al.*, 1998). This so-called H-channel, named after the partially conserved residue His_I413^{bovine}, begins at the N-side of the membrane and leads to Asp_I51^{bovine} on the P-side. Depending on the reduction state of heme *a*, Asp_I51^{bovine} changes its conformation from protonic equilibrium with the matrix space, when heme *a* is oxidized, to equilibrium with the intermembrane space when heme *a* is reduced, providing a gate for proton translocation across the membrane. Replacements, using a bovine gene expression system, of amino acid residues involved in the formation of this channel (like Asp_I51 to asparagine) abolish pumping without impairment of catalytic activity (Tsukihara *et al.*, 2003). However, it seems that this channel (if it exists) is strictly a property of mammalian oxidases, since bacterial oxidases lack some of the key residues involved in its formation, and extensive mutations of other residues in the proposed area have shown no functional significance for proton translocation (Pfitzner *et al.*, 1998; Lee *et al.*, 2000). Thus, either the mechanism of proton pumping in the mammalian CcO is different from the bacterial one, which seems quite unlikely due to their similar properties and structures, or the H-channel has another function, for example charge compensation upon heme *a* reduction.

2.4.3 Oxygen-transfer Pathways

As a small, uncharged molecule, dioxygen can easily permeate membranes and on a first sight should be able to reach the catalytic site of the oxidase even without any specific route, through loosely packed regions, using conformational fluctuations of the protein. However, the rate of

such uncontrolled diffusion is slow, and most likely insufficient to maintain normal catalytic activity of the oxidase. Thus, the protein must have certain structures that function as channels for oxygen delivery to the reaction center. And indeed, analysis X-ray crystal structures (Tsukihara *et al.*, 1996; Svensson-Ek *et al.*, 2002), supplemented by experimental (Riistama *et al.*, 1996&2000a; Salomonsson *et al.*, 2004) and theoretical examinations (Hofacker and Schulten, 1998), reveals from one (in *P. denitrificans*) to three (in bovine) highly hydrophobic passages from the middle of the membrane bilayer, where oxygen is concentrated, towards the active site. Interestingly, even a single amino-acid mutation can dramatically influence the binding of oxygen, causing partial (in Val_I279 to isoleucine mutant, Riistama *et al.*, 1996&2000a) or even complete inhibition (in Gly_I283 to valine mutant of *R. sphaeroides*, Salomonsson *et al.*, 2004).

2.5 Intermediates of the Catalytic Cycle

In contrast to most cell proteins, the redox centers of CcO are colored and characterized by distinct optical spectra in oxidized and reduced states, and mainly because of this our basic description of the intermediates of the catalytic cycle was obtained by optical absorbance spectroscopy. At the same time, for a deeper understanding of internal processes in the catalytic cycle the optical studies must often be supplemented with other measurements, such as resonance Raman studies of intermediates, determination of potential generation across the membrane, measurements of proton uptake and release, *etc.*

Approximately up to ten intermediates of the catalytic cycle have been identified (Fig. 9); some of them are more or less stable, while the others appear only for a fraction of a millisecond. It should be noted that the letter abbreviations accepted in the literature for the different states reflect only the state of the binuclear site and do not specify the redox states of heme *a* and Cu_A.

*Fully oxidized **O**-state.* The enzyme after purification is in the fully-oxidized "as prepared" state, where all redox centers of the protein are oxidized and the enzyme cannot react with dioxygen. Sometimes, depending on the details of the purification protocol, it may contain a subpopulation in the **E** (one-electron reduced) state. The enzyme in the **O** state is often includes populations of different substates that differ with respect to the ligation state of the high-spin heme. These substates can roughly be divided into two groups based on their ability to react with cyanide (Baker *et al.*, 1987; Moody *et al.*, 1991a). One - the "slow" form has a maximum in the Soret

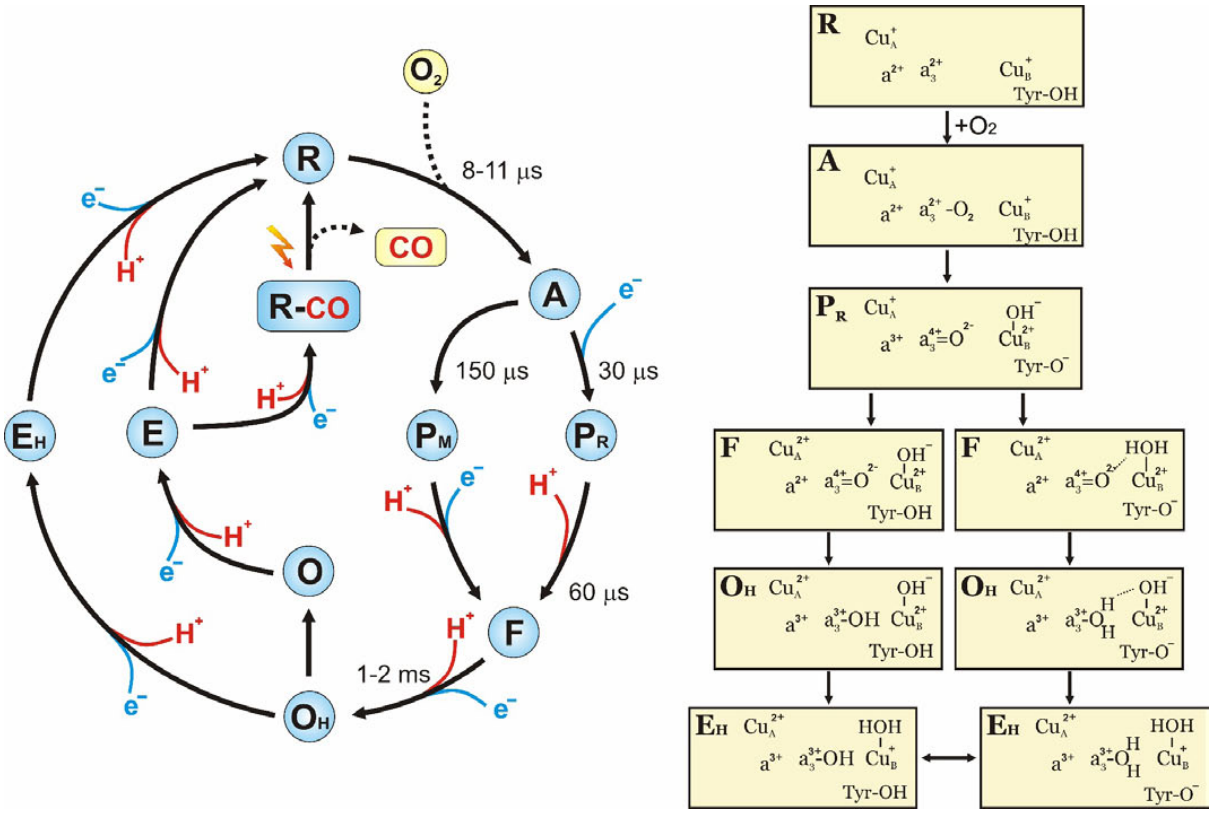

Figure 9. The catalytic cycle of cytochrome *c* oxidase supplemented with plausible structures of the intermediates. The definitive structure of the **F** state is still unclear and two possible configurations may be proposed.

region below 418 nm and is characterized by slow kinetics of cyanide binding to the oxidized heme a_3. The absorbance maximum of the other - "fast" - is several nanometers red-shifted; this form binds cyanide at least 100-fold more rapidly. The enzyme in the "slow" form can be obtained when the protein is incubated or purified in a low pH buffer (~6), especially in the presence of certain anions such as Br^-, $HCOO^-$, or Cl^- (Baker *et al.*, 1987; Moody *et al.*, 1991a). At the same time, the fully-oxidized "as prepared" state is often referred to as the "resting" form of the oxidase, and it can include both "slow" and "fast" forms. Reduction and re-oxidation (*pulsing*) of the "resting" oxidase produces the homogeneous population of the oxidized **O** state – the so-called "oxygen pulsed" form (Antonini *et al.*, 1977). The "pulsed" form is highly active and has properties very similar to the "fast" form, though most likely these forms represent different states of the enzyme discriminated by their ability to pump protons upon reduction (Verkhovsky *et al.*, 1999b; Paper III&V). Thus, the "pulsed" form is probably the same state as the $\mathbf{O_H}$ intermediate in the catalytic cycle (see below).

*One-electron reduced **E**-state.* In the **E** state an electron is shared between heme a_3 and Cu_B in the binuclear center. This state can be obtained in potentiometric titrations where it is characterized by the presence of a g = 6 EPR signal. This signal originates from the oxidized high-spin heme a_3 (when Cu_B is reduced) and the maximal amplitude of the g = 6 EPR signal (Wilson *et al.*, 1976) in a potentiometric redox titration would indicate maximal yield of the **E** state. Alternatively, it is possible to create **E** by several kinetic techniques such as flash-induced chemical photoreduction (FIRE) (Moody *et al.*, 1991b), or electron injection from RubiPy (Nilsson, 1992; Ruitenberg *et al.*, 2000; Verkhovsky *et al.*, 2001b). However it should be stressed that formation of the **E** state by the kinetic techniques takes seconds, due to extremely slow proton uptake to the binuclear center for charge compensation. Taking into account that the complete cycle of CcO occurs in a few milliseconds, it is rather unlikely that the **E** state is a natural state during catalytic turnover of the oxidase. Unlike hemoglobin or myoglobin one electron reduced CcO cannot bind either oxygen or carbon monoxide (Lindsay *et al.*, 1975; Malatesta *et al.*, 1990).

*Reduced **R**-state.* The **R** state is the state which is capable of dioxygen binding and can have from 2 to 4 electrons in the redox centers. Delivery of an electron alone into low dielectric media deep in the middle of the membrane, where three out of four enzyme redox centers are located, is energetically unfavorable, but can be enhanced when coupled with proton uptake. Indeed, Mitchell and Rich (1994) based on experimental determination of proton uptake upon reduction and binding of anions (azide, formate, fluoride, or cyanide) suggested an "electroneutrality principle", which postulates that reduction of the binuclear center is coupled to uptake of two protons for charge compensation. Complete reduction of the oxidase by 4 electrons is coupled to uptake of 2.1-2.4 H^+/CcO in *R. sphaeroides* and bovine oxidases (Mitchell & Rich, 1994; Capitanio *et al.*, 1997; Ädelroth *et al.*, 1998b). At least two of these protons are taken up via the K-pathway and most likely are used for water formation (Hosler *et al.*, 1996; Konstantinov *et al.*, 1997; Ädelroth *et al.*, 1998a; Wikström *et al.*, 2000; Paper III). Both fully-reduced and mixed-valence (two-electron reduced) oxidases can bind CO to heme a_3. Binding of CO to the binuclear center increases midpoint potentials of heme a_3 and Cu_B, and stabilizes their reduced form (Wilson & Nelson, 1982). Depending on the reduction level of the oxidase, two types of CO-bound compounds are defined: the fully-reduced CO-bound (*COFR*) form with all four redox centers in the reduced state and the mixed-valenced CO-bound (*COMV*) form, where only a_3 and Cu_B are reduced. Both forms, COFR and COMV, are widely used as starting points for studies of intermediates in the reaction cycle.

*Ferrous-oxy **A** intermediate.* As mentioned in the previous paragraph, the oxidase in the two-electron reduced state can already react rapidly with dioxygen producing the so-called compound **A**. Compound **A** is the first spectroscopically detectable intermediate, originally reported by Chance *et al.* (1975) in their low-temperature "triple-trapping" experiments, with a 591 nm peak and a 611 nm trough in the difference (**A** -*minus*- **R**) spectrum. At room temperature compound **A** is formed with a time constant of 8 μs at 1 mM oxygen concentration (Oliveberg *et al.*, 1989; Verkhovsky *et al.*, 1994) and has an absorbance maximum in the difference spectrum at 595 nm (Hill & Greenwood, 1983; Verkhovsky *et al.*, 1996a; Sucheta *et al.*, 1998). Similar to oxyhemoglobin and oxymyoglobin, the Raman spectrum of compound **A** (Varotsis *et al.*, 1989; Han *et al.*, 1990a) has a stretching mode at 568 cm^{-1} which characterizes the $Fe^{2+}_{a_3} - O_2$ structure of the binuclear center.

Peroxy intermediate, P_M. Compound **A** is unstable and in the case of the mixed-valence enzyme decays with τ ~150 μs (Hill & Greenwood, 1983; Oliveberg *et al.*, 1989) into the so-called peroxy (**P_M**)[4] intermediate, originally named compound **C** (Chance *et al.*, 1975). This intermediate is stable and the reaction stops here unless an additional electron enters the enzyme. This compound was named "peroxy" because it was thought that the oxygen-oxygen bond was still intact, and heme a_3 had a peroxy structure $Fe^{3+}_{a_3} - O^- - O^-$. But more recent examination by time-resolved resonance Raman (Proshlyakov *et al.*, 1998), and mass-spectrometry (Fabian *et al.*, 1999) clearly demonstrated that the oxygen-oxygen bond is already broken, and that heme a_3 is in the oxo-ferryl state ($Fe^{4+}_{a_3} = O$) with the other oxygen atom, spatially derived from O_2, bound to Cu_B as a hydroxide ion. The **P_M** state can also be formed directly in the reaction of the oxidized CcO at alkaline pH with stoichiometric amounts of H_2O_2 (Bickar *et al.*, 1982; Wrigglesworth, 1984; Vygodina & Konstantinov, 1989), where the resulting spectrum has characteristic peaks at 607 (ε_{607}-ε_{630} ~ 11 $mM^{-1}\cdot cm^{-1}$) and 570 nm in the **P_M**-*minus*-**O** difference spectrum. Cleavage of the O-O bond requires simultaneous transfer of four electrons to the molecule of dioxygen. Three of these electrons are donated from the metals of the binuclear center: one from Cu_B ($Cu_B^+ \rightarrow Cu_B^{2+}$) and two from the heme a_3 iron ($Fe^{2+}_{a_3} \rightarrow Fe^{4+}_{a_3}$), while the source of the fourth electron is still under debate. Presumably, the fourth electron is donated from one of the amino-acid residues in the proximity of the catalytic site. High-resolution X-ray crystallographic structures (Yoshikawa *at al.*, 1998; Ostermeier *et al.*, 1997) and biochemical

[4] Subscripts 'M'/'R' in **P** were introduced to distinguish the origins of two peroxy-oxygen intermediate forms: mixed-valence and fully-reduced, respectively.

analysis (Buse *et al.*, 1999) have revealed that the conserved residue $Tyr_I280(244)$, in the catalytic center, is covalently linked (Fig. 6) to one of the ligands of Cu_B ($His_I276(240)$). It has therefore been proposed to serve as a source of the remaining electron. In addition to electron transfer, O-O bond cleavage requires delivery of a proton. The reaction of COMV with O_2 occurs without external proton uptake (Oliveberg *et al.*, 1991), indicating that the required proton must be borrowed from one of the groups within the oxidase. At the same time, electrometric results show virtually no phase of potential generation upon the **R→P$_M$** reaction (Jasaitis *et al.*, 1999); thus it is most likely that the required proton is taken from a group which is very close to the catalytic center. Taken together, these findings suggest that it is reasonable to propose that Tyr_I280 provides both an electron and a proton for O-O bond splitting, producing a neutral tyrosine radical (Proshlyakov et al., 1998; Proshlyakov et al, 2000).

*Peroxy intermediate, **P$_R$**.* When the oxygen reacts with the fully-reduced oxidase, compound **A** relaxes in about 30-40 μs (Oliveberg *et al.*, 1989; Verkhovsky *et al.*, 1994) into another unstable peroxy intermediate (**P$_R$**). As was shown by optical absorbance (Hill 1991; 1994) and resonance Raman spectroscopy (Han *et al.*, 1990b), in a significant subpopulation of the enzyme, heme *a* becomes oxidized upon formation of **P$_R$**, while Cu_A stays reduced (Oliveberg and Malmström, 1992). Also, **P$_M$** and **P$_R$** have very similar kinetic difference spectra with peaks at 607 nm (Morgan *et al.*, 1996; Sucheta *et al.*, 1998), with the only significant difference being due to heme *a* oxidation in the latter, indicating similar structures of the catalytic site with the O-O bond already broken (Morgan *et al.*, 2001) in both of these intermediates. However, due to electron transfer from heme *a* in the latter case, it can be proposed that during formation of **P$_R$** the tyrosine radical is not formed, and the proton, required for O-O bond breakage, is picked up from the cross-linked tyrosine with formation of the deprotonated tyrosinate. As with the formation of **P$_M$**, the appearance of **P$_R$** is not coupled to proton uptake from the bulk solution (Ädelroth *et al.*, 1998b; Karpefors *et al.*, 2000), but internal proton movement is very likely to occur (Karpefors *et al.*, 2000; Morgan *et al.*, 2001; Paper IV). Formation of **P$_R$** is a unique transition in the catalytic cycle, because the electron transfer into the binuclear center during this reaction is not coupled to external proton uptake, which occurs only in the next transition. Such a feature of the **A→P$_R$** transition could be due to preceding protonation of some internal sites upon formation of COFR which would favor fast electron transfer.

*Ferryl-oxo intermediate **F**.* Intermediate **F** can be obtained in several ways: by the reversal of electron transfer (Wikström, 1981) when high proton-motive force is applied to mitochondria (in

fact, by increasing the strength of the proton-motive force, it is possible to reverse the oxygen reaction even beyond **F** and reach $\mathbf{P_M}$); in the flow-flash reaction after $\mathbf{P_R}$ with $\tau \sim 120\text{-}140$ μs in bovine CcO (Hill & Greenwood, 1984; Oliveberg *et al.*, 1989) or 50 μs in CcO from *P.denitrificans* (Ribacka *et al.*, 2005); by electron injection into the stable $\mathbf{P_M}$ state (Verkhovsky *et al.*, 1996b); or by incubation of oxidized CcO with excess amounts of H_2O_2 (Wrigglesworth, 1984; Vygodina & Konstantinov, 1988). Intermediate **F** can be easily detected by optical absorbance spectroscopy as it has a characteristic peak at 580 nm in the **F**-*minus*-**O** difference spectrum ($\varepsilon_{580}\text{-}\varepsilon_{630} \sim 5.3\ mM^{-1}\cdot cm^{-1}$). From the structural point of view one of the differences between **F** and $\mathbf{P_R}$ is an extra proton in the catalytic center in the former intermediate. This proton is taken up from the N-side of the membrane via the D-pathway (Fig. 8), though the **F** state can be formed even when the D-channel entrance is blocked by mutation (Smirnova *et al.*, 1999). In this case, the required proton may be borrowed from one of the amino-acid residues forming the channel - presumably $Glu_I278(242)$. The final destination of the proton during the **P→F** transition is uncertain but two possible candidates can be proposed: in one scenario this proton reprotonates Tyr-O^-, while in another it transforms the hydroxyl group on Cu_B to a water molecule (Fig. 9). Proton uptake to the catalytic center during the **P→F** transition is also coupled to $Cu_A \leftrightarrow$ heme *a* electron re-equilibration (Oliveberg *et al.*, 1989), where approximately 60% of Cu_A becomes oxidized (Hill, 1991).

Fully-Oxidized High-Energy state, $\boldsymbol{O_H}$**.** The $\mathbf{O_H}$ state is a final product in the classical flow-flash reaction of the fully reduced CcO with dioxygen. It appears with a time constant of 1-2 ms (Hill and Greenwood, 1984; Oliveberg *et al.*, 1989; Hill, 1991) from **F** and requires delivery of both an electron and a proton to the catalytic site. While the electron migrates from the Cu_A/heme *a* couple, the proton is taken up via the D-pathway (Konstantinov *et al.*, 1997) as in the $\mathbf{P_R}$**→F** transition. Most likely, this proton goes to the oxygen atom at the heme a_3 iron, resulting in two possible configurations of the catalytic center: in one case (left branch in scheme, Fig. 9) both heme a_3 and Cu_B have hydroxide ligands, while in the other, these two metal centers share water and hydroxide molecules. In the latter case, the hydroxide ion and the molecule of water form a resonance structure with a preferable configuration in which the water molecule is bound to the heme a_3 iron and hydroxide to Cu_B. The fully-oxidized $\mathbf{O_H}$ state is referred to as a "high-energy" state implying that the energy released in the redox reactions of the oxidative part of the catalytic cycle is conserved in this intermediate (Verkhovsky *et al.*, 1999b), and will be used in the next transitions of the cycle for proton pumping (Paper III&V). The $\mathbf{O_H}$ state is not stable and in certain conditions, when the electron donors are exhausted, it relaxes into the low energy **O** state

(incapable of pumping protons upon reduction) possibly by a protonation of a hydroxyl to water, or tyrosinate to tyrosine. In spite of the energetic difference no spectral distinction between **O** and $\mathbf{O_H}$ intermediates has been found (Jancura *et. al.*, 2006).

One-electron reduced $\boldsymbol{E_H}$**.** Discovery of the metastable high-energy $\mathbf{O_H}$ state had led to the conclusion that its reduction will result in formation of a one-electron reduced state, which will be different from the relaxed **E** state created by the reduction of the resting CcO (Paper III&V). Not much is yet known about the structure of this intermediate; however recent results indicate that the Cu_B center receives an electron upon the $\mathbf{O_H \rightarrow E_H}$ transition ($Cu_B^{2+} \rightarrow Cu_B^{+}$) with a "chemical" proton being delivered to the catalytic center (Paper V).

2.6 Proton Pumping

From the discovery of cytochromes by David Keilin in the 1920s (Keilin, 1925&1927) it took more than 40 years of investigation (Slater, 2003 for historical review) to find that CcO conserves energy by maintaining a $\Delta\mu_H$ on a membrane, by virtue of the vectorial organization of its chemistry (Chapter 2.1), and 10 more years to discover that for maximal efficiency the enzyme can perform active transport of protons from one side of the membrane dielectric to the other (pumping). As was first shown by Wikström (1977) with rat-liver mitochondria and confirmed later with bovine CcO reconstituted in phospholipids vesicles (Wikström & Saari, 1977; Krab & Wikström, 1978; Casey *et al.*, 1979), reduction of each dioxygen to two molecules of water is coupled to pumping of protons across the membrane.

2.6.1 Stoichiometry of Proton Translocation in the Catalytic Cycle

The first attempts to correlate proton pumping with certain transitions in the catalytic cycle were done by a quasi equilibrium approach involving reversal of the oxygen reduction reaction. The application of a high electrochemical proton gradient across the inner mitochondrial membrane, with high E_h, and relatively high pH of the medium, creates specific conditions in which some catalytic steps of dioxygen reduction can be reversed. Thus, addition of a high concentration of ATP to well-coupled mitochondria in the presence of ferricyanide leads to formation of the **P** and **F** states (Wikström, 1981; Wikström and Morgan, 1992). Analysis of the yields of the **F** and **P** intermediates as a function of the applied driving force at different pH values (Wikström, 1989) led to the conclusion that the four electron transfer steps in the catalytic cycle are not equal

with respect to proton pumping, and all four protons are pumped in two equal parts only during the **P→F** and **F→O** transitions.

These conclusions were challenged by Michel (1998), who re-analyzed the original experiments and proposed a new model. The stoichiometry of the proton pumping predicted by this model was two protons in **P** to **F**, one in **F** to **O**, and one more proton in the reductive part of the cycle presumably during the **E** to **R** transition.

Detailed analysis of membrane potential generation combined with parallel optical measurements of the flow-flash reaction showed that both **P→F** and **F→O** transitions generate approximately equal amounts of potential (Verkhovsky *et al.*, 1997; Jasaitis *et al.*, 1999). However, despite having an extremely good $^{signal}/_{noise}$ ratio for the electrometric signals, this method does not directly give the number of transferred charges. One solution to this problem is to use an internal standard for the calibration. Such independent calibration of potential generation can be obtained, for example, from the electron backflow reaction (chapters 4.1&5.2), which, at neutral pH, consists of a single electrogenic event – electron transfer from heme *a* to Cu_A. But even in this case calibration is complicated by uncertainty about the dielectric distance between these redox centers, *i.e.* how deep heme *a* is buried in the membrane and thus, the distance traversed through the membrane by an electron moving from heme *a* to Cu_A (Jasaitis *et al.*, 1999). The X-ray crystallographic structure of the oxidase (Iwata *et al.*, 1995; Tsukihara *et al.*, 1995) and experimental determination (Verkhovsky *et al.*, 1999b; Paper II) of the dielectric depth of heme *a* both gave the value $^1/_3$ – implying that the pumping stoichiometry is one in both the **P→F** and **F→O** transitions.

Direct measurements of both proton and charge translocations in CcO vesicles during partial turnover of the enzyme (Verkhovsky *et al.*, 1999b; Paper III) show that only two protons are pumped in the oxidative part of the catalytic cycle: one during **P→F**, and another during **F→O**. However the reaction is supplemented by two more pumped protons when the oxidation is followed by immediate re-reduction. Since reduction of the fully-oxidized **O** state is not coupled to proton pumping (Verkhovsky *et al.*, 1999b; Ruitenberg *et al.*, 2000; Verkhovsky *et al.*, 2001b; Paper III), a new "high-energy" fully-oxidized $\mathbf{O_H}$ intermediate with energy conserved for proton translocation was proposed. Indeed, by electron injection experiments it was demonstrated that one electron reduction of $\mathbf{O_H}$ leads to formation of a new $\mathbf{E_H}$ state and that this process is coupled to translocation of one proton across the membrane (Paper III&V). Since the overall

stoichiometry of proton translocation is four protons per dioxygen, reduction of the $\mathbf{E_H}$ state must also be coupled to a translocation of a proton (Paper III). The proton pumping during reduction of the $\mathbf{E_H}$ state is consistent with the experiments by Ruitenberg *et al.* (2002), who produced the $\mathbf{E_H}$ state during the reduction of the **F** state by CO.

The recent results have been developed into a symmetrical scheme of the pumping events during the catalytic cycle of CcO (Fig. 10). Under continuous turnover conditions CcO proceeds via four relatively stable intermediates: $\mathbf{P_M}$, **F**, $\mathbf{O_H}$, and $\mathbf{E_H}$. Single electron reduction of each of these four intermediates from cytochrome *c* leads to uptake of a "chemical" proton from the N-side with simultaneous translocation of another proton across the membrane.

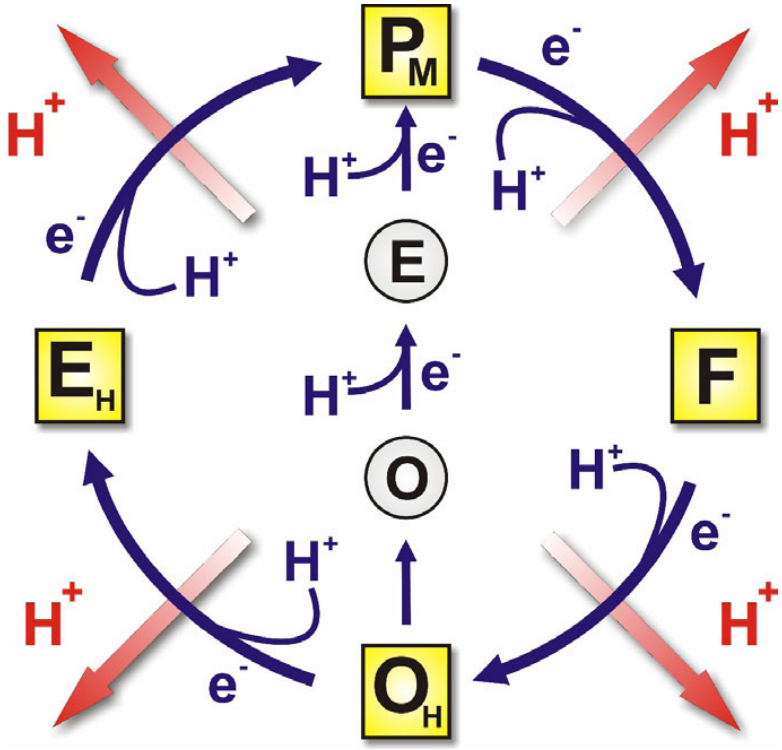

Figure 10. The proton translocation during the catalytic cycle of cytochrome *c* oxidase. The active states are shown in squares. The transitions between each of them are coupled to proton pumping. The relaxed states are shown in circles; their reduction is not coupled to proton pumping.

2.6.2. Models of Proton Translocation

For many years, it was an almost universal assumption that proton pumping is coupled to the reduction and oxidation of certain redox centers of CcO, and at different times each of the four redox centers was considered to be a crucial element in the mechanism of proton translocation.

A model based on ligand exchange at the Cu_A site linked to its oxidoreduction was proposed by the Chan group (Gelles *et al.*, 1986). In this model reduction of Cu_A induces a change of the Cu_A ligation state, which results in transfer of a proton from a tyrosine residue below Cu_A to one of the cysteine ligands of Cu_A. Upon subsequent oxidation of Cu_A by the binuclear center, the system returns to its original configuration with release of the translocated proton from the cysteine and reprotonation of the tyrosine residues. However this model seems to be unfeasible because structurally similar quinol oxidases are still able to pump protons even in the absence of a Cu_A center.

Heme *a* was probably the most popular candidate to be the key cofactor for proton pumping. For more than 20 years after discovery of proton pumping the idea of tight coupling between heme *a* oxidoreduction to proton pumping was the basis for many models (Wikström *et al.*, 1977; Artzatbanov *et al.*, 1978; Babcock and Callahan, 1983; Rich *et al.*, 1998; Yoshikawa *et al.*, 1998; Michel, 1998; Papa *et al.*, 1998). In general it was proposed that reduction of heme *a* is coupled to uptake of a pumped proton from the N-side of the membrane. Subsequent electron transfer from heme *a* to the binuclear center would be linked to uptake of another proton from the N-side for water formation, and release of the preloaded proton towards the P-side of the membrane.

Rousseau *et al.* (1993) proposed a model where oxidoreduction of heme a_3 is linked to a change in its ligand configuration: in one redox state a histidine residue occupies the fifth coordination site of the heme, while in another the histidine may be substituted by a tyrosine. Such exchange at heme a_3 would lead to proton translocation from the tyrosine to histidine and further to the P-side of the membrane.

Several models have put oxidoreduction of Cu_B as a central element in the proton translocation mechanism. Mitchell (1988) proposed that protonation of a hydroxyl ligand on the copper, by a proton taken from the N-side of the membrane, resulting in a water molecule bound to Cu_B. This would be followed by re-orientation of the water molecule towards the P-side, after which the proton is released due to Cu_B oxidation. Another model (Larsen *et al.*, 1992) that posits Cu_B as a

central element in the proton pump is derived from Chan's Cu_A model of ligand exchange. A "histidine cycle" model presented in 1994 (Morgan *et al.*, 1994) specifies one of the conserved histidine ligands of Cu_B as a pump element. According to this model, this histidine shuttles between two conformations depending on the reduction level of Cu_B. In one conformation, the histidine is deprotonated (imidazolate form, Im^-) and bound to Cu_B, while in another form, it is protonated (imidazolium, $ImHH^+$) and rotated away from Cu_B. Arrival of a chemical proton at oxygen induces proton ejection from the imidazolium towards the P-side of the membrane, and provides driving force for the reaction.

In contrast, recent models do not focus on any individual redox cofactor as the driving element of proton translocation but rather the transfer of an electron from heme *a* to the binuclear center (Siegbahn *et al.*, 2003; Popović and Stuchebrukhov, 2004; Siletsky *et al.*, 2004); or of a proton from the conserved $Glu_I278(242)$ to a proton pump site above the hemes via a chain of water molecules (Wikström *et al.*, 2003; Paper IV&V) which then triggers electron equilibration between the hemes. In spite of the fact that these two types of models differ with respect to the order of the electron and proton steps, and which one drives the reaction, these models are quite similar. The initial electron (heme *a* to the binuclear center) and proton (from Glu_I278 to the pump site) transfers are followed by uptake of a chemical proton to the active site, which leads to release of the pumped proton from the protein on the P-side.

A model that is completely different from the electrostatic models just described has recently been proposed by the Brzezinski group. Based on the kinetics of proton uptake and release on both aqueous sides of the membrane, it is suggested that proton pumping is not coupled to internal electron transfer, but rather occurs as a result of energy conservation in the protein structure in response to transfer of a chemical proton to the active site (Brzezinski and Larsson, 2003; Faxen *et al.*, 2005).

So, the long history of CcO studies has produced a large number of models to explain the proton pump mechanism; many of these models have already been disproved, but we should admit that there is still no single widely accepted theory present.

3. AIMS OF THE PRESENT STUDY

The first crystallographic structures of CcO with atomic resolution were obtained more than 10 years ago; however at the time when this work was started there was still no clear information about the molecular mechanism of the proton pump in CcO. Results obtained by different groups were sometimes contradictory making understanding of CcO functioning, which is extremely complicated itself, even more complex. The main task of this work was to carry out extensive studies of pumping and non-pumping terminal oxidases by a variety of different complementary techniques (absorbance spectroscopy, potentiometric electrometry, and proton pumping measurements) examining full and partial steps of the catalytic cycle. More specifically, the main aims were:

- To explore and compare the dioxygen binding properties of the terminal oxidases from the distinct heme-copper and *bd*-type families.
- To study the electron reversal reaction after CO photolysis from the mixed-valence CO-bound CcO under different pH conditions, and to use this reaction to estimate the relative dielectric depth of the binuclear center within the membrane.
- To perform a detailed analysis of the oxidative and reductive parts of the catalytic cycle to clarify the steps in the reaction that are coupled to proton translocation, and estimate the number of protons translocated at each of these steps.
- To study the individual steps of proton translocation to locate the reaction that drives the proton pumping mechanism.
- To explore one of the single proton translocation steps in CcO in real time to define thermodynamic and kinetic properties of the proton pump, and describe the proton pump mechanism at the atomic level.

4. METHODOLOGY

4.1. Methodological Approaches

The typical rate of oxygen reduction by CcO under steady-state conditions is approximately 100-200 enzyme revolutions per second. This means that a single turnover of the enzyme is extremely fast and occurs in the millisecond time domain. At the same time, each turnover has a number of distinct intermediates which are formed in times ranging from a few microseconds to several milliseconds after the beginning of the reaction. Thus, because of a large number of catalytic intermediates, complicated by a large hierarchy of transition rate constants between them, it is impossible to study the mechanism of CcO functioning by means of conventional steady-state techniques. The main problem in the steady-state approach is that under such conditions only the longest lived intermediate is populated, leaving all other intermediates completely invisible. The transient kinetics approach makes it possible to overcome these difficulties, but requires a certain number of conditions which have to be fulfilled.

- First, the measuring system must allow time resolution faster than the fastest reaction step under investigation. This is actually the least difficult matter nowadays due to developments in the field of modern electronics (*e.g.* development of the CCD (Charge Coupled Device, an image sensor consisting of a large number of capacitors for light registration), fast Analog-to-Digital converters, powerful computers for real-time processing *etc.*).
- Second, the sample solution consists of a very large number of individual protein molecules that function independently, and it is very important to set all of them into the same state before initiation of the reaction.
- Third, addition of substrates to the enzyme has to be carried out faster than the fastest transition under investigation. This is a real challenge because the fastest mixing time of a conventional stopped-flow apparatus is in the range of milliseconds, which is much slower than most of the intermediate transitions in the catalytic cycle. A possible solution to this problem is to start the reaction by instant enzyme activation, for example by a laser flash.

The catalytic reaction of CcO consists of oxygen reduction chemistry together with proton and electron transfers. In general, electron transfer can occur in two opposite directions: *to* and *from* the binuclear center. In the first case, the movement of electrons coincides with the normal

physiological direction of electron transfer, while the other case is an artificial experimental model used for detailed studies of electron transfer reactions (*backflow* reaction).

Two main approaches have been introduced for measurements of the catalytic reactions in CcO in real time. One of them - the *flow-flash* method (Gibson and Greenwood, 1963) - is a combination of the conventional stopped-flow technique with laser-induced initiation of the reaction. In this method, instead of initiating the reaction by the actual mixing of the fully-reduced CcO with dioxygen, the enzyme is first allowed to react with carbon-monoxide, which binds to the reduced heme a_3 at the oxygen binding site; after that the CO-bound oxidase is mixed in a stopped-flow apparatus with an oxygen-containing buffer. Under these conditions, the reaction of dioxygen with the CO-bound oxidase is limited by the CO-dissociation rate (*ca.* 0.02 s^{-1} (Gibson and Greenwood, 1963&1964)[5]. However the Fe–CO bond is photolabile and before spontaneous dissociation can take place, the entire population can be instantly photolysed by a laser flash. The laser flash photolyzes CO from heme a_3 allowing dioxygen to bind and begin the reaction. The subsequent transitions can be monitored by a number of different time-resolved detection techniques such as optical absorption spectroscopy (Gibson and Greenwood, 1963; Hill and Greenwood, 1984; Orii, 1988; Oliveberg *et al.*, 1989; Hill, 1991&1994; Blackmore *et al.*, 1991; Verkhovsky *et al.*, 1994&1996a; Sucheta *et al.*, 1998), potentiometric electrometry (Verkhovsky *et al.*, 1997; Jasaitis *et al.*, 1999; Verkhovsky *et al.*, 1999b), resonance Raman (Varotsis *et al.*, 1989; Han *et al.*, 1990a; Ogura *et al.*, 1990; Varotsis and Babcock, 1990; Varotsis *et al.*, 1993) *etc*. The flow-flash method is very useful; however its scope is restricted and it is usually applied to studying the oxidative part of the catalytic cycle only. In addition, the beginning of the reaction is complicated by the phase of CO release, which takes the same route via Cu_B (Alben *et al.*, 1981) as subsequent dioxygen binding (Verkhovsky *et al.*, 1994). Fortunately, CO dissociation from the binuclear center seems to be much faster (Woodruff *et al.*, 1991) than the subsequent step of oxygen binding, and should not affect it.

The second approach is the initiation of the reaction by the injection of a single electron into the enzyme. The most successful implementation to date has been the use of photo-activated ruthenium derivatives (Mayo *et al.*, 1986; Nilsson, 1992; Zaslavsky *et al.*, 1993; Geren *et al.*, 1995; Zaslavsky *et al.*, 1998; Ruitenberg *et al.*, 2000; Verkhovsky *et al.*, 2001b; Siletsky *et al.*,

[5] The rate of CO dissociation strongly depends on the intensity of the measuring light and under particular experimental conditions it can be much faster than the cited value.

2004; Papers III&V) such as tris(2,2'-bipyridyl) ruthenium (RubiPy) for the reaction initiation in CcO. Under low ionic strength conditions RubiPy binds electrostatically to the oxidase at the cytochrome *c* binding pocket. A laser flash promotes the molecule of RubiPy to an excited state with an E_m of about -1.5 V, which can then donate an electron to Cu_A in less than 0.5 μs. The injected electron is further redistributed among all redox cofactors according to their midpoint potentials. The reverse reaction of enzyme reoxidation by the oxidized RubiPy is prevented by addition of a sacrificial electron donor such as, for example, aniline or EDTA. Electron injection is a very powerful and useful technique, albeit with certain limitations: the main one is the relatively small quantum yield, which is typically less than 10%.

An alternative way to study electron transfer in CcO is investigation of the electron *backflow* reaction and processes coupled to it by the *perturbed equilibrium* method. In this method, CO binding is used to maintain the apparent midpoint potentials of heme a_3 and Cu_B at high level prior to the flash. The bound molecule of CO can then be dissociated by a flash of light causing the midpoint potentials of heme a_3 and Cu_B to drop, and allowing electron redistribution among all redox centers according to the new redox equilibrium (see Section 5.2).

4.2. Time-resolved Potential Electrometry

The functioning of CcO is directly linked to the translocation of both electrons and protons across the membrane. Whereas the transfer of electrons can be relatively easily followed by various spectroscopic methods, the time-resolved transfer of protons can conveniently be measured by potential electrometry. Potential electrometry is a technique of direct measurement of electric charge translocation by membrane proteins. It was originally developed for the study of bacterial reaction centers and bacteriorhodopsin (Drachev *et al.*, 1974&1979), but later also applied to CcO (Zaslavsky *et al.*, 1993). In recent years this technique has advanced extensively allowing detection of $\Delta\Psi$ generated not only in the light-induced reactions, but also after addition of other substrates such as O_2, or NO (Verkhovsky *et al.*, 1997; Hendriks *et al.*, 2002). The idea of the electrometric technique is that, firstly, the molecules of CcO are incorporated into phospholipid vesicles by gradual removal of detergent from the protein/lipid mixture (Hinkle *et al.*, 1979; Rigaud *et al.*, 1995). Then the vesicles with CcO are fused to a planar lipid measuring membrane through neutralization of the membrane surface negative charges by Ca^{2+} or Mg^{2+} ions (Fig. 11). The measuring membrane must be very thin in order to possess a high electric capacitance to allow the recording of fast charge translocation. During the enzymatic

reaction, CcO creates a $\Delta\Psi$ across the vesicle membrane which is then proportionally divided with the measuring membrane and thus can be detected by Ag/AgCl electrodes situated on on the two sides of the measuring membrane. Typically, the measuring membrane has a resistance of about 1-5 GOhm, and the measured $\Delta\Psi$ decays with a time constant of several seconds, which is slower than the typical rates of $\Delta\Psi$ generation due to the enzymatic processes.

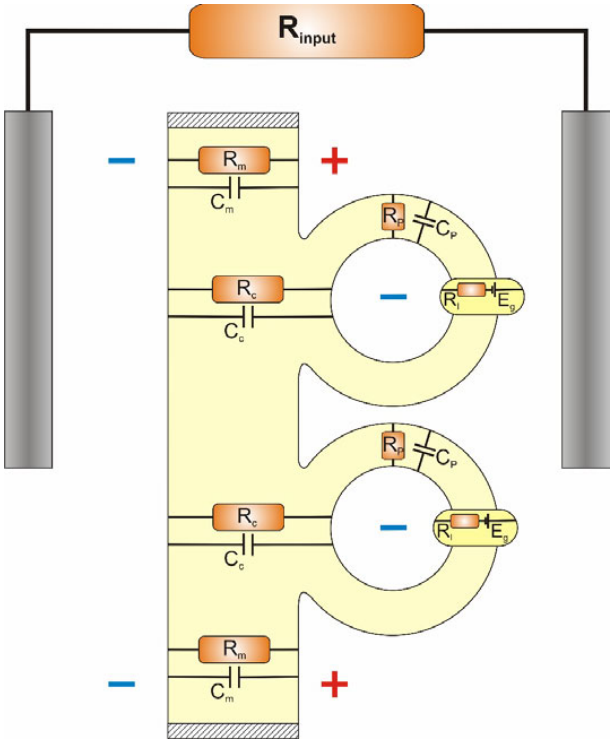

Figure 11. Scheme of the electrometric setup. CcO is reconstituted into phospholipid vesicles that are fused to the phospholipid measuring membrane. The potential measured between Ag/AgCl electrodes is proportional to the potential generated by the enzyme. C_m, C_p, C_c are the capacitances of the measuring membrane, the liposomal membrane, and their contact region respectively. R_m, R_p, R_c are the corresponding resistances. R_i is internal resistance and E_g is the electromotive force of the molecular generator.

This method is extremely sensitive, allowing detection of charge translocation of less than 1 Å across the membrane dielectric in the direction perpendicular to the membrane plane. At the same time it has certain limitations natural for any vesicle-related technique, for instance the enzyme molecules may not all be oriented in the same direction, decreasing the amplitude of the signal, or the substrate binding sites may be unreachable if they are located on the inner side of the vesicle membrane.

5. RESULTS AND DISCUSSION

5.1 Oxygen Binding Properties of Terminal Oxidases

5.1.1 Determination of the Oxygen Binding Constant

In contrast to mitochondria, bacteria are usually characterized by a highly branched composition of the respiratory chain where up to at least three different terminal oxidases are available for expression (Anraku and Gennis, 1987; Garcia-Horsman *et al.*, 1994). One of the main functions of the branched organization of the respiratory chain is to adapt bacteria to a variety of environmental growth conditions. Indeed, unlike the mitochondria that can benefit from the stable conditions of the eukaryotic cell, bacteria are often exposed to a constantly variable environment and deprived of such stability. Since dioxygen is one of the main substrates essential for survival of aerobic organisms, nature developed several types of terminal oxidases that function under different oxygen conditions. Under normal oxygen concentration terminal oxidases are presented by a proton-pumping heme-copper type of oxidases, while under low oxygen tension the most pronounced is expression of non-pumping (Miller and Gennis, 1985; Puustinen *et al.*, 1991) cytochrome *bd*. Thus, it is interesting to compare the oxygen binding properties of these oxidases. But, if for CcO both oxygen dissociation constant (K_d = 280-320 μM (Chance *et al.*, 1975; Verkhovsky *et al.*, 1994)) and Michaelis constant - the concentration yielding half-maximal steady-state turnover (K_m = 0.95-1 μM (Petersen *et al.*, 1976; Verkhovsky *et al.*, 1996c)) are well defined, the same characteristics measured for cytochrome *bd* are less certain. There is only one reported value of K_d = 25 nM for *bd*-oxidase (Hill *et al.*, 1994), which was however obtained indirectly using results from different experiments - the forward rate constant (k_1) from the oxygen reaction, and the reverse rate constant (k_{-1}) from a ligand-exchange (O_2/CO) experiment without presenting real data for the latter case. Because of that the high affinity of cytochrome *bd* to oxygen was always considered to be based on K_m values. But on one hand, the published K_m values vary extensively from 3 nM to 2μM depending on the concentration and nature of the primary substrate, experimental techniques, and other factors (Rice and Hempfling, 1978; Kita *et al.*, 1984; Kolonay *et al.*, 1994; Jünemann *et al.*, 1995; D'mello *et al.*, 1996). And on the other, the use of K_m as a measure of the enzyme affinity to oxygen (*i.e.* $K_d = K_m$) may often be incorrect, except in the simplest case of a single substrate reaction when k_2 is very small, otherwise the $^{k2}/_{k1}$ ratio should be added to K_d to obtain K_m:

$$\mathrm{Enz} + \mathrm{O_2} \underset{k_{-1}}{\overset{k_1}{\rightleftharpoons}} \mathrm{Enz\text{-}O_2} \xrightarrow{k_2} \mathrm{Product}$$

$$K_d = \frac{k_{-1}}{k_1} \qquad K_m = \frac{k_{-1} + k_2}{k_1} \qquad K_m = K_d + \frac{k_2}{k_1} \tag{3}.$$

The difference between K_m and K_d can be emphasized by comparing these values for CcO where they differ more than 100-fold (Verkhovsky *et al.*, 1996c).

In contrast to heme-copper oxidases, cytochrome *bd* can bind oxygen even in the one-electron reduced state, forming a stable oxygenated complex ($b_{558}^{3+}b_{595}^{3+}d^{2+}-O_2$) characterized by an absorbance spectrum with a maximum at 650 nm (**I**, Fig. 1A). Under anaerobic conditions it is possible to remove all bound oxygen from cytochrome *bd*, and later regenerate the oxygenated form by successive addition of aliquots of oxygen to the sample. The regeneration of the oxygenated form is seen in the difference optical spectrum as an increase at 648 nm and a decrease at 626 nm, due to a shift of the heme *d* α band maximum (**I**, Fig. 1B). The K_d value for *bd*-oxidase can be defined by plotting and fitting of the fraction of oxygenated form (measured as the absorbance difference between 648 and 626 nm) as a function of O_2 concentration (**I**, Fig. 2). The fit to the experimental data was based on a simple model of reversible oxygen binding:

$$\mathrm{Enz} + \mathrm{O_2} \underset{k_{-1}}{\overset{k_1}{\rightleftharpoons}} \mathrm{Enz\text{-}O_2} \Rightarrow k_1 \cdot [\mathrm{Enz}] \cdot [\mathrm{O_2}] = k_{-1} \cdot [\mathrm{Enz\text{-}O_2}]$$

$$\begin{cases} K_d = \dfrac{k_{-1}}{k_1} = \dfrac{[\mathrm{Enz}] \cdot [\mathrm{O_2}]}{[\mathrm{Enz\text{-}O_2}]} \\ [\mathrm{Enz\text{-}O_2}] + [\mathrm{Enz}] = 1 \end{cases} \Rightarrow [\mathrm{Enz\text{-}O_2}] = \frac{[\mathrm{O_2}]}{K_d + [\mathrm{O_2}]}$$

and yielded K_d ~ 280 nM. Thus the oxygen affinity of *bd*-oxidase is indeed extremely high; it is about 3-fold higher than that of sperm whale myoglobin (~880 nM, Draghi *et al.*, 2002), and 3 orders of magnitude higher than that of CcO.

Taking the values for K_d and the bimolecular rate constant for the interaction of oxygen with the enzyme, it is possible to estimate and compare the population of the oxygenated complex at a typical oxygen concentration in tissues (3 μM, Gnaiger, 2003) for both terminal oxidases, as $k_{on} = k_1 \times [O_2]$ and $k_{off} = k_1 \times K_d$.

Taking k_1 as 1.38×10^8 $M^{-1}s^{-1}$ for CcO (Verkhovsky *et al.*, 1994) results in k_{on} = 414 s^{-1} (τ ~ 2.4 ms), and k_{off} = 3.9×10^4 s^{-1} (τ ~ 25 μs), which indicates very weak binding of oxygen. This raises a question; how is CcO ever able to work with such low affinity to oxygen, when the population of

oxygenated form is only about 1%? A possible explanation may be in the rate of transformation of compound **A** into the "peroxy" state (τ = 30-40 μs (Oliveberg *et al.*, 1989; Verkhovsky *et al.*, 1994)), which is approximately similar to the k_{off} value. This means that CcO functions as a kinetically effective trap for oxygen (Chance *et al.*, 1975; Verkhovsky *et al.*, 1996c), where the molecule of bound dioxygen is rapidly reduced, before it can dissociate. In contrast, cytochrome *bd* tends to populate the oxygenated complex, as can be estimated from the obtained $k_{on} = 6\times10^3$ s^{-1} (τ ~ 170 μs) and $k_{off} = 560$ s^{-1} (τ ~ 2 ms) rates, based on $k_1 = 2\times10^9$ $M^{-1}s^{-1}$ (Hill *et al.*, 1994). Since cytochrome *bd* is a non-pumping oxidase it does not spend energy for proton translocation across the membrane. Also it accepts electrons, not from cytochrome *c*, but from ubiquinol, which is about 150 mV more negative (E_m ~ 100 mV). Thus, this significant excess of redox energy drop from ubiquinol/quinone to the oxygen/water couple can be invested solely into tight binding of oxygen. After isolation, cytochrome *bd* in the "as prepared" state already exists in the oxygen bound form (Lorence and Gennis, 1989) and the removal of oxygen is not an easy task. Only exposing the enzyme to a medium with an oxygen concentration lower than K_d, or the use of strong light under microaerobic conditions (see Section 5.1.2), can do the job.

5.1.2 Photolability of the Heme d-O_2 Bond in Cytochrome bd

Despite the fact that oxygen binding to the "as isolated" form of cytochrome *bd* is reversible, attempts to photolyse the heme *d*-O_2 bond in the mixed-valence enzyme have not been successful (Borisov *et al.*, 2002). It has been concluded that, in contrast to myoglobin and some other synthetic oxy-hemes (Ye *et al.*, 2002; Fry *et al.*, 2004), the quantum yield for photodissociation of the heme *d*-O_2 bond is effectively zero. In order to check this feature of cytochrome *bd*, we investigated the oxygenated form of the enzyme under strong continuous illumination. Because O_2 binding to cytochrome *bd* is extremely tight, it is feasible to study photodissociation under lower O_2 concentration. Under *microaerobic* conditions ([O_2]~800nM) the illumination of the oxygenated cytochrome *bd* induced a decrease of absorbance at 648 nm and increase at 626 nm (**I**, Fig. 3A). The obtained difference spectrum of optical changes was virtually identical to the inverted spectrum of oxygen binding to heme *d* (**I**, Fig. 3B), which indicates that the heme *d*-O_2 bond is actually photolabile.

It seems that the difference between our present and previously reported results is most likely due to different oxygen concentrations in the sample: while Borisov *et al.* (2002) tried to photolyse heme *d*-O_2 bond under high oxygen tension, we conducted the measurements under

microaerobiosis. It is possible that, in addition to the high-affinity oxygen binding site at heme *d*, there is also a low-affinity binding site within the protein, somewhere in a possible oxygen-conducting channel. We propose that under microaerobiosis this putative low-affinity site is empty allowing oxygen photodissociation away from heme *d*, whereas at high oxygen tension, this site will be occupied, locking the photoexcited oxygen at heme *d*. From our data it is not possible to make a specific assignment of the low-affinity site, but we can exclude heme b_{595} since in our measurement this heme is oxidized and thus incapable of oxygen binding.

5.2 Electron Backflow Reaction

The coupling between internal electron and proton transfers in CcO can be studied not only in the forward reaction of oxygen reduction to water, but also in a simpler experimental model - electron backflow. Under anaerobic conditions a molecule of CO binds to reduced heme a_3 in place of oxygen and significantly increases the midpoint potential of heme a_3 and Cu_B, trapping electrons at the binuclear center (Fig. 12). However, the heme a_3-CO bond is photolabile and can be broken by a laser flash. Upon the flash, in several hundreds of femtoseconds, CO leaves heme a_3 and transiently binds to Cu_B (Woodruff *et al.*, 1991). After CO dissociation the midpoint potential of heme a_3 returns to its original value, and the electron equilibrates among the redox

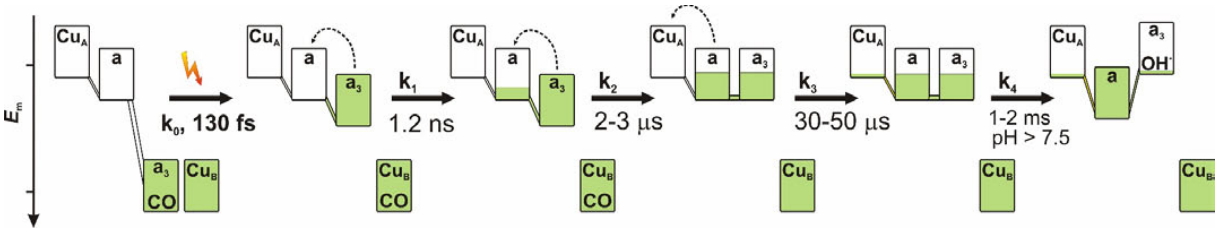

Figure 12. The scheme of the electron backflow reaction from the mixed-valence CcO. Each box represents one of the redox centers, and can be completely or partially filled (reduced), or emptied (oxidized).

centers (Boelens and Wever, 1979; Morgan *et al.*, 1989; Oliveberg and Malmström, 1991; Verkhovsky *et al.*, 1992; Ädelroth *et al*, 1995; Jasaitis *et al.*, 1999) approaching a distribution that depends on their midpoint potentials. Fast electron equilibration between heme a_3 and heme *a* takes place on the nanosecond time scale (Verkhovsky *et al.*, 2001a; Pilet *et al.*, 2004), followed by a slower 2-3 µs process connected with a protein relaxation that takes place upon CO release from Cu_B. The next step happens in 30-50 µs and includes further electron equilibration among the hemes and Cu_A. At high pH, electron backflow is also supplemented by a millisecond phase ($\tau \sim 2$ ms, pH 9) caused by additional electron equilibration among the redox

centers in response to proton release from the binuclear center. It has been proposed that this proton originates from a water molecule and is released to the bulk solution via the K-pathway (Hallén *et al.*, 1994; Brändén *et al.*, 2003). This proton movement should create an electric potential ($\Delta\Psi$) that can be detected and used to estimate the relative dielectric depth of the binuclear center within the membrane (*d*).

Typical traces of $\Delta\Psi$ generation in the backflow reaction in the COMV state at different pH values are shown in **II**, Figure 4. Only a very small (~0.25mV) amplitude of $\Delta\Psi$ generation was detected in CcO in *P. denitrificans* at neutral pH. However upon increasing the pH, the amplitude of $\Delta\Psi$ generation increased, reaching 8.2 mV at pH 10. In the pH range 7-8.5, the time constant of charge translocation was about 50-60 μs, but in alkaline conditions it slowed to ~200 μs at pH 10.5 (**II**, Fig. 5), however without any detectable component in the millisecond time domain. Thus there is a clear difference between the optical and electrometrical results in alkaline conditions. To clarify the source of this difference a definitive assignment of the electrometric signal was performed by means of parallel optical measurements and the use of proton channel blocking mutants.

On one hand the rate of $\Delta\Psi$ generation is very close to the rate of electron transfer between heme *a* and the Cu_A center, and it is possible that in alkaline conditions the extent of the electron transfer to Cu_A in the two-electron reduced enzyme is much higher than at neutral pH. However, the direct comparison of optical traces of Cu_A oxidoreduction in the electron backflow reaction in alkaline conditions from COMV, COFR, and $3e^-$ reduced enzyme clearly showed that there was no Cu_A reduction in the COMV case (**II**, Fig. 6, reduction of Cu_A corresponds to a decrease in absorbance at 820 nm). All other redox centers in CcO are located at about the same depth within the membrane dielectric and electron equilibration among them cannot produce any $\Delta\Psi$. Thus, the 50-200 μs phase of $\Delta\Psi$ generation should derive only from the proton transfer towards the N-side of the membrane. Indeed $\Delta\Psi$ generation measurements with D- and K- channel blocking mutants supported this assignment (**II**, Fig. 7). While the amplitude of $\Delta\Psi$ generation for the D124N enzyme was almost unaffected by the mutation (it had approximately the same amplitude and the same rate as for the wild type oxidase), blockage of the K-channel (K354M mutant) resulted in complete disappearance of the signal in the mixed-valence enzyme. This agrees with previous results from time-resolved optical measurements on the analogous K-channel mutant in *Rhodobacter sphaeroides* CcO, where the millisecond electron-transfer phase was also not detected (Ädelroth *et al.*, 1998a). Taken together, the obtained results suggest that

the 50-200 μs phase of ΔΨ generation is due to proton transfer through the K-pathway, and are consistent with the fact that uptake of the first and second protons during reduction of CcO from the **O** state happens also via the K-pathway (Ädelroth *et al.*, 1998a; Wikström *et al.*, 2000). If so, what can explain the apparent contradiction that when proton release, coupled to electron re-equilibration, is measured by the electrometric method, a time constant of about 150 μs is found, whereas the proton ejection from the enzyme, as measured using pH-sensitive dye (Brändén *et al.*, 2003), and electron equilibration itself is observed only on millisecond time scale? It seems that the difference in the rates is due to the fact that the enzyme is not in the same physical environment in typical optical and electrometrical measurements. In one case the enzyme is exposed to a detergent containing environment, while in the other it is reconstituted into phospholipid vesicles. This idea is supported by optical measurement of the backflow reaction with the reconstituted CcO, where the rate of the second electron transfer phase was significantly faster than in detergent solution: about 6.7×10^4 s^{-1} (τ = 150 μs) at pH 9.5 (**II**, Fig. 8). Two feasible explanations of this increase may be proposed: either incorporation of the enzyme into the vesicles significantly changes the conductivity of the K-channel, or the large number of negative charges on the membrane surface may serve as a proton acceptor pool increasing the proton release rate.

Taking the maximal amplitude of ΔΨ in the backflow reaction from the fit to the experimental data as 9.84 mV (**II**, Fig. 4B), it is possible to estimate the relative dielectric depth of the hemes within the membrane. But that requires knowledge of the total extent of electron transfer between the binuclear center and the heme *a*/Cu_A couple after CO dissociation from COMV. The amplitude of electron transfer in this process can be obtained from the CO recombination rates in the COMV and COFR enzymes (**II**, Fig. 1). In both cases the kinetics of CO recombination were monophasic at any pH from 7 to 11. In the COFR enzyme the observed rate was about 44 s^{-1}, and pH independent, while in the mixed-valence enzyme the rate decreased from 20 s^{-1} at pH 7 to 1 s^{-1} at pH 11, which is similar to the CO recombination rates measured on *R. sphaeroides* CcO (Sigurdson *et al.*, 2002). The pH independence in the COFR case indicates that the CO recombination as such does not involve protonation events. In COMV however, the decrease in the rate with pH can be explained by a decrease of the occupancy of the fully-reduced binuclear site after CO photolysis, due to electron transfer to heme *a* (Morgan *et al.*, 1993). Therefore, the rate of CO recombination in the mixed-valence enzyme can be described by the equation:

$$k_{rec}(pH) = k_0 \cdot [a_3^{red}(pH)],$$

where k_{rec} is the apparent rate constant of CO recombination at a particular pH value; k_0 is the CO recombination rate constant in fully-reduced enzyme; and $[a_3^{red}]$ is the fraction of fully-reduced binuclear center. $[a_3^{red}]$ can be estimated from the measured rates of CO recombination in COMV at different pH values. Amplitudes of $[a_3^{red}]$ were fitted with a Henderson-Hasselbalch one-proton titration curve (**II**, Fig. 1C) giving a pK_a value of 8.66 (Hill coefficient 0.6). From the fit the maximal extent of the fully-reduced binuclear center after the fast phase can be calculated to be 50.5%. A Hill coefficient less than unity indicates negative cooperativity with several other titratable groups. Since there is only a decrease in the Hill coefficient without any splitting of the titration curve, we can conclude that these titratable groups are located, not near, but rather quite far away from the titratable water molecule in the binuclear center.

The amplitude of $\Delta\Psi$ generation in the reaction of the fully-reduced CcO with dioxygen was 105 mV which corresponds to the translocation of $2+d+(1-d)\times 2$ charges - two protons across the membrane (pumping); one electron via *d*-span of the membrane due to electron transfer from Cu_A to heme *a*, and two more protons through (1-*d*) span of the membrane for water formation. At the same time, the translocation of 0.505 protons via (1-*d*) in the backflow reaction from COMV in alkaline conditions generates 9.84 mV of potential. When these numbers are taken together they can be used to estimate the relative dielectric depth of the binuclear center within the membrane (*d*):

$$\frac{105\,mV}{2+d+(1-d)\times 2}=\frac{9.84\,mV}{(1-d)\times 0.505},\qquad \Rightarrow\quad d=0.32\,.$$

The value of d = 0.32 is in a good agreement with the previous estimate based on electron equilibration between heme *a* and Cu_A in the 3-electron reduced enzyme (Verkhovsky *et al.*, 1999b), and with the crystallographic structure (Iwata *et al.*, 1995).

5.3 Stoichiometry of Proton Translocation

The results from direct measurements of both proton and charge translocation processes in CcO reconstituted into phospholipid vesicles suggested (Verkhovsky *et al.*, 1999b) that only two out of four protons are pumped during the oxidative phase of the catalytic cycle (one in **P→F**, and one in **F→O**). However, when the oxidative phase is followed by immediate re-reduction, this results in additional pumping of two more protons. In contrast, reduction of oxidized, as isolated enzyme (state **O**) is not coupled to proton pumping (Verkhovsky *et al.*, 1999b; Ruitenberg *et al.*, 2000; Verkhovsky *et al.*, 2001b) in agreement with the low midpoint potentials (E_m) of heme a_3

and Cu_B from anaerobic redox titrations (Dutton and Wilson, 1974). It was proposed (Verkhovsky *et al.*, 1999b) that the intermediates formed in the reductive phase starting from the oxidized enzyme, as isolated, and from the oxidized enzyme in the continuous turnover are different, implying existence of two alternative catalytic pathways that differ in efficiency of proton pumping.

To establish the stoichiometry of proton pumping in the re-reductive phase of the catalytic cycle (**O_H→E_H→R**) we conducted direct measurements of proton translocation in CcO vesicles. These experiments showed that only two protons are pumped when the enzyme, fully reduced by a stoichiometric amounts of donor, is oxidized by dioxygen (**III**, Fig. 2), and nicely fits a simulation curve in which it is assumed that one proton is pumped during the each **P→F** and **F→O** transition step. At the same time, when two additional electron equivalents were present after the oxidation (in the form of reduced cytochrome *c*) this led to translocation of two more protons by CcO. Even though these results provide further support for suggestion by Verkhovsky and coworkers (1999b), they are not precise enough to make a distinction between two possible models for proton pumping during enzyme re-reduction. In the first model (**III**, Fig.2, upper curve) the **O_H→E_H** transition is associated with pumping of two protons, while **E_H→R** is completely non-pumping; in the second, both of these steps are associated with pumping of one proton (**III**, Fig.2, lower curve).

The re-reduction of the **O_H** state can also be studied by laser-induced electron injection from the photosensitive dye RubiPy (tris(2,2'-bispyridyl)ruthenium [II]) and measured by time-resolved potential electrometry. In these experiments CcO was incorporated into phospholipid vesicles and was initially fully reduced in the presence of CO to form a stable heme a_3-CO complex. Addition of dioxygen into the anaerobic sample was followed by a laser flash to photolyse CO which allows the binding of O_2, followed by the oxidation of the enzyme (**III**, Fig. 3AB, blue trace). The first flash was then followed by a series of flashes to photoinject electrons from RubiPy into the **O_H** state (**III**, Fig. 3AB, red traces) with a quantum yield of about 20% (as measured using K354M mutant enzyme, similar to Verkhovsky *et al.* (2001b)). Upon excitation, during each flash, the Cu_A site becomes reduced in a 20% population of the enzyme, with a time constant of less than 0.5 μs. After that, the injected electron first equilibrates between Cu_A and heme *a* with a time constant of ~10 μs. This is then followed by a slower reaction phases that includes electron delivery to the catalytic site and several phases of proton transfer. Since electron equilibration between Cu_A and heme *a*, and transfer of protons occur across the

membrane they will be involved into ΔΨ generation. The amplitude of ΔΨ generation during each flash remained almost constant for more than 16 flashes with wild-type CcO, while the mutation of the conserved Lys_I354 in the K-pathway to methionine (K354M) resulted in strong inhibition of ΔΨ generation (**III**, Fig. 3B, red traces). This effect was, however, expected because it is well known that the reduction process in the K354M variant is strongly inhibited (Vygodina *et al.*, 1998; Ädelroth *et al.*, 1998a; Wikström *et al.*, 2000).

The kinetics of ΔΨ generation from a single flash into the $\mathbf{O_H}$ state of wild-type CcO comprised four kinetically distinguishable phases (**III**, Fig. 3C; **V**, Fig. 2B). First, a ~10 μs event (relative amplitude 12%) is due to electron equilibration between Cu_A and heme *a*, where approximately 70% of the electron population has moved to heme *a* (Paper **V**). The fast phase was followed by three phases of proton translocation with time constants of 150 μs, 800 μs, and 2.6 ms and relative amplitudes 42%, 30%, and 16% respectively.

The fast (10 μs) electron transfer phase can serve as an internal calibration of the proton transfer steps and makes it possible to estimate the overall charge translocation during the slower processes.

$\frac{12\%}{d \times 0.7} = \frac{42\% + 30\% + 16\%}{\text{number of charges}} \Rightarrow$ number of charges $= 1.64$, where d = 0.32 is the relative dielectric depth of the hemes in the membrane (section 5.2). Hence, the data suggest that the electron transfer to the binuclear site at the $\mathbf{O_H}$ state is accompanied by uptake of a substrate proton (across 1-*d*, ~0.64 charges), and pumping of another proton across the membrane.

We conclude that anaerobic reduction of the $\mathbf{O_H}$ state is coupled to translocation of two protons across the membrane: one of these protons is translocated during the $\mathbf{O_H}$ to $\mathbf{E_H}$ transition, which defines the pumping stoichiometry for the next $\mathbf{E_H}$ to **R** step also as one proton. This conclusion is supported by the virtual independence of the amplitudes of ΔΨ generation during more than 16 successive flashes. Each flash injects a single electron into a subpopulation of the enzyme, and as the sequence of flashes proceeds, and electrons accumulate in the enzyme, a considerable amount of the enzyme will then proceed through the $\mathbf{P_M}$ to **F**, and **F** to $\mathbf{O_H}$ steps due to the aerobic conditions. Comparison of the amplitude of ΔΨ generation during the initial O_2-reaction phase (first laser shot) with the amplitude generated during subsequent electron photoinjection events provides an additional control of the signal calibration. The amplitude of ΔΨ generation during the electron injection events was approximately 10 times smaller than during the

oxidation phase (**III**, Fig.3A). The quantum yield of electron injection was ~20%; when the signal was extrapolated to 100% it became about two times smaller than the amplitude in the oxidative phase (~34 mV *vs.* 60 mV), which is in a good agreement with the number of charges transferred in each of these reactions: 2 charges *vs.* 3.68 charges.

Based on the results presented here a general picture of the proton translocation steps can be drawn. The oxidative phase of the catalytic cycle is coupled to pumping of two protons: one in **P** to **F**, and one in the **F** to $\mathbf{O_H}$ transition. In continuous turnover, oxidation is followed by immediate re-reduction of CcO from cytochrome *c*, and in this case each transition in the reductive part of the catalytic cycle is also coupled to proton pumping of a single proton during each $\mathbf{O_H}$ to $\mathbf{E_H}$ and $\mathbf{E_H}$ to **R** (Fig. 10).

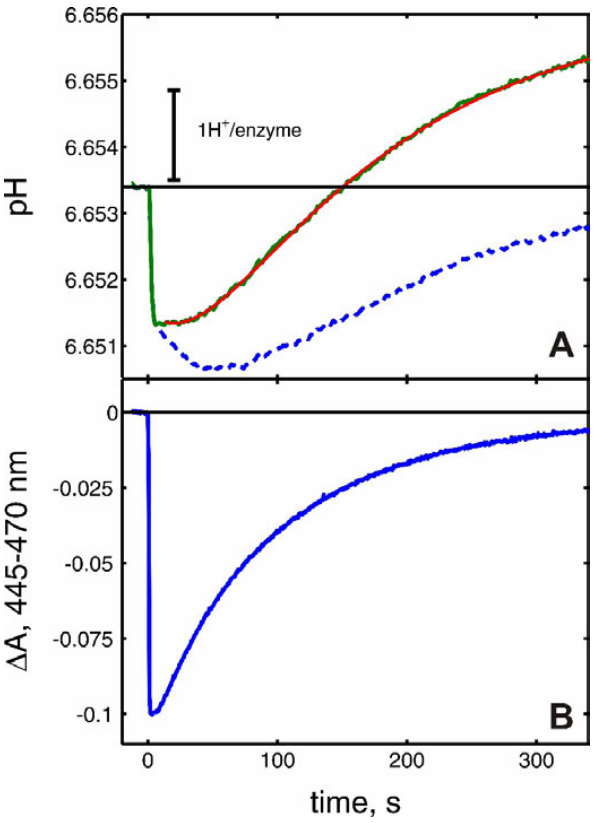

Figure 13. Proton pumping on oxidation and re-reduction after a pulse of oxygen saturated water. **A.** measurements of pH changes. Blue line, experimental curve; green line, after subtraction of protons originating from ascorbate oxidation; red line, the fit of the re-reduction part of the reaction with parameters: τ_1 ~ 42 s (amplitude, -0.0030), and τ_2 ~ 150 s (amplitude, 0.0076). **B.** Optical changes at 445-470 nm. Conditions: CcO in liposomes; KCl, 100mM; valinomycin, 1μM; sodium ascorbate, 1mM; monensin, 3nM.

The lifetime of the $\mathbf{O_H}$ state is unknown due to experimental difficulties. However we can try to estimate the lifetime of this intermediate based on results from the proton pumping measurements (Fig. 13). For these measurements, CcO reconstituted into vesicles was made anaerobic and fully reduced using a small amount of ascorbate. After that, the oxygen reaction was initiated by a stoichiometric pulse of oxygen and the resulting reaction was followed by optical spectroscopy as well as with simultaneous measurement of pH changes in the medium. The slow rate of the re-reduction process under these experimental conditions makes it possible to separate proton release during the oxidative and the subsequent re-reductive phases. The pH changes which follow the pulse consist of two phases (Fig. 13A, dashed trace): the fast phase is due to the proton pumping during the oxidative part, and the slow phase consists of events that take place during re-reduction of the enzyme: the release

of protons pumped in this phase, as well as protons released when ascorbate becomes oxidized. Under present experimental conditions, about 0.5 H^+/e^- are released into the medium due to oxidation of ascorbate. The rate of ascorbate oxidation (and therefore the rate of proton release from ascorbate) is determined by the rate of the enzyme re-reduction (Fig 13B). Using these data, it is possible to determine the pH changes that result from the oxygen pulse, excluding the protons from ascorbate (Fig. 13A, black solid line). According to a calibration using injections of anaerobic acid, about 1.5-1.6 protons per O_2 were pumped in the oxidative part of the cycle. The pH changes during the re-reduction phase could be fitted by a 2 exponential function with the following parameters: τ_1 ~ 42 s (amplitude, -0.0030), and τ_2 ~ 150 s (amplitude, 0.0076). The amplitude of the first component reflects additional pumping, which is linked to the enzyme re-reduction, of about 2.2 H^+ per enzyme. Since this is the full amplitude of proton pumping expected, it appears that little decay of the $\mathbf{O_H}$ intermediate has taken place, and that the lifetime of this state must be at least 30-40 seconds. The second component has the opposite sign, and reflects the uptake of protons for the reduction of oxygen to water and is defined by the slow rate of proton exchange between the vesicles' interior and the external reaction medium.

5.4 Proton-linked Electron Transfer from Heme a to Heme a_3 is the Driving Reaction in the Mechanism of Proton Translocation by CcO

As discussed in the previous section, proton translocation occurs four times during the catalytic cycle of CcO. Each of these transitions is associated with delivery of an electron to the catalytic site, and is coupled to uptake of a substrate proton from the N-side of the membrane to form the equivalent of water. Thus, it is very likely that the mechanism of proton translocation at each step is essentially the same, with the only variation in the final destination of the injected electron. But in order to proceed further in understanding the actual mechanism of the proton pump, it is important to establish a driving element or reaction that pushes the pump into the right direction. One approach to this problem is to study the earliest part of the oxygen reaction with fully-reduced CcO, because here it is possible to kinetically distinguish electron transfer from heme *a* to the binuclear center (during $\mathbf{A \rightarrow P_R}$) from the next step ($\mathbf{P_R \rightarrow F}$) - when uptake of both the substrate and the pumped protons take place from the aqueous N-side.

The combination of time-resolved optical spectroscopy with potential electrometry is a tool that gives information about both redox changes of the metal centers and vectorial movement of protons during transitions of the catalytic cycle. The $\Delta\Psi$ generation in the reaction of the fully-

reduced CcO with oxygen at neutral pH develops in two major kinetically distinguishable phases (**IV**, Fig. 2a) that were previously assigned to the $\mathbf{P_R \rightarrow F}$ and **F→O** transitions (Jasaitis *et al.*, 1999). In the first two phases, **R→A** and $\mathbf{A \rightarrow P_R}$, Jasaitis *et al.* (1999) observed little or no electrometric signal and concluded that there was essentially no charge transfer during these transitions. Formation of compound **A** is indeed not linked to any charge movement, while the next phase includes electron equilibration between heme *a* and the binuclear center. Even though this electron equilibration is electrometrically silent itself, due to the location of donor and acceptor at the same depth within the membrane, it is possible that this process is linked to some internal proton movement. However the large amplitude of ΔΨ in the subsequent reaction step might overwhelm possible signal of such charge translocation during $\mathbf{A \rightarrow P_R}$, obscuring the amplitude of the earlier phase in a multi-exponential fit. When we studied the oxygen reaction in alkaline conditions, where the rates of both $\mathbf{P_R \rightarrow F}$ and **F→O** transitions are known to be decelerated (Brändén *et al.*, 2005), the rate of the slow ΔΨ generation step (**F→O**) was indeed slowed down, but the rate of the preceding electrometric phase appeared to be accelerated with a shortening of the initial lag phase (**IV**, Fig. 2ab). Furthermore, in alkaline conditions the fast phase of ΔΨ generation overlapped in time with the kinetics of the earlier reaction step ($\mathbf{A \rightarrow P_R}$) as measured spectroscopically (**IV**, Fig. 2c). This indicates that ΔΨ is already beginning to develop during $\mathbf{A \rightarrow P_R}$ and that the fast phase of ΔΨ generation actually consists of two electrogenic phases that are differently affected by pH. The amplitude of ΔΨ generation during $\mathbf{A \rightarrow P_R}$ is pH-independent, while during the following $\mathbf{P_R \rightarrow F}$ it is initially large but decreases with pH.

Additional support for ΔΨ generation during $\mathbf{A \rightarrow P_R}$ was obtained from measurements on the Asp_I124 to asparagine (D124N) mutant enzyme. In the D124N mutant the entrance of the D-pathway is blocked by the mutation, which impairs proton pumping (Thomas *et al.*, 1993a; Fetter *et al.*, 1995) and strongly inhibits proton transfer through the D-channel (Smirnova *et al.*, 1999). Because the amplitude of the major electrogenic phases during the $\mathbf{P_R \rightarrow F}$ and **F→O** transition steps are decreased in D124N, it is possible to resolve the early transient during $\mathbf{A \rightarrow P_R}$. The fast phase of ΔΨ generation in D124N, measured at pH 7, coincided with the fast phase in the wild-type enzyme at pH 10.5 indicating that the early phase of charge translocation during the $\mathbf{A \rightarrow P_R}$ transition also occurs at neutral pH (**IV**, Fig. 2b).

The importance, for the proton pumping mechanism, of the electron transfer that takes place during $\mathbf{A \rightarrow P_R}$ can be assessed by studying the oxygen reaction starting from the mixed-valence

state of the enzyme, where only heme a_3 and Cu_B are reduced, and the electron transfer from heme *a* does not take place. In this case the oxygen reaction is not coupled to any charge translocation (Jasaitis *et al.*, 1999), though the scission of the O-O bond occurs in the normal way. This demonstrates that the early charge translocation during **A→P$_R$** completely depends on the electron transfer from heme *a* to the binuclear center.

From the amplitude of ΔΨ generation during **A→P$_R$** (~8% of ΔΨ generation during oxidative part of the catalytic cycle) it is possible to estimate the relative distance of the charge transfer in this step. Since during **R→O** about 3.68 charges are transferred across the membrane (Verkhovsky *et al.*, 1999b), the **A→P$_R$** transition will be coupled to transfer of one electrical charge across ~27% of the membrane dielectric. From the fact that the electron equilibration from heme *a* and the binuclear center is electrometrically silent, we can assign this charge translocation phase to internal proton movement towards the P-side of the membrane. The conserved residue Glu_I278 at the end of the D-pathway may be proposed as a proton donor. Electrometric measurements of charge translocation in the E278Q mutant enzyme strengthen this assignment, as virtually no charge transfer was detected during **A→P$_R$** (Paper **IV**, supplementary material). The acceptor of the proton in this reaction is most likely some as yet unidentified group ("pump site") above the hemes; this cannot be the binuclear center itself since proton arrival at this center would produce **F**, which is formed only in the subsequent reaction step. Our results suggest that the proton transfer from Glu_I278 to this unidentified location above the heme groups is responsible for ΔΨ generation during **A→P$_R$**, and that this is the initial step of the proton pump mechanism.

With these new results, the stoichiometry of charge translocation during each single transition in the oxidative phase of the catalytic cycle can be deduced. The total amplitude of charge translocation during the oxidative part of the cycle corresponds to transfer of 3.68 charges across the membrane (Verkhovsky *et al.*, 1999b). This number includes transfer of an electron from Cu_A to heme *a* across 0.32 of the membrane, transfer of 2 protons across the membrane, and delivery of 2 protons to the catalytic site for water formation across 0.68 of the membrane. How is the movement of all of these charges organized during the oxidative part of the catalytic cycle?

1. The first transition **R→A** comprises oxygen binding to heme a_3 and is electrically silent.
2. The next step, **A→P_R** includes the transfer of a proton across 0.27 of the membrane, from Glu_I278 at the end of the D-pathway to the "pump site". There is simultaneous electron redistribution between hemes *a* and a_3, but this takes place in the plane of the membrane and is thus electrically silent.
3. During **P_R→F** the charge translocation is due to
   - delivery of the a "chemical" proton to the catalytic site across 0.68 of the membrane;
   - electron redistribution between Cu_A and heme *a*, which gives a relative electrometric amplitude of: 0.32 × 0.6 = 0.19, where 0.6 is the extent of electron transfer from Cu_A in this step (Hill, 1991), and 0.32 is the fraction of the total membrane dielectric crossed by the electron;
   - proton pumping events such as reprotonation of Glu_I278 from the N-side of the membrane and ejection of a proton that was preloaded to the "pump site". In total these events will account for proton transfer across 1 - 0.27 = 0.73 of the membrane dielectric.

→→ Total: 0.68 + 0.19 + 0.73 = 1.6 charges across the membrane.

4. The final transition in the oxidative part of the cycle, **F→O_H,** consists of delivery of another chemical proton to the catalytic site across 0.68 of the membrane, electron transfer from Cu_A to heme *a*: 0.32 × 0.4 = 0.13, where 0.32 is the fraction of the total membrane dielectric crossed by the electron and 0.4 the extent of electron transfer from Cu_A, and pumping of a proton across the membrane – 1.0. In total the **F→O_H** transition is responsible for transfer of 0.68 + 0.13 + 1.0 = 1.81 charges.

5.5 Single Proton Translocation Cycle

In the continuous turnover regime, the catalytic cycle of CcO consists of four proton translocation steps (section 5.3; Fig. 10). In each step delivery of an electron to the enzyme starts a proton pump cycle, which is likely to occur by essentially the same mechanism every time the electron arrives. In principle, the mechanism of proton translocation during a single pump event can be studied at any of these steps; however the **O_H→E_H** transition is favorable for study due to high yield (almost 100%) of the **O_H** state in the reaction of the fully-reduced CcO with dioxygen.

The $\mathbf{O_H \rightarrow E_H}$ reaction was initiated by electron injection from the photosensitive dye RubiPy (see section 5.3) and followed by both time-resolved optical spectroscopy and electrometry. Upon a laser flash, an excited molecule of RubiPy donated an electron to Cu_A with a time constant less than 0.5 μs. This reduction of Cu_A was seen as an unresolved drop of absorption at 820 nm (**V**, Fig. 2A). This process was followed by electron equilibration ($\tau \sim 10$ μs) between Cu_A and heme *a*, in which about 70% of the electron population has been transferred (**V**, Fig. 2A, 3A). From the amplitude of $\Delta\Psi$ generation measured under the same conditions (**V**, Fig. 2B) we can conclude that the 10 μs phase is due to electron transfer only, without any internal proton translocation. Since the midpoint redox potential (E_m) of Cu_A is about 250 mV (Zickermann *et al.*, 1995; Gorbikova *et al.*, 2006) it is possible to estimate the E_m value for heme *a* as ~270 mV. Electron equilibration between Cu_A and heme *a* is not coupled to proton uptake (Oliveberg *et al.*, 1989; Ruitenberg *et al.*, 2000; Siletsky *et al.*, 2004) which accounts for the relatively low "operational" E_m of heme *a*, which is much lower than the "high asymptotic" E_m found in equilibrium redox titrations (Artzatbanov *et al.*, 1978; Wikström *et al.*, 1981; Blair *et al.*, 1986; Moody and Rich, 1990; Gorbikova *et al*, 2006). However, this potential is still high enough for heme *a* to accept part of the electron population from Cu_A without charge compensation by a proton. We saw no electron transfer to the binuclear center during the 10 μs phase, which indicates that the E_m values of heme a_3 and Cu_B must be at least as low as 150 mV.

The next phase with $\tau \sim 150$ μs consisted of complete oxidation of Cu_A, and in reoxidation of about 45% of the population of reduced heme *a*, by electron transfer to the binuclear center (new equilibrium: ~40% of electron on heme *a*, and ~60% on heme a_3). Electrometric measurements showed charge transfer across a fraction of about 0.84 of the membrane dielectric (**V**, Fig. 2B) during this phase. Of this, proton transfer accounts for $0.84 - 0.32 \times 0.3 = 0.74$, where 0.32 is the fraction of the total membrane dielectric crossed by the electron and 0.3 is the extent of electron transfer from Cu_A. Proton uptake in this phase (as was judged from the amplitude of $\Delta\Psi$ formation) raises the E_m of both hemes to approximately similar values ($\Delta E_m \sim 10$ mV); unfortunately, it is not possible to make a quantitative assessment of their E_m values at this point in the reaction because our internal redox indicator - Cu_A - is completely oxidized. However, we can conclude that the potentials of the two hemes are both about 370 mV, which corresponds to the "high-asymptotic" E_m value measured in anaerobic redox titrations where there is equilibrium with protons (Blair *et al.*, 1986; Wikström *et al.*, 1981; Gorbikova *et al.*, 2006). The intrinsic electron equilibration between heme a_3 and heme *a* occurs in about 1 ns (Verkhovsky *et al.*, 2001a; Pilet *et al.*, 2004) in agreement with the short edge-to-edge distance between the

hemes (Page *et al.*, 1999). This rate is however much faster than the observed electron equilibration between these centers during $\mathbf{O_H \rightarrow E_H}$ (150 μs), which also indicates involvement of protons in this reaction step. The acceptor of the electron during 150 μs phase can be identified from the kinetic spectra of this and the following phases, after subtracting the contribution from oxidation of heme *a* (**V**, Fig. 3C). Based on reversibility of changes in the 560-620 nm spectral region during the 150 μs and the subsequent 800 μs phases we were able to assign heme a_3 as the electron acceptor during the 150 μs phase.

The last phase observed by optical absorbance has $\tau \sim 800$ μs; here heme *a* becomes completely oxidized by electron transfer to the binuclear center. The final acceptor of the electron can be deduced from the spectral difference between the final state and the initial state before electron injection (**V**, Fig. 3B). The only feature seen in the difference spectrum is a blue shift of the 665-nm charge transfer band that can be ascribed to reduction of Cu_B. Because after this phase all redox centers except Cu_B are oxidized we were able to estimate the E_m value of Cu_B as more than 100 mV higher than that of heme *a*. Based on electrometric results, the 800 μs phase is coupled to proton transfer across a ~0.60 fraction of the membrane.

The 150 and 800 μs phases together make the largest contribution to the total $\Delta\Psi$ generation in this reaction, and it is these two phases where uptake and transfer of pumped and substrate protons takes place. The fate of the proton which is being transferred at each phase can be established based on an estimation of the E_m values of the redox cofactors in the binuclear center. Arrival of the pumped proton at the "pump site" in proximity to the binuclear center should increase the E_m of the binuclear center much less than the entry of the "chemical" proton directly into the binuclear center. Based on this logic it is possible to assign the 150 μs phase to uptake of the pumped proton from the N-side of the membrane, and the 800 μs phase to uptake of the substrate proton.

Interestingly, in addition to the three phases that are coupled to the electron transfer reaction, the kinetics of $\Delta\Psi$ generation included an extra component that was not detected in the optical measurements. This phase has $\tau \sim 2.6$ ms and is linked to transfer of 0.32 charges across the membrane dielectric. Most likely this phase is due to relaxation of the protein and release of the pumped proton from the "pump site" towards the P-side of the membrane.

Based on the data obtained we can propose a possible mechanism of proton pumping by CcO. During single-electron reduction of the $\mathbf{O_H}$ state of CcO, the electron first enters the Cu_A center. In the next phase the electron equilibrates between Cu_A and heme *a*, with $\tau \sim 10$ μs (**V**, Fig. 4, I→II). The arrival of electron on heme *a* raises the pK_a of a yet unidentified "pump site" above the heme groups, which takes up a proton with $\tau \sim 150$ μs (**V**, Fig. 4, II→III). The protonation of the "pump site" occurs from the conserved $Glu_I278(242)$ via a chain of water molecules by the Grotthuss mechanism (de Grotthuss, 1806&2006; Nagle and Morowitz, 1978; Agmon, 1995) (Fig. 7). Three or four water molecules are predicted to reside inside the hydrophobic cavity between the glutamate, the Δ-propionate of heme a_3, and the binuclear center (Riistama *et al.*, 1997; Zheng *et al.*, 2003). These water molecules are sensitive to the redox-state-dependent electric field between heme *a* and the binuclear center, and arrange themselves into two different configurations for proton transfer (Wikström *et al.*, 2003). When the binuclear center is oxidized and the electron is on heme *a*, the array of water molecules is oriented towards the Δ-propionate of heme a_3 ("pump site" direction); however this array switches towards the binuclear center (the direction for chemical reaction) after reduction of the binuclear center from heme *a*. The rate-limiting protonation of the "pump site" raises the E_m of both hemes, and leads to further electron equilibration between Cu_A and the two hemes in the same time window (**V**, Fig. 4, III→IV). At the end of the 150 μs phase Cu_A is fully oxidized, while heme *a* and heme a_3 have 40% and 60% of the injected electron population respectively. In addition, the 150 μs phase includes reprotonation of Glu_I278 from the N-side of the membrane via the proton conducting D-pathway.

In the next phase ($\tau \sim 800$ μs), transfer of a substrate proton to the OH^- ligand of Cu_B (Fann *et al.*, 1995) raises the E_m of Cu_B to a value much higher than those of all other redox centers, which induces ultimate movement of the injected electron to the Cu_B center (**V**, Fig. 4, IV→V).

During the last step ($\tau \sim 2.6$ ms) of the single proton pump cycle, the proton, which has been "preloaded" into the "pump site", is expelled towards the P-side of the membrane due to electrostatic repulsion from the substrate proton.

It seems feasible that the mechanism of proton translocation during $\mathbf{P_M \rightarrow F}$, $\mathbf{F \rightarrow O_H}$, and $\mathbf{E_H \rightarrow R}$ is essentially the same as in the $\mathbf{O_H \rightarrow E_H}$ transition with the only difference being the final destination of the injected electron. After oxygen activation, CcO has 4 high potential acceptors that are sequentially filled with electrons during each of the pumping transition steps. Thus, the

sequence of events shown in Figure 4 (Paper **V**) would be repeated every time an electron enters the Cu_A site. In each case the electron travels from cytochrome *c* to Cu_A, and subsequently through heme *a* to the binuclear center, driving proton pumping across the membrane.

6. SUMMARY

In this work we have applied a complex approach using a variety of different techniques to study the properties and the mechanism of proton translocation by the terminal oxidases. The combination of direct measurements of pH changes during catalytic turnover, time-resolved potentiometric electrometry and optical spectroscopy, made it possible to obtain valuable information about various aspects of oxidase functioning.

We compared oxygen binding properties of oxidases from the distinct heme-copper and cytochrome *bd* families and found that cytochrome *bd* indeed has a high affinity for oxygen, which is 3 orders of magnitude higher than that of CcO. Interestingly, the difference between CcO and cytochrome *bd* is not only in higher affinity of the latter to oxygen, but also in the way that each of these enzymes traps oxygen during catalysis. CcO traps oxygen kinetically - the molecule of bound dioxygen is rapidly reduced before it can dissociate. In contrast cytochrome *bd* employs an alternative mechanism of oxygen trapping - part of the redox energy is invested into tight oxygen binding, and the price paid for this is the lack of proton pumping.

A single cycle of oxygen reduction to water is characterized by translocation of four protons across the membrane. Our results make it possible to assign the pumping steps to discrete transitions of the catalytic cycle and indicate that during *in vivo* turnover of the oxidase these four protons are transferred, one at a time, during the **P→F**, **F→O_H**, **O_H→E_H**, and **E_H→R** transitions. At the same time, each individual proton translocation step in the catalytic cycle is not just a single reaction catalyzed by CcO, but rather a complicated sequence of interdependent electron and proton transfers. We assume that each single proton translocation cycle of CcO is assured by internal proton transfer from the conserved Glu_I278(242) to an as yet unidentified “pump site” above the hemes. Delivery of a proton to the “pump site” serves as a driving reaction that forces the proton translocation cycle to continue.

Based on our study of the electron backflow reaction we conclude that it is important to be particularly cautious about comparison of results that are obtained with membrane proteins under different environmental conditions, especially when comparing the results from reconstituted and soluble systems, because it is possible that some functional properties may be altered.

7. ACKNOWLEDGEMENTS

This study was performed in the Helsinki Bioenergetics Group at the Institute of Biotechnology and at the Division of Biochemistry, Faculty of Biosciences, University of Helsinki. The Academy of Finland, the University of Helsinki, Biocentrum Helsinki, and the Sigrid Jusélius Foundation are kindly acknowledged for financial support of the work.

I would like to thank my academic advisers Dr. Michael Verkhovsky and Prof. Mårten Wikström sincerely for providing me continuous support, help, and the great opportunity to work in their team over these years. Their enthusiastic approach was extremely encouraging.

I would like to express my gratitude to all past and present members of the Helsinki Bioenergetics Group for their invaluable assistance, enjoyable discussions, company in trips, banters and inspiration. In particular, I especially would like thank Audrius Jasaitis, Dima Bloch, Anne Tuukkanen, Anne Puustinen, Camilla Ribacka for collaboration; Pamela David, Liliya Euro, Mika Molin, Vivek Sharma, and Ville Kaila for being able to share the office space with me; Marina Verkhovskaya, Virve Rauhamäki, Elena Gorbikova, Liisa Laakkonen, Markus Kaukonen for kind and efficient help in the lab premises and *in silico* matters. The huge special thank is to my external co-authors - Vitaliy Borisov, and Alexander Konstantinov from the Moscow State University.

I thank the reviewers, Prof. Ilmo Hassinen and Prof. Joel Morgan for critical reading of the thesis and their constructive comments, which I found extremely valuable.

The kindest appreciation is to our lab technicians and research assistants Eija Haasanen, Tarja Salojärvi, and Anne Hakonen for their excellent technical expertise. Also I want to express a special thank is to our former secretary Satu Sankkila who was solving all practical problems with confidence, and took a good care of me from my first days in Finland.

I deeply thank all my friends who are now all other the world but still are able to share with me their kindness and friendship. Especially I would like to thank those who are now in Finland - Tolya Verkhovsky, Rasa Gabrenaite-Verkhovskaya, Evgeny Kulesskiy, Alexey Adamov, Niina Juuti, Dima Tisnek, Petteri Kuuskoski, Dima Shchigel, and my other friends for the great time and the lighting up the dull autumn days.

Finally and most importantly, I would like to thank my family. I am sincere grateful to my wife Katya and to my parents Galina and Nikolay for their love. This work would never have been completed without their support.

Ilya Belevich,
Helsinki, September 2007

8. REFERENCES

Aasa, R., Albracht, S.P.J., Falk, K-E., Lanne, B., and Vanngård, T. (1976) // *Biochim. Biophys. Acta*, **422**, 260-272.

Abramson, J., Riistama, S., Larsson, G., Jasaitis, A., Svensson-Ek, M., Laakkonen, L., Puustinen, A., Iwata, S. and Wikström, M. (2000) // *Nat. Struct. Biol.*, **7**, 910-917.

Agmon, N. (1995) // *Chem. Phys. Lett.*, **244**, 456-462.

Alben, J.O., Moh, P.P., Fiamingo, F.G., and Altschuld, R.A. (1981) // *Proc. Natl. Acad. Sci. USA*, **78**, 234-237.

Anraku, Y., and Gennis, R.B. (1987) // *Trends Biochem. Sci.*, **12**, 262-266.

Antalis, T.M., and Palmer, G. (1982) // *J. Biol. Chem.*, **257**, 6194-6206.

Antholine, W.E., Kastrau, D.H.W., Steffens, G.C.M., Buse, G., Zumft, W.G., and Kroneck, P.M.H. (1992) // *Eur. J. Biochem.*, **209**, 875-881.

Antonini, E., Brunori, M., Colosimo, A., Greenwood, C., and Wilson, M.T. (1977) // *Proc. Natl. Acad. Sci. USA*, **74**, 3128-3132.

Arnold, S., Goglia, F., and Kadenbach, B. (1998) // *Eur. J. Biochem.*, **252**, 325-330.

Artzatbanov, V.Yu., Konstantinov, A.A., and Skulachev, V.P. (1978) // *FEBS Lett.*, **78**, 180-185.

Babcock, G.T., Vickery, L.E., and Palmer, G. (1976) // *J. Biol. Chem.*, **251**, 7907-7919.

Babcock, G.T., Callahan, P.M., Ondrias, M.R., and Salmeen, I. (1981) // *Biochemistry*, **20**, 959-966.

Babcock, G.T., and Callahan, P.M. (1983) // *Biochemistry*, **22**, 2314-2319.

Babcock, G.T., and Wikström, M. (1992) // *Nature*, **356**, 301-309.

Baker, G.M., Noguchi, M., and Palmer, G. (1987) // *J. Biol. Chem.*, **262**, 595-604.

Beinert, H., Griffiths, D.E., Wharton, D.C., and Sands, R.H. (1962) // *J. Biol. Chem.*, **237**, 2337-2346.

Beinert, H., Hansen, R.E., and Hartzell, C.R. (1976) // *Biochim. Biophys. Acta*, **423**, 339-355.

Berry, E.A., and Trumpower, B. (1985) // *J. Biol. Chem.*, **260**, 2458-2467.

Berry, S., Schneider, D., Vermaas, W.F.J., and Rönger, M. (2002) // *Biochemistry*, **41**, 3422-3429.

Bickar, D., Bonaventura, J., and Bonaventura, C. (1982) // *Biochemistry*, **21**, 2661-2666.

Blackmore, R.S., Greenwood, C., and Gibson, Q.H. (1991) // *J. Biol. Chem.*, **266**, 19245-19249.

Blair, D.F., Witt, S.N., and Chan, S.I. (1985) // *J. Am. Chem. Soc.*, **107**, 7389-7399.

Blair, D.F., Ellis, W.R.Jr., Wang, H., Gray, H.B., and Chan, S.I. (1986) // *J. Biol. Chem.*, **261**, 11524-11537.

Boelens, R., and Wever, R. (1979) // *Biochim. Biophys. Acta*, **547**, 296-310.

Bogachev, A.V., Murtazina, R.A., and Skulachev V.P. (1996) // *J. Bacteriol.*, **178**, 6233-6237.

Borisov, V.B., Liebl, U., Rappaport, F., Martin, J.-L., Zhang, J., Gennis, R.B., Konstantinov, A.A., and Vos, M.H. (2002) // *Biochemistry*, **41**, 1654-1662.

Brzezinski, P. (1996) // *Biochemistry*, **35**, 5611-5615.

Brzezinski, P., and Larsson, G. (2003) // *Biochim. Biophys. Acta*, **1605**, 1-13.

Brändén, G., Brändén, M., Schmidt, B., Mills, D.A., Ferguson-Miller, S., and Brzezinski, P. (2005) // *Biochemistry*, **44**, 10466-10474.

Brändén, M., Sigurdson, H., Namslauer, A., Gennis, R.B., Ädelroth, P., and Brzezinski, P. (2001) // *Proc. Natl. Acad. Sci. USA*, **98**, 5013-5018.

Brändén, M., Tomson, F., Gennis, R.B., and Brzezinski, P. (2002) // *Biochemistry*, **41**, 10794-10798.

Brändén, M., Namslauer, A., Hansson, O., Aasa, R., and Brzezinski, P. (2003) // *Biochemistry*, **42**, 13178-13184.

Buse, G., Soulimane, T., Dewor, M., Meyer, H.E., and Blüggel, M. (1999) // *Prot. Sci.*, **8**, 985-990.

Bushnell, G.W., Louie, G.V., and Brayer G.D. (1990) // *J. Mol. Biol.*, **214**, 585-595.
Calhoun, M.W., Thomas, J.W., and Gennis R. (1994) // *Trends Biochem. Sci.*, **19**, 325-330.
Callahan, P.M., and Babcock, G.T. (1983) // *Biochemistry*, **22**, 452-461.
Cao, J., Shapleigh, J., Gennis, R., Revzin, A., and Ferguson-Miller, S. (1991) // *Gene*, **101**, 133-137.
Cao, J., Hosler, J., Shapleigh, J., Revzin, A., and Ferguson-Miller, S. (1992) // *J. Biol. Chem.*, **267**, 24273-24278.
Capaldi, R.A. (1990) // *Annu.Rev.Biochem.*, **59**, 569-596.
Capitanio, N., Vygodina, T.V., Capitanio, G., Konstantinov, A.A., Nicholls, P., and Papa, S. (1997) // *Biochim. Biophys. Acta*, **1318**, 255-265.
Carroll, J., Shannon, R.J., Fearnley, I.M., Walker, J.E., and Hirst, J. (2002) // *J. Biol. Chem.*, **277**, 50311– 50317.
Casey, R.P., Chappell, J.B., and Azzi, A. (1979) // *Biochem. J.*, **182**, 149-156.
Caughey, W.S., Smythe, G.A., O'Keeffe, D.H., Maskasky, J.E., and Smith, M.L. (1975) // *J. Biol. Chem.*, **250**, 7602-7622.
Chance, B., Saronio, C., and Leigh, J.S.Jr. (1975) // *J. Biol. Chem.*, **250**, 9226-9237.
Crofts, A.R. (2004) // *Annu. Rev. Physiol.*, **66**, 689-733.
de Grotthuss, C.J.T. (1806) // *Ann. Chim. (Paris)*, **LVIII**, 54-74.
de Grotthuss, C.J.T. (2006) // *Biochim. Biophys. Acta*, **1757**, 871-875.
D'mello, R., Hill, S., and Poole, R.K. (1996) // *Microbiology*, **142**, 755-763.
Drachev, L.A., Jasaitis, A.A., Kaulen, A.D., Kondrashin, A.A., Liberman, E.A., Nemecek, I.B., Ostroumov, S.A., Semenov, A.Y., and Skulachev, V.P. (1974) // *Nature*, **249**, 321-324.
Drachev, L.A., Kaulen, A.D., Semenov, A.Y., Severina, I.I., and Skulachev, V.P. (1979) // *Anal. Biochem.*, **96**, 250-262.
Draghi, F., Miele, A.E., Traveglini-Allocatelli, C., Vallone, B., Brunori, M., Gibson, Q.H., and Olson, J.S. (2002) // *J. Biol. Chem.*, **277**, 7509-7519.
Dutton, P.L., and Wilson, D.F. (1974) // *Biochim. Biophys. Acta*, **346**, 165-212.
Einarsdóttir, Ó., and Caughey, W.S. (1985) // *Biochem. Biophys. Res. Commun.*, **129**, 840-847.
Einarsdóttir, Ó., Georgiadis, K.E., and Sucheta, A. (1995) // *Biochemistry*, **34**, 496-508.
Fabian, M., Wong, W.W., Gennis, R.B., and Palmer, G. (1999) // *Proc. Natl. Acad. Sci. USA*, **96**, 13114-13117.
Fann, Y.C., Ahmed, I., Blackburn, N.J., Boswell, J.S., Verkhovskaya, M.L., Hoffman, B.M., and Wikström, M. (1995) // *Biochemistry*, **34**, 10245-10255.
Faxén, K., Gilderson, G., Ädelroth, P., and Brzezinski, P. (2005) // *Nature*, **437**, 286-289.
Ferguson-Miller, S., Brautigan, D.L., and Margoliash, E. (1978) // *J. Biol. Chem.*, **253**, 149-159.
Fetter, J.R., Qian, J., Shapleigh, J., Thomas, J.W., Garcia-Horsman, A., Schmidt, E., Hosler, J., Babcock, G.T., Gennis, R.B., and Ferguson-Miller, S. (1995) // *Proc. Natl. Acad. Sci. USA*, **92**, 1604-1608.
Fry, H.C., Hoertz, P.G., Wasser, I.M., Karlin, K.D., and Meyer, G.J. (2004) // *J. Am. Chem. Soc.*, **126**, 16712-16713.
Fuller, S.D., Darley-Usmar, V.M., and Capaldi, R.A. (1981) // *Biochemistry*, **20**, 7046-7053.
Garcia-Horsman, J.A., Barquera, B., Rumbley, J., Ma., J., and Gennis, R. (1994) // *J. Bacteriol.*, **176**, 5587-5600.
Gelles, J., Blair, D.F., and Chan, S.I. (1986) // *Biochim. Biophys. Acta*, **853**, 205-236.
Geren, L.M., Beasley, J.R., Fine, B.R., Saunders, A.J., Hibdon, S., Pielak, G.J., Durham, B., and Millet, F. (1995) // *J. Biol. Chem.*, **270**, 2466-2472.
Gibson, Q.H., and Greenwood, C. (1963) // *Biochem. J.*, **86**, 541-555.
Gibson, Q.H., and Greenwood, C. (1964) // *J. Biol. Chem.*, **239**, 586-590.
Gnaiger, E. (2003) // *Adv. Exp. Med. Biol.*, **543**, 39-55.
Gorbikova, E.A., Vuorilehto, K., Wikström, M., and Verkhovsky, M.I. (2006) // *Biochemistry*, **45**, 5641-5649.

Gray, H.B., and Winkler, J.R. (1996) // *Annu. Rev. Biochem.*, **65**, 537-561.
Green, G.N., Lorence, R.M., and Gennis, R.B. (1986) // *Biochemistry*, **25**, 2309-2314.
Hallén, S., Brzezinski, P., and Malmström, B.G. (1994) // *Biochemistry*, **33**, 1467-1472.
Haltia, T., Finel, M., Harms, N., Nakari, T., Raitio, M., Wikström, M., and Saraste, M. (1989) // *EMBO J.*, **8**, 3571-3579.
Haltia, T., Saraste, M., and Wikström, M. (1991) // *EMBO J.*, **10**, 2015-2021.
Haltia, T., Semo, N., Arrondo, J.L.R., Goñi, F.M., and Freire, E. (1994) // *Biochemistry*, **33**, 9731-9740.
Han, S., Ching, Y.-C., and Rousseau, D.L. (1990a) // *Proc. Natl. Acad. Sci. USA*, **87**, 2491-2495.
Han, S., Ching, Y.-C., and Rousseau, D.L. (1990b) // *Proc. Natl. Acad. Sci. USA*, **87**, 8408-8412.
Harrenga, A. and Michel, H.(1999) // *J. Biol. Chem.*, **274**, 33296-33299.
Hazzard, J.T., Rong, S-Y., and Tollin, G. (1991) // *Biochemistry*, **30**, 213-222.
Hendler, R.W., Pardhasaradhi, K., Reynafarje, B., and Ludwig, B. (1991) // *Biophys. J.*, **60**, 415-423.
Hendriks, J.H.M., Jasaitis, A., Saraste, M., and Verkhovsky, M.I. (2002) // *Biochemistry*, **41**, 2331-2340.
Hill, B.C. (1991) // *J. Biol. Chem.*, **266**, 2219-2226.
Hill, B.C. (1994) // *J. Biol. Chem.*, **269**, 2419-2425.
Hill, B.C., and Greenwood, C. (1983) // *Biochem. J.*, **215**, 659-667.
Hill, B.C., and Greenwood, C. (1984) // *Biochem. J.*, **218**, 913-921.
Hill, B.C., Hill, J.J., and Gennis, R.B. (1994) // *Biochemistry*, **33**, 15110-15115.
Hill, S., Viollet, S., Smith, A.T., and Anthony, C. (1990) // *J. Bacteriol.*, **172**, 2071-2078.
Hinchliffe, P., and Sazanov L.A. (2005) // *Science*, **309**, 771-774.
Hinkle, P.C. (1979) // *Methods Enzymol.*, **55**, 748-751.
Hirst, J. (2005) // *Biochem. Soc. Trans.*, **33(3)**, 525-529.
Hofacker, I., and Schulten, K. (1998) // *Proteins: Structure, Function and Genetics*, **30**, 100-107.
Horie, S., and Morrison, M. (1963) // *J. Biol. Chem.*, **238**, 1855-1860.
Horsefield, R., Iwata S., and Byrne., B. (2004) // *Curr. Protein Pept. Sci.*, **5**, 107-118.
Hosler, J.P., Ferguson-Miller, S., Calhoun, M.W., Thomas, J.W., Hill, J., Lemieux, L, Ma, J., Georgiou, C., Fetter, J., Shapleigh, J., Tecklenburg, M.M.J., Babcock, G.T., and Gennis, R. (1993) // *J. Bioenerg. Biomembr.*, **25**, 121-136.
Hosler, J.P., Espe, M.P., Zhen, Y., Babcock, G.T., Ferguson-Miller, S. (1995) // *Biochemistry*, **34**, 7586-7592.
Hosler, J.P., Shapleigh, J.P., Mitchell, D.M., Kim, Y., Pressler, M.A., Georgiou, C., Babcock, G.T., Alben, J.O., Ferguson-Miller, S., and Gennis, R.B. (1996) // *Biochemistry*, **35**, 10776-10783.
Hunsicker-Wang, L.M., Pacoma, R.L., Chen, Y., Fee, J.A. and Stout, C.D. (2005) // *Acta Crystallogr., Sect.D,* **61**, 340-343.
Iwata, S., Ostermeier, C., Ludwig, B., and Michel, H. (1995) // *Nature*, **376**, 660-669.
Jancura, D., Berka, V., Antalik, M., Bagelova, J., Gennis, R.B., Palmer, G., and Fabian, M. (2006) // *J. Biol. Chem.*, **281**, 30319-30325.
Jasaitis, A., Verkhovsky, M.I., Morgan, J.E., Verkhovskaya, M.L., and Wikström, M. (1999) // *Biochemisty*, **38**, 2697-2706.
Jasaitis, A., Backgren, C., Morgan, J.E., Puustinen, A., Verkhovsky, M.I., and Wikström, M. (2001) // *Biochemistry*, **40**, 5269-5274.
Joseph-Horne, T., Hollomon, D.W., and Wood, P.M. (2001) // *Biochim. Biophys. Acta*, **1504**, 179-195.
Jünemann, S., Butterworth, P.J., and Wrigglesworth, J.M. (1995) // *Biochemistry*, **34**, 14861-14867.
Kadenbach, B., and Merle, P. (1981) // *FEBS Lett.*, **135**, 1-11.

Kadenbach, B., Hüttemann, M., Arnold, S., Lee, I., and Bender, E. (2000) // *Free Radical Biol. Med.*, **29**, 211-221.

Kannt, A., Lancaster, C.R.D., and Michel, H. (1998) // *J. Bioenerg. Biomembr.*, **30**, 81-87.

Kannt, A., Pfitzner, U., Ruitenberg, M., Hellwig, P., Ludwig, B., Mäntele, W., Fendler, K., and Michel, H. (1999) // *J. Biol. Chem.*, **274**, 37974-37981.

Karlsson, B., and Andreasson, L.-E. (1981) // *Biochim. Biophys. Acta*, **635**, 73-81.

Karlsson, B., Aasa, R., Vänngård, T., and Malmström, B.G. (1981) // *FEBS Lett.*, **131**, 186-188.

Karpefors, M., Ädelroth, P., Zhen, Y., Ferguson-Miller, S., and Brzezinski, P. (1998) // *Proc. Natl. Acad. Sci. USA*, **95**, 13606-13611.

Karpefors, M., Ädelroth, P., Namslauer, A., Zhen, Y., and Brzezinski, P. (2000) // *Biochemistry*, **39**, 14664-14669.

Keilin, D. (1925) // *Proc. R. Soc. Lond. B Biol. Sci.*, **98**, 312-339.

Keilin, D. (1927) // *Nature*, **119**, 670-671.

Kelly, M.J.S., Poole, R.K., Yates, M.G., and Kennedy, C. (1990) // *J. Bacteriol.*, **172**, 6010-6019.

Kelly, M., Lappalainen, P., Talbo, G., Haltia, T., van der Oost, J., and Saraste, M. (1993) // *J. Biol. Chem.*, **268**, 16781-16787.

Kirichenko, A., Vygodina, T., Mkrtchyan, H.M., and Konstantinov, A. (1998) // *FEBS Lett.*, **423**, 329-333.

Kita, K., Konishi, K., and Anraku, Y. (1984) // *J. Biol. chem.*., **259**, 3375-3381.

Kobayashi, K., Une, H., and Hayashi, K. (1989) // *J. Biol. Chem.*, **264**, 7976-7980.

Kolonay, J.F.Jr., Moshiri, F., Gennis, R.B., Kaysser, T.M., and Maier, R.J. (1994) // *J. Bacteriol.*, **176**, 4177-4181.

Konstantinov, A.A., Siletsky, S., Mitchell, D., Kaulen, A., and Gennis, R.B. (1997) // *Proc. Natl. Acad. Sci. USA*, **94**, 9085-9090.

Krab, K., and Wikström, M. (1978) // *Biochim. Biophys. Acta*, **504**, 200-214.

Kroneck, P.M.H., Antholine, W.E., Kastrau, D.H.W., Buse, G., Steffens, G.C.M., and Zumft, W.G. (1990) // *FEBS Lett.*, **268**, 274-276.

LaMarche, A.E.P., Abate, M.I., Chan, S.H.P., and Trumpower, B.L. (1992) // *J. Biol. Chem.*, **267**, 22473-22480.

Lanyi, J.K. (2004) // *Mol. Membr. Biol.*, **21**, 143-150.

Lappalainen, P., Aasa, R., Malmström, B.G., and Saraste, M. (1993) // *J. Biol. Chem.*, **268**, 26416-26421.

Larsen, R.W., Pan, L.-P., Musser, S.M., Li, Z., and Chan, S.I. (1992) // *Proc. Natl. Acad. Sci. USA*, **89**, 723-727.

Lee, H., Das, T.K., Rousseau, D.L., Mills, D., Ferguson-Miller, S., and Gennis, R.B. (2000) // *Biochemistry*, **39**, 2989-2996.

Lee, A., Kirichenko, A., Vygodina, T., Siletsky, S.A., Das, T.K., Rousseau, D.L., Gennis, R., and Konstantinov, A. (2002) // *Biochemistry*, **41**, 8886-8898.

Lemberg, R. (1962) Action of alkali on cytochrome oxidase. // *Nature*, **193**, 373-374.

Liao, G.-L., and Palmer, G. (1996) // *Biochim. Biophys. Acta*, **1274**, 109-111.

Lindsay, J.G., Owen, C.S., and Wilson, D.F. (1975) // *Archs. Biochem. Biophys.*, **169**, 492-505.

Lorence, R.M., and Gennis, R.B. (1989) // *J. Biol. Chem.*, **264**, 7135-7140.

Ma, J., Tsatsos, P.H., Zaslavsky, D., Barquera, B., Thomas, J.W., Katsonouri, A., Puustinen, A., Wikström, M., Brzezinski, P., Alben, J.O., and Gennis, R.B. (1999) // *Biochemistry*, **38**, 15150-15156.

Malatesta, F., Sarti, P., Antonini, G., Vallone, B., and Brunori, M. (1990) // *Proc. Natl. Acad. Sci. USA*, **87**, 7410-7413.

Malmström, B.G., and Aasa, R. (1993) // *FEBS Lett.*, **325**, 49-52.

Marcus, R.A., and Sutin, N. (1985) // *Biochim. Biophys. Acta*, **811**, 265-322.

Mayo, S.L., Ellis, W.R.Jr., Crutchley, R.J., and Gray, H.B. (1986) // *Science*, **233**, 948-952.

McCauley, K.M., Vrtis, J.M., Dupont, J., and van der Donk, W.A. (2000) // *J. Am. Chem. Soc.*, **122**, 2403-2404.
Michel, H. (1998) // *Proc. Natl. Acad. Sci. USA*, **95**, 12819-12824.
Miller, M.J., and Gennis, R.B. (1985) // *J. Biol. Chem.*, **260**, 14003-14008.
Mitchell, P. (1961) // *Nature*, **191**, 144-184.
Mitchell, P. (1976) // *J. Theor. Biol*, **62**, 327-367.
Mitchell, P. (1988) // *Ann. N. Y. Acad. Sci.*, **550**, 185-198.
Mitchell, R., Mitchell, P., and Rich, P.R. (1991) // *FEBS Lett.*, **280**, 321-324.
Mitchell, R., and Rich, P.R. (1994) // *Biochim. Biophys. Acta*, **1186**, 19-26.
Moody, A.J., and Rich, P.R. (1990) // *Biochim. Biophys. Acta*, **1015**, 205-215.
Moody, A.J., Cooper, C.E., and Rich, P.R. (1991a) // *Biochim. Biophys. Acta*, **1059**, 189-207.
Moody, A.J., Brandt, U., and Rich, P.R. (1991b) // *FEBS Lett.*, **293**, 101-105.
Morgan, J.E., Li, P.M., Jang, D.-J., El-Sayed, M.A., and Chan, S.I. (1989) // *Biochemistry*, **28**, 6975-6983.
Morgan, J.E., Verkhovsky, M.I., Puustinen, A., and Wikström, M. (1993) // *Biochemistry*, **32**, 11413-11418.
Morgan, J.E., Verkhovsky, M.I., and Wikström, M. (1994) // *J. Bioenerg. Biomembr.*, **26**, 599-608.
Morgan, J.E., Verkhovsky, M.I., and Wikström, M. (1996) // *Biochemistry*, **35**, 12235-12240.
Morgan, J.E., Verkhovsky, M.I., Palmer, G., and Wikström, M. (2001) // *Biochemistry*, **40**, 6882-6892.
Moser, C.C., Keske, J.M., Warncke, K., Farid, R.S., and Dutton, P.L. (1992) // *Nature*, **355**, 796-802.
Muramoto, K., Hirata, K., Shinzawa-Itoh, K., Yoko-o, S., Yamashita, E., Aoyama, H., Tsukihara, T., and Yoshikawa, S. (2007) // *Proc. Natl. Acad. Sci. USA*, **104**, 7881-7886.
Nagle, J.F., and Morowitz, H.J. (1978) // *Proc. Natl. Acad. Sci. USA*, **75**, 298-302.
Nilsson, T. (1992) // *Proc. Natl. Acad. Sci. USA*, **89**, 6497-6501.
Ogura, T., Takahashi, S., Shinzawa-Itoh, K., Yoshikawa, S., and Kitagawa, T. (1990) // *J. Biol. Chem.*, **265**, 14721-14723.
Oliveberg, M., Brzezinski, P., and Malmström, B.G. (1989) // *Biochim. Biophys. Acta*, **977**, 322-328.
Oliveberg, M., and Malmström, B.G. (1991) // *Biochemistry*, **30**, 7053-7057.
Oliveberg, M., Hallén, S., and Nilsson, T. (1991) // *Biochemistry*, **30**, 436-440.
Oliveberg, M., and Malmström, B.G. (1992) // *Biochemistry*, **31**, 3560-3563.
Orii, Y. (1988) // *Ann. N.Y. Acad. Sci.*, **550**, 105-117.
Ostermeier, C., Harrenga, A., Ermler, U. and Michel, H. (1997) // *Proc. Natl. Acad. Sci. USA*, **94**, 10547-10553.
Page, C.C., Moser, C.C., Chen, X., and Dutton, P.L. (1999) // *Nature*, **402**, 47-52.
Papa, S., Capitanio, N., and Villani, G. (1998) // *FEBS Lett.*, **439**, 1-8.
Pelletier, H., and Kraut, J. (1992) // *Science*, **258**, 1748-1755.
Petersen, L.C., Nicholls, P., and Degn, H. (1976) // *Biochim. Biophys. Acta*, **452**, 59-65.
Pezeshk, A., Torres, J., Wilson, M.T., and Symons, M.C.R. (2001) // *J. Inorg. Biochem.*, **83**, 115-119.
Pfitzner, U., Odenwald, A., Ostermann, T., Weingard, L., Ludwig, B., and Richter, O.-M.H. (1998) // *J. Bioenerg. Biomembr.*, **30**, 89-97.
Pfitzner, U., Kirichenko, A., Konstantinov, A.A., Mertens, M., Wittershagen, A., Kolbesen, B.O., Steffens, G.C.M., Harrenga, A., Michel, H., and Ludwig, B. (1999) // *FEBS Lett.*, **456**, 365-369.
Pilet, E., Jasaitis, A., Liebl, U., and Vos, M.H. (2004) // *Proc. Natl. Acad. Sci. USA*, **101**, 16198-16203.
Poole, R.K. (1983) // *Biochim. Biophys. Acta*, **726**, 205-243.

Popović, D.M., and Stuchebrukhov, A.A. (2004) // *FEBS Lett.*, **566**, 126-130.
Proshlyakov, D.A., Pressler, M.A., and Babcock, G.T. (1998) // *Proc. Natl. Acad. Sci. USA*, **95**, 8020-8025.
Proshlyakov, D.A., Pressler, M.A., DeMaso, C., Leykam, J.F., DeWitt, D.L., and Babcock, G.T. (2000) // *Science*, **290**, 1588-1591.
Puustinen, A., Finel, M., Virkki, M., and Wikström, M. (1989) // *FEBS Lett.*, **249**, 163-167.
Puustinen, A., Finel, M., Haltia, T., Gennis, R.B., and Wikström, M. (1991) // *Biochemistry*, **30**, 3936-3942.
Puustinen, A., and Wikström, M. (1999) // *Proc. Natl. Acad. Sci. USA*, **96**, 35-37.
Qin, L., Hiser, C., Mulichak, A., Garavito, R.M., and Ferguson-Miller, S. (2006) // *Proc. Natl. Acad. Sci. USA*, **103**, 16117-16122.
Raitio, M., Tuulikki, J., and Saraste, M. (1987) // *EMBO J.*, **6**, 2825-2833.
Rauhamäki, V., Baumann, M., Soliymani, R., Puustinen, A., and Wikström, M. (2006) // *Proc. Natl. Acad. Sci. USA*, **103**, 16135-16140.
Reinhammar, B., Malkin, R., Jensen, P., Karlsson, B., Andreasson, L.-E., Aasa, R., Vänngård, T., and Malmström, B.G. (1980) // *J. Biol. Chem.*, **255**, 5000-5003.
Ribacka, C., Verkhovsky, M.I., Belevich, I., Bloch, D.A., Puustinen, A., Wikström, M. (2005) // *Biochemistry*, **44**, 16502-16512.
Rice, C.R., and Hempfling, W.P. (1978) // *J. Bacteriol.*, **134**, 115-124.
Rich, P.R., Jünemann, S., and Meunier, B. (1998) // *J. Bioenerg. Biomembr.*, **30**, 131-138.
Rieder, R., and Bosshard, H.R. (1980) // *J. Biol. Chem.*, **255**, 4732-4739.
Rigaud, J.-L., Pitard, B., and Levy, D. (1995) // *Biochim. Biophys. Acta*, **1231**, 223-246.
Riistama, S., Puustinen, A., Garcia-Horsman, A., Iwata, S., Michel, H., and Wikström, M. (1996) // *Biochim. Biophys. Acta*, **1275**, 1-4.
Riistama, S., Hummer, G., Puustinen, A., Dyer, R.B., Woodruff, W.H., and Wikström, M. (1997) // *FEBS Lett.*, **414**, 275-280.
Riistama, S., Laakkonen, L., Wikström, M., Verkhovsky, M.I., and Puustinen, A. (1999) // *Biochemistry*, **38,** 10670-10677.
Riistama, S., Puustinen, A., Verkhovsky, M., Morgan, J.E., and Wikström, M. (2000a) // *Biochemistry*, **39**, 6365-6372.
Riistama, S., Verkhovsky, M.I., Laakkonen, L., Wikström, M and Puustinen, A. (2000b) // *Biochim. Biophys. Acta*, **1456**, 1-4.
Rousseau, D.L., Ching, Y.-C., and Wang, J. (1993) // *J. Bioenerg. Biomembr.*, **25**, 165-176.
Ruitenberg, M., Kannt, A., Bamberg, E., Ludwig, B., Michel, H., and Fendler, K. (2000) // *Proc. Natl. Acad. Sci. USA*, **97**, 4632-4636.
Ruitenberg, M., Kannt, A., Bamberg, E., Fendler, K., and Michel H. (2002) // *Nature*, **417**, 99-102.
Saiki, K., Mogi, T., Ogura, K., and Anraku, Y. (1993) // *J. Biol. Chem.*, **268**, 26041-26045.
Salomonsson, L., Lee, A., Gennis, R.B., and Brzezinski, P. (2004) // *Proc. Natl. Acad. Sci. USA*, **101**, 11617-11621.
Saraste, M. (1990) // *Q. Rev. Biophys.*, **23**, 331-366.
Saraste, M. (1999) // *Science*, **283**, 1488-1493.
Schmidt, B., McCracken, J., and Ferguson-Miller, S. (2003) // *Proc. Natl. Acad. Sci. USA*, **100**, 15539-15542.
Seelig, A., Ludwig, B., Seelig, J., and Schatz, G. (1981) // *Biochim. Biophys. Acta*, **636**, 162-167.
Shapleigh, J.P., and Gennis, R.B. (1992) // *Mol. Microbiol.*, **6**, 635-642.
Shapleigh, J.P., Hosler, J.P., Tecklenburg, M.M.J., Kim, Y., Babcock, G.T., Gennis, R.B., and Ferguson-Miller, S. (1992) // *Proc. Natl. Acad. Sci. USA*, **89**, 4786-4790.
Shaw, R.W., Hansen, R.E., and Beinert, H. (1978) // *Biochim. Biophys. Acta*, **504**, 187-199.
Siegbahn, P.E.M., Blomberg, M.R.A, and Blomberg, M.L.. (2003) // *J. Phys. chem. B*, **107**, 10946-10955.

Sigurdson, H., Brändén, M., Namslauer, A., and Brzezinski, P. (2002) // *J. Inorg. Biochem.*, **88**, 335-342.

Siletsky, S.A., Pawate, A.S., Weiss, K., Gennis, R.B., and Konstantinov, A.A. (2004) // *J. Biol. Chem.*, **279**, 52558-52565.

Slater, E.C. (2003) // *J. Biol. Chem.*, **278**, 16455-16461.

Smirnova, I.A., Ädelroth, P., Gennis, R.B., and Brzezinski, P. (1999) // *Biochemistry*, **38**, 6826-6833.

Solioz, M., Carafoli, E., and Ludwig, B. (1982) // *J. Biol. Chem.*, **257**, 1579-1582.

Soulimane, T., Buse, G., Bourenkov, G. P., Bartunik, H. D., Huber, R. and Than, M. E. (2000) // *EMBO J.*, **19**, 1766-1776.

Steinrucke, P., Steffens, G.C.M., Panskus, G., Buse, G., and Ludwig, B. (1987) // *Eur. J. Biochem.*, **167**, 431-439.

Stevens, T.H., and Chan, S.I. (1981) // *J. Biol. Chem.*, **256**, 1069-1071.

Stock, D., Gibbons, C., Arechaga, I., Leslie A.GW., and Walker J.E. (2000) // *Curr. Opin. Struct. Biol.*, **10**, 672-679.

Sucheta, A., Szundi, I., and Einarsdóttir, Ó. (1998) // *Biochemistry*, **37**, 17905-17914.

Svensson-Ek, M., Thomas, J.W., Gennis, R.B., Nilsson, T., and Brzezinski, P. (1996) // *Biochemistry*, **35**, 13673-13680.

Svensson-Ek, M., Abramson, J., Larsson, G., Tornroth, S., Brezezinski, P. and Iwata, S. (2002) // *J. Mol. Biol.*, **321**, 329-339.

Thomas, J.W., Puustinen, A. Alben, J.O., Gennis, R.B., and Wikström, M. (1993a) // *Biochemistry*, **32**, 10923-10928.

Thomas, J.W., Lemieux, L.J., Alben, J.O., and Gennis, R.B. (1993b) // *Biochemistry*, **32**, 11173-11180.

Thomas, J.W., Calhoun, M.W., Lemieux, L.J., Puustinen, A., Wikström, M., Alben, J.O., and Gennis, R.B. (1994) // *Biochemistry*, **33**, 13013-13021.

Tsukihara, T., Aoyama, H., Yamashita, E., Tomizaki, T., Yamaguchi, H., Shinzawa-Itoh, K., Nakashima, R., Yaono, R., and Yoshikawa, S. (1995) // *Science*, **269,** 1069-1074.

Tsukihara, T., Aoyama, H., Yamashita, E., Tomizaki, T., Yamaguchi, H., Shinzawa-Itoh, K., Nakashima, R., Yaono, R. and Yoshikawa, S. (1996) // *Science,* **272**, 1136-1144.

Tsukihara, T., Shimokata, K., Katayama, Y., Shimada, H., Muramoto, K., Aoyama, H., Mochizuki, M., Shinzawa-Itoh, K., Yamashita, E., Yao, M., Ishimura, Y. and Yoshikawa, S. (2003) // *Proc. Natl. Acad. Sci. USA*, **100**, 15304-15309.

Tweedle, M.F., Wilson, L.J., Garcia-Iñiguez, L., Babcock, G.T., and Palmer, G. (1978) // *J. Biol. Chem.*, **253**, 8065-8071.

van der Oost, J., Lappalainen, P., Musacchio, A., Warne, A., Lemieux, L., Rumbley, J., Gennis, R.B., Aasa, R., Pascher, T., Malmström, B.G., and Saraste, M. (1992) // *EMBO J.*, **11**, 3209-3217.

van Gelder, B.F., and Beinert, H. (1969) // *Biochim. Biophys. Acta*, **189**, 1-24.

Vanneste, W.H. (1966) // *Biochemistry*, **5**, 838-848.

Varotsis, C., Woodruff, W.H., and Babcock, G.T. (1989) // *J. Am. Chem. Soc.*, **111**, 6439-6440.

Varotsis, C., and Babcock, G.T. (1990) // *Biochemistry*, **29**, 7357-7362.

Varotsis, C., Zhang, Y., Appelman, E.H., and Babcock, G.T. (1993) // *Proc. Natl. Acad. Sci. USA*, **90**, 237-241.

Verkhovskaya, M., Verkhovsky, M., and Wikström, M. (1992) // *J. Biol. Chem.*, **267**, 14559-14562.

Verkhovskaya, M.L., Garcia-Horsman, A., Puustinen, A., Rigaud, J.-L., Morgan, J.E., Verkhovsky, M.I., and Wikström, M. (1997) // *Proc. Natl. Acad. Sci. USA*, **94**, 10128-10131.

Verkhovsky, M.I., Morgan, J.E., and Wikström, M. (1992) // *Biochemistry*, **31**, 11860-11863.

Verkhovsky, M.I., Morgan, J.E., and Wikström, M. (1994) // *Biochemistry*, **33**, 3079-3086.

Verkhovsky, M.I., Morgan, J.E., and Wikström, M. (1995) // *Biochemistry*, **34**, 7483-7491.
Verkhovsky, M.I., Morgan, J.E., Puustinen, A., and Wikström, M. (1996a) // *Biochemistry*, **35**, 16241-16246.
Verkhovsky, M.I., Morgan, J.E., and Wikström, M. (1996b) // *Proc. Natl. Acad. Sci. USA*, **93**, 12235-12239.
Verkhovsky, M.I., Morgan, J.E., Puustinen, A., and Wikström, M. (1996c) // *Nature*, **380**, 268-270.
Verkhovsky, M.I., Morgan, J.E., Verkhovskaya, M.L., and Wikström, M. (1997) // *Biochim. Biophys. Acta*, **1318**, 6-10.
Verkhovsky, M.I., Belevich, N., Morgan, J.E., and Wikström, M. (1999a) // *Biochim. Biophys. Acta*, **1412**, 184-189.
Verkhovsky, M.I., Jasaitis, A., Verkhovskaya, M.L., Morgan, J.E., and Wikström, M. (1999b) // *Nature*, **400**, 480-483.
Verkhovsky, M.I., Jasaitis, A., and Wikström, M. (2001a) // *Biochim. Biophys. Acta*, **1506**, 143-146.
Verkhovsky, M.I., Tuukkanen, A., Backgren, C., Puustinen, A., and Wikström, M. (2001b) // *Biochemistry*, **40**, 7077-7083.
Verkhovski, M.I., Belevich, I., Bloch, D.A., and Wikström, M. (2006) // *Biochim. Biophys. Acta*, **1757**, 401-407.
Vygodina, T., and Konstantinov, A. (1988) // *Ann. N Y Acad. Sci.*, **550**, 124-138.
Vygodina, T., and Konstantinov, A. (1989) // *Biochim. Biophys. Acta*, **973**, 390-398.
Vygodina, T.V., Pecoraro, C., Mitchell, D., Gennis, R., and Konstantinov, A.A. (1998) // *Biochemistry*, **33**, 3053-3061.
Wikström, M.K.F. (1977) // *Nature*, **266**, 271-273.
Wikström, M. (1981) // *Proc. Natl. Acad. Sci. USA*, **78**, 4051-4054.
Wikström, M. (1984) // *FEBS Lett.*, **169**, 300-304.
Wikström, M. (1989) // *Nature*, **338**, 776-778.
Wikström, M.K.F., and Saari, H.T. (1977) // *Biochim. Biophys. Acta*, **462**, 347-361.
Wikström, M., Saari, H., Penttilä, T., and Saraste, M. (1977) in Nicholls, P., Moller, J.V., Jorgensen, A.J., and Moody, A.J. (Eds.), *Membrane Proteins 11th FEBS Meeting*, Symp. A4, **45**, Pergamon, Oxford, 85-94.
Wikström, M., and Morgan, J.E. (1992) // *J. Biol. Chem.*, **267**, 10266-10273.
Wikström, M., Saari, H., Penttilä, T., and Saraste, M. (1977) in Membrane proteins 11th FEBS Meeting, Symposium A4, **45**, Pergamon, Oxford, 85-94.
Wikström, M., Krab, K., and Saraste, M. (1981) // *Cytochrome Oxidase: A Synthesis*, (Academic Press, London).
Wikström, M., Jasaitis, A., Backgren, C., Puustinen, A., and Verkhovsky, M. (2000) // *Biochim. Biophys. Acta*, **1459**, 514-520.
Wikström, M., Verkhovsky, M.I., and Hummer, G. (2003) // *Biochim. Biophys. Acta*, **1604**, 61-65.
Wilson, D.F., Erecińska, M., and Owen, C.S (1976) // *Arch. Biochem. Biophys.*, **175**, 160-172.
Wilson, D.F., and Nelson, D. (1982) // *Biochim. Biophys. Acta*, **680**, 233-241.
Winkler, J.R., Malmström, B.G., and Gray, H.B. (1995) // *Biophys. Chem.*, **54**, 199-209.
Witt, H., and Ludwig, B. (1997) // *J. Biol. Chem.*, **272**, 5514-5517.
Witt, H., Malatesta, F., Nicoletti, F., Brunori, M., and Ludwig, B. (1998) // *J. Biol. Chem.*, **273**, 5132-5136.
Woodruff, W.H., Einarsdóttir, Ó., Dyer, R.B., Bagley, K.A., Palmer, G., Atherton, S.J., Goldbeck, R.A., Dawes, T.D., and Kliger, D.S. (1991) // *Proc. Natl. Acad. Sci. USA*, **88**, 2588-2592.
Wrigglesworth, J.M. (1984) // *Biochem. J.*, **217**, 715-719.

Yang, W.-L., Iacono, L., Tang, W.-M., and Chin, K.-V. (1998) // *Biochemistry*, **37**, 14175-14180.

Yano, T. (2002) // *Mol. Asp. Med.*, **23**, 345-368.

Ye, X., Demidov, A., and Champion, P.M. (2002) // *J. Am. Chem. Soc.*, **124**, 5914-5924.

Yoshikawa, S., Shinzawa-Itoh, K., Nakashima, R., Yaono, R., Yamashita, E., Inoue, N., Yao, M., Fei, M. J., Libeu, C. P., Mizushima, T., Yamaguchi, H., Tomizaki, T. and Tsukihara, T. (1998) // *Science*, **280**, 1723-1729.

Zaslavsky, D., Kaulen, A.D., Smirnova, I.A., Vygodina, T., and Konstantinov, A.A. (1993) // *FEBS Lett.*, **336**, 389-393.

Zaslavsky, D., Sadoski, R.C., Wang, K., Durham, B., Gennis, R.B., and Millett, F. (1998) // *Biochemistry*, **37**, 14910-14916.

Zhen, Y., Hoganson, C.W., Babcock, G.T., and Ferguson-Miller, S. (1999) // *J. Biol. Chem.*, **274**, 38032-38041.

Zheng, X., Medvedev, D.M., Swanson, J., and Stuchebrukhov,A.A. (2003) // *Biochim. Biophys. Acta*, **1557**, 99-107.

Zickermann, V., Verkhovsky, M., Morgan, J., Wikström, M., Anemüller, S., Bill, E., Steffens, G.C.M., and Ludwig, B. (1995) // *Eur. J. Biochem.*, **234**, 686-693.

Ädelroth, P., Brzezinski, P., and Malmström, B.G. (1995) // *Biochemistry*, **34**, 2844-2849.

Ädelroth, P., Svensson Ek, M., Mitchell, D.M., Gennis, R.B., and Brzezinski, P. (1997) // *Biochemistry*, **36**, 13824-13829.

Ädelroth, P., Gennis, R.B., and Brzezinski, P. (1998a) // *Biochemistry*, **37**, 2470-2476.

Ädelroth, P., Ek, M., and Brzezinski, P. (1998b) // *Biochim. Biophys. Acta*, **1367**, 107-117.